

**UNIVERSIDADE FEDERAL DO RIO GRANDE DO SUL**  
**INSTITUTO DE QUÍMICA**  
**PROGRAMA DE PÓS-GRADUAÇÃO EM QUÍMICA**

**HÍBRIDOS À BASE DE ANILINA/SÍLICA OBTIDOS ATRAVÉS**  
**DO PROCESSO SOL-GEL: SÍNTESE, CARACTERIZAÇÃO**  
**E PROPRIEDADES**

**FLÁVIO ANDRÉ PAVAN**

**PORTO ALEGRE**  
**Julho 2003**

**UNIVERSIDADE FEDERAL DO RIO GRANDE DO SUL**  
**INSTITUTO DE QUÍMICA**  
**PROGRAMA DE PÓS-GRADUAÇÃO EM QUÍMICA**

**HÍBRIDOS À BASE DE ANILINA/SÍLICA OBTIDOS ATRAVÉS  
DO PROCESSO SOL-GEL: SÍNTESE, CARACTERIZAÇÃO  
E PROPRIEDADES**

**FLÁVIO ANDRÉ PAVAN**

Mestre em Química Analítica

Tese apresentada ao Programa de Pós-Graduação em Química da UFRGS como parte dos  
requisitos para a obtenção do título de Doutor em Química

**PORTO ALEGRE**  
**Julho 2003**

## **DECLARAÇÃO DE AUTORIA**

Este trabalho foi orientado pelo Professor Dr. Edilson Valmir Benvenuti e com a co-orientação da Professora Dr. Tania M. H. Costa. As atividades inerentes ao trabalho foram realizadas no Laboratório de Sólidos e Superfícies, do Instituto de Química da UFRGS no período entre Setembro de 1999 e Julho de 2003.

---

---

Esta Tese foi julgada adequada para a obtenção do título de Doutor em Química e aprovada em sua forma final, pelo Orientador e pela Banca Examinadora do Curso de Pós-Graduação.

Orientador: Prof. Dr Edilson Valmir Benvenuti

Banca Examinadora:

Prof Dr. Yoshitaka Gushikem

Prof Dr. Lauro Kubota

Profa Dra. Marcia Gallas

Profa Dra. Adriana Ruffin Pohlmann

Prof. Dr Adriano Lisboa Monteiro  
Coordenador do PPGQ-UFRGS

*Dedico este trabalho em especial a minha família e a minha querida noiva Ana Cristina Mazzocato por estarem sempre ao meu lado incentivando-me e confortando-me com palavras de esperança e carinho.*

## **AGRADECIMENTOS**

Ao professor Edilson V. Benvenuti pela orientação, dedicação e amizade durante a realização deste trabalho.

À professora Tania M. H. Costa pela sua valiosa contribuição, conhecimentos compartilhados e dedicação.

Aos professores membros da Banca Examinadora, Márcia Gallas, Lauro Kubota, Yoshitaka Gushikem e Adriana Ruffin Pohlmann pelas contribuições sugeridas.

Aos colegas do Laboratório de Sólidos e Superfícies desta instituição pela convivência, receptividade e apoio.

Aos meus pais Gelso e Irma Pavan pela lição de vida, sabedoria e nobreza de seus pensamentos e atitudes.

Aos demais familiares e também aos meus verdadeiros amigos que sempre estiveram ao meu lado acreditando que quando sentimos prazer em fazer algo que gostamos, mesmo que o caminho a percorrer seja árduo, o enriquecimento humano e a superação de limites é uma consequência.

Ao sofrido povo brasileiro, que através do pagamento do seus impostos permitiu a minha qualificação acadêmica.

Ao CNPq pela bolsa concedida.

A todos aqueles que contribuíram de alguma forma para esta conquista, o meu apreço.

---

---

## SUMÁRIO

RESUMO	viii
ABSTRACT	ix
CONSIDERAÇÕES PRELIMINARES	x
1. INTRODUÇÃO	1
1.1 - PROCESSO SOL-GEL	1
1.1.1 - Considerações Gerais	2
1.1.2 - Química do Processo Sol-Gel	2
1.1.2.1 - Natureza dos Precursores	2
1.1.2.2 - Hidrólise	3
1.1.2.3 - Condensação	4
• - Alcoólica	
• - Aquosa	
1.1.3 - Etapas do Processo Sol-Gel	6
1.1.3.1 - Gelatinização/Policondensação	6
1.1.3.2 - Envelhecimento	7
1.1.3.3 - Secagem	7
1.2 - MATERIAIS HÍBRIDOS ORGANO-INORGÂNICOS	8
1.2.1 Aplicações de Materiais Híbridos Organo-Inorgânicos	10
1.3 - MOTIVAÇÃO PARA A REALIZAÇÃO DESSE TRABALHO	10
1.4 - INTRODUÇÃO ÀS TÉCNICAS DE CARACTERIZAÇÃO UTILIZADAS NESSE TRABALHO	11
1.4.1 - BET	11
1.4.2 - Espectroscopia no Infravermelho ( <i>FT-IR</i> )	12
1.4.3 - Análise Termogravimétrica ( <i>TGA</i> )	13
1.4.4 - Análise de Tamanho de Poros	13
1.4.4.1 - Poros Totais	13
1.4.4.2 - Poros Abertos	14

---

---

1.4.5 - Microscopia Eletrônica de Varredura (SEM)	14
2. OBJETIVOS	15
3. REFERÊNCIAS BIBLIOGRÁFICAS	16
4. ARTIGOS	20

4.1- F. A. Pavan, S. Leal, T. M. H. Costa, Y. Gushiken and E. V. Benvenutti. A Sol-Gel Synthesis for Termally Stable Aniline/ Silica Material. *Journal of Sol-Gel Science and Technology* 23, 129-133, 2002

4.2.- F. A. Pavan, W. F. Magalhães, M. A. de Luca, C. C. Moro, T. M. H. Costa and E. V. Benvenutti. A characterization study of xerogel silicapropylaniline powders. *Journal of Non-Crystalline Solids* 311 (2002) 54-60

4.3 - F. A. Pavan, Y. Gushiken, C. Moro, T. M. H. Costa and E. V. Benvenutti. The influence of Na<sup>+</sup> on the aniliepropylsilica xerogel synthesis by using the fluoride nucleophilic catalyst. *Colloid Polym Sci* (2003) 281: 173- 177

4.4 - F. A. Pavan, S. A. Gobbi, T. M. H. Costa and E. V. Benvenutti. FTIR Thermal analysis on anilinepropylsilica xerogel. *Journal of Thermal Analysis and Calorimetry*, 68 (2002) 199-206

4.5 - F. A. Pavan, S. A. Gobbi, C. C. Moro, T. M. H. Costa and E. V. Benvenutti. The Influence of the Amount of Fluoridre Catalyst on the Morphological Properties of the Anilinepropylsilica Xerogel Prepared in Basic Medium. *Journal of Porous Materials* 9: 307-311, 2002

4.6 - F. A. Pavan, S. A. H. S. Hoffmann, Y. Gushiken, T. M. H. Costa, E. V. Benvenutti. The gelation temperature effects in the anilinepropylsilica xerogel properties. *Materials Letters* 55, (2002) 378-382



4.7 - F. A. Pavan, A. M. S. Lucho, R. S. Gonçalves, T. M. H. Costa and E. V. Benvenuti. Anilinepropylsilica xerogel used as a selective Cu(II) adsorbent in aqueous solution. *Journal Colloid Interface Science*

4.8 - F. A. Pavan, T. M. H. Costa, E. V. Benvenuti. Adsorption of CoCl<sub>2</sub>, ZnCl<sub>2</sub> and CdCl<sub>2</sub> on aniline/silica hybrid material obtained by sol-gel method. *Colloid and Surface A: Physicochemical and Engineering Aspects* (trabalho aceito)

5. CONCLUSÕES	83
6. SUGESTÕES PARA TRABALHOS FUTUROS	85
7. ANEXOS	86

## RESUMO

Neste trabalho inicialmente foi sintetizado o precursor organoalcoxisilano 3-anilina-propiltrimetoxissilano, APTMS, a partir da reação entre a anilina e o 3-cloropropiltrimetoxissilano, CPTMS, usando hidreto de sódio, NaH, como ativador de base. O precursor inorgânico tetraetilortossilicato, TEOS, foi polimerizado na presença do precursor orgânico, e catalisador. Durante a etapa de polimerização dos precursores alcóxidos, foram investigadas as influências da temperatura, do tipo e concentração do catalisador e da concentração de precursor orgânico adicionado nas propriedades finais dos híbridos anilina-propilsilica resultantes. Os materiais híbridos foram caracterizados através das técnicas: espectroscopia no infravermelho (*FT-IR*), técnica de espalhamento de Raios-x a baixos ângulos (*SAXS*), microscopia eletrônica de varredura (*SEM*), isotermas de adsorção e dessorção de nitrogênio, análise elementar, espectroscopia de aniquilação de pósitrons (*PALS*), análise termogravimétrica (*TGA*), espectroscopia de elétrons dispersos (*EDS*). A potencialidade de aplicação dos híbridos obtidos como materiais adsorventes na extração dos cátions Cu(II), Zn(II), Cd(II) e Co(II), em solução, foi investigada usando-se isotermas de adsorção pelo método batelada.

Através das técnicas de caracterização foi possível observar que as propriedades morfológicas dos materiais como área superficial, distribuição do tamanho de poros, forma e tamanho das partículas, além da estabilidade e grau de incorporação orgânica podem ser controladas em maior ou menor grau, dependendo da variável usada durante a polimerização dos precursores alcóxidos. O material apresentou propriedades promissoras como adsorvente seletivo para o cobre.

## **ABSTRACT**

In this work, firstly, it was synthesized the 3-aminepropyltrimethoxysilane, APTMS, starting from the reaction between the aniline and the 3-chloropropyltrimethoxysilane, CPTMS, using the sodium hydride as base activator. The inorganic precursor tetraethylorthosilicate, TEOS, was polymerized together with the organic precursor using a catalyst. During the polymerization step, it was investigated the influences of the temperature, type and quantity of catalyst and the concentration of the organic precursor added, in the properties of the resulting anilinepropylsilica xerogels. The hybrid materials were characterized by using elemental analysis (CHN), infrared spectroscopy (FTIR), scanning electron microscopy (SEM), positron annihilation lifetime spectroscopy (PALS), small angle x-ray scattering (SAXS), thermal gravimetric analysis (TGA), electron dispersive spectroscopy (EDS) and N<sub>2</sub> adsorption desorption isotherms. The potential application of the obtained hybrid materials as metal sorbent for solutions containing Cu(II), Zn (II), Co (II) and Cd (II), was investigated by using of batch technique.

From the characterization study it was possible to observe that the xerogel properties as surface area, pore size distribution, particle size and shape, thermal stability and organic content can be controlled starting from the synthesis conditions. The anilinepropylsilica xerogel presents promising properties as copper selective adsorbent.

## **CONSIDERAÇÕES PRELIMINARES**

A apresentação de Teses em forma de artigos científicos, é uma tendência nacional, visto que, a produção científica discente tem sido um dos fatores relevantes na avaliação dos órgãos de fomento à pesquisa. Esta forma de apresentação, ao mesmo tempo que incentiva à publicação científica, possibilita a exposição e discussão dos resultados e idéias frente a uma comunidade científica maior.

Frente a esta tendência, o Programa de Pós-Graduação em Química da Universidade Federal do Rio Grande do Sul, recentemente tem adotado e incentivado a apresentação de Tese em forma de artigos científicos.

A presente Tese será apresentada sob a forma de artigos levando em consideração as exigências de formatação segundo as regras das revistas de publicação dos referidos artigos. A primeira etapa consta de uma introdução geral que trata das generalidades que justificam a proposta de trabalho e seus objetivos. Numa segunda etapa serão apresentados os trabalhos publicados e submetidos, inerentes ao trabalho desenvolvido. Numa terceira e última parte, será apontada uma síntese de conclusões dos trabalhos publicados, bem como um enfoque de aspectos fundamentais para realização de futuros estudos na área.

## 1. INTRODUÇÃO

O constante surgimento de novas tecnologias trouxe como imposição e desafio para a comunidade científica a necessidade de desenvolver materiais capazes de preencher as exigências requeridas por estes avanços. Não há exagero em dizer que o avanço tecnológico de uma nação depende da disponibilidade e qualidade dos materiais por ela produzidos.

Em muitas áreas da ciência, o emprego de materiais convencionais tem sido limitado devido às propriedades por eles apresentadas. Desta forma, materiais que contemplam propriedades que não são encontradas em materiais convencionais têm recebido uma atenção especial. A escolha adequada dos constituintes de um material, como também as propriedades físicas complementares, tem levado ao desenvolvimento de materiais híbridos organo-inorgânicos.

Dentre os processos existentes para a preparação de materiais híbridos, o processo sol-gel aparece como uma rota alternativa e bastante vantajosa. A possibilidade de controlar as propriedades morfológicas dos materiais através dos parâmetros de síntese usados permite a obtenção de materiais com propriedades específicas e com ampla aplicabilidade em diferentes áreas tecnológicas.

### 1.1 - PROCESSO SOL – GEL

#### 1.1.1 - Considerações Gerais

O processo sol-gel é conhecido pelos químicos a mais de 150 anos, e teve seu início com o trabalho pioneiro de Ebelmen e Graham <sup>1-2</sup> em 1844. Comercialmente tem sido aplicado desde 1930, na produção de filmes de óxidos com propriedades ópticas e protetoras. Em 1960, com o trabalho de Dislich <sup>1</sup>, que demonstrou a viabilidade de preparação de vidros multicomponentes controlando-se as taxas de hidrólise e condensação dos precursores, é que o processo sol-gel mostrou-se uma técnica versátil com potencialidade de aplicação em várias áreas tecnológicas. Entretanto, só a partir da década de 80, o processo sol-gel ganhou notoriedade, quando adquiriu importância científica e tecnológica. Um marco importante da escala evolutiva do processo sol-gel, foram os trabalhos realizados por Schimidt e *et al.*,(1984)<sup>1-3</sup>, que demonstraram a possibilidade de inserção de um componente orgânico

a uma estrutura inorgânica, dando surgimento a classe de materiais híbridos organo-inorgânicos.<sup>2</sup>

O processo sol-gel como o próprio nome implica, envolve a síntese de uma rede polimérica inorgânica por reações químicas em solução a baixas temperaturas, tendo como resultante a transição de um líquido no estado sol (dispersão coloidal) para o estado de gel.<sup>4</sup>

Indiscutivelmente o processo sol-gel apresentou-se como uma rota alternativa e bastante vantajosa para a síntese de materiais, tanto inorgânicos poliméricos como híbridos orgânico-inorgânicos. Este fato é comprovado pelo expressivo número de trabalhos científicos publicados, mais de 6000 artigos até o ano de 1995<sup>5</sup>, e chegando a mais de 17.700 publicações até o presente (julho de 2003). Como vantagens do processo sol-gel no processamento de materiais pode-se destacar: a) a alta pureza dos precursores, resultando desta forma, na obtenção de materiais também com alta pureza; b) reações podem ser processadas à temperatura ambiente, o que torna possível por exemplo, incorporar à rede inorgânica biomoléculas (enzimas, proteínas, anticorpos, etc.) de difícil incorporação pelos métodos tradicionais; c) o controle dos processos químicos envolvidos, com possibilidade de arquitetar as propriedades dos materiais como por exemplo, tamanho e forma de partículas, volume e distribuição de poros, área superficial; d) possibilidade de obter materiais sob diferentes configurações como monolitos, fibras, corpos cerâmicos, filmes, membranas e pós. Já como desvantagens pode-se destacar: a) o alto custo de alguns precursores, b) longos tempos de processamento, c) em alguns casos a reprodutibilidade se torna difícil.<sup>4,6-10</sup>

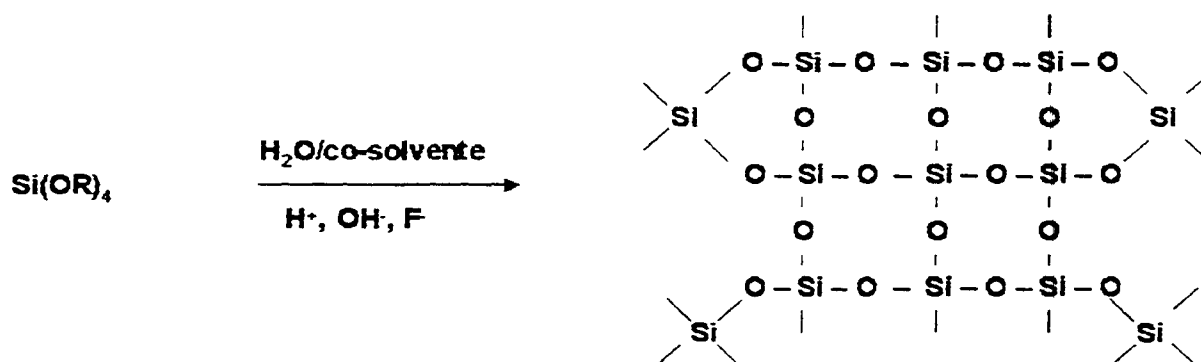
## **1.1.2 - Química do Processo Sol- Gel**

### **1.1.2.1- Natureza do Precursor**

Em princípio, para que um composto possa ser usado como precursor no processo sol-gel, é necessário que o mesmo cumpra os seguintes requisitos fundamentais: ser solúvel no meio reacional e apresentar reatividade capaz de participar das reações para formação do gel. Assim, compostos como sais inorgânicos ou orgânicos; hidróxidos, óxidos, e alcóxidos podem ser usados como tais. Comumente, os precursores consistem de um metal ou não metal circundado por espécies ligantes reativas.

Os alcóxidos são amplamente usados como precursores no processo sol-gel, pois são facilmente hidrolisáveis, solúveis na maioria dos solventes orgânicos e facilmente purificados.<sup>4,6,11-12</sup> Dependendo da natureza, os precursores alcóxidos podem ser: a) metálico

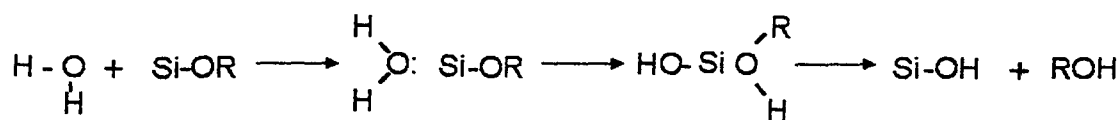
(M(OR)<sub>n</sub>, onde M= Al, Sn, Mo, Ce, Ti, etc, e b) silício (alcoxissilano, Si(OR)<sub>n</sub>), onde R= grupo alquila. Alcoxissilanos organofuncionalizados (R'-Si(OR)<sub>3</sub> e (OR)<sub>3</sub>-Si-R'-(OR)<sub>3</sub> onde R'= C<sub>6</sub>H<sub>5</sub>, SH, etc, são empregados para a obtenção de materiais híbridos. Dentre os alcoxissilanos, podemos destacar o tetrametilortosilicato (TMSO); Si(OCH<sub>3</sub>)<sub>4</sub> e o tetraetilortosilicato TEOS; Si(OC<sub>2</sub>H<sub>5</sub>)<sub>4</sub>. No esquema abaixo, está representado o produto da hidrólise e condensação polimérica desses precursores, dissolvido em solvente orgânico na presença de água e catalisador <sup>4,6,12-13</sup>.



As reações químicas envolvidas durante o processo sol-gel para a obtenção de materiais inorgânicos poliméricos e híbridos são duas: I) *hidrólise do precursor* II) *condensação dos grupos silanóis*. Essas reações serão discutidas a seguir, para alcóxidos de silício.

### 1.1.2.2 - Hidrólise

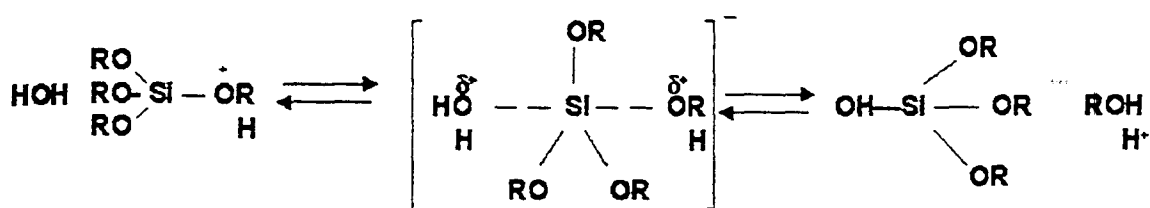
Os precursores alcóxidos de silício, Si(OR)<sub>4</sub>, sofrem hidrólise por meio da reação direta entre o grupo alcóxido e a molécula de água, para formar as espécies Si(OH)<sub>4</sub>, com a liberação de álcool, envolvendo: a) adição nucleofílica de H<sub>2</sub>O ao silício; b) transferência de próton (estado de transição) da molécula de água para o oxigênio do grupo OR, e; c) saída do álcool, conforme ilustrado abaixo. <sup>4,6,12-13</sup>



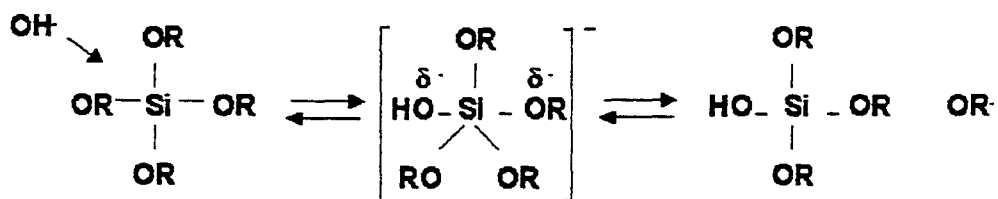
Tanto a hidrólise como a condensação dos alcóxidos podem ser processadas na presença de catalisadores que proporcionam um aumento na velocidade dessas reações. A

catálise é particularmente importante no caso dos alcóxidos de silício que apresentam uma baixa reatividade em relação aos alcóxidos metálicos. Os catalisadores usados podem ser: HCl, H<sub>2</sub>SO<sub>4</sub>, HNO<sub>3</sub>, HF; NH<sub>3</sub><sup>+</sup>, dimetilformamida, ácido acético, ácido oxálico etc.<sup>4,12,14</sup>

Sob condições ácidas, a hidrólise se processa mais rapidamente que a condensação. O mecanismo envolvido durante a catálise ácida, consiste na protonação do grupo alcóxido e substituição do mesmo pela água, *via* mecanismo de substituição nucleofílica bimolecular (S<sub>N</sub>2), com inversão do tetraedro de silício.<sup>4,12,14</sup>



Já em condições básicas, a hidrólise se dá *via* um ataque nucleofílico do grupo hidroxila sobre o silício, resultando na formação de um estado de transição pentacoordenado negativo, com liberação do íon alcóxido.<sup>4,14</sup>



Um outro tipo de catálise é a catálise nucleofílica. Nesse caso usa-se preferencialmente fluoreto. Segundo Brinker e Scherer<sup>15</sup>, o mecanismo envolvido na catálise por F<sup>-</sup> consiste em um ataque nucleofílico do F<sup>-</sup> ao alcóxido de silício, com formação de um intermediário de silício pentacoordenado ou hexacoordenado com formação do álcool e silanol. Como envolve um ataque nucleofílico ao silício, tem semelhanças com o mecanismo da catálise básica.<sup>4,12,14</sup>

### 1.1.2.3. - Condensação

As reações de condensação ocorrem após a formação de espécies hidrolisadas. O mecanismo envolvido consiste de um ataque nucleofílico de silanos desprotonados, SiO<sup>-</sup>, a

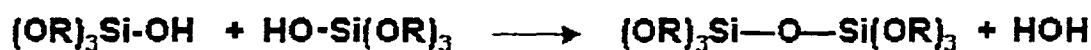


espécies neutras SiOH ou SiOR, originando um siloxano, Si-O-Si. Quando o sub-produto formado for um álcool, a condensação é denominada de alcoólica ou heterogênea, por outro lado, se for a água, a condensação é dita aquosa ou homogênea. O esquema abaixo descreve de forma sintética estas reações:<sup>4,12</sup>

- *Condensação alcoólica*



- *Condensação aquosa*



As reações de condensação também são aceleradas por catálise ácida ou básica. Na catálise ácida, a condensação ocorre preferencialmente nas extremidades dos oligômeros, nas espécies menos condensadas, ou seja, que apresentam uma maior fração silícios mais básicos Si-OR. Os polímeros resultantes da catálise ácida são mais lineares, compactos, geralmente com predomínio de microporos e estreita distribuição de diâmetro de poros.<sup>4,16</sup>

Na catálise básica, a condensação ocorre preferencialmente no centro dos oligômeros, onde se encontram os silícios mais ácidos, o que resulta geralmente na formação de polímeros menos densos, particulados, com partículas geralmente esféricas.<sup>4,16-17</sup>

A catálise nucleofílica também influencia a condensação e da mesma forma que na reação de hidrólise, o mecanismo envolvido é muito similar ao da catálise básica. Portanto, seria previsível esperar que os materiais obtidos por estes dois tipos de catálise apresentem características semelhantes. Entretanto, já foi relatado por Tigner *et al.*<sup>18</sup>, que a catálise nucleofílica com fluoreto pode favorecer o crescimento de cadeia linear dos oligômeros, contrariando a hipótese proposta de Brinker e Scherer<sup>15</sup>, visto que o crescimento linear da cadeia é uma característica da catálise ácida. Portanto, não há consenso na literatura, quanto aos mecanismos envolvidos no processo sol-gel. Conflitos dessa natureza fazem desses sistemas alvo de muita pesquisa científica.

As reações do processo sol-gel podem ser resumidamente descritas como:



Durante as reações de hidrólise e condensação importantes variáveis como natureza e quantidade de catalisador <sup>19-26</sup>, concentração das espécies reativas <sup>27-31</sup> temperatura de condensação <sup>32-35</sup>, pH <sup>36-40</sup>, natureza dos precursores <sup>41-45</sup> e solvente <sup>46-51</sup> podem influenciar significativamente na velocidade relativa destas reações e portanto influenciar nas propriedades estruturais dos materiais resultantes. Outras variáveis, como velocidade de agitação <sup>52-53</sup> ou ordem de adição das espécies reativas <sup>54</sup> também podem influenciar no processo. Portanto, como são muitas variáveis, o sistema torna-se muito atrativo sob o ponto de vista da pesquisa científica, pois embora exista uma certa dificuldade na reprodutibilidade dos materiais, justamente pela dificuldade de manutenção das condições de síntese, a variação de qualquer uma dessas condições resulta em alterações nas propriedades finais dos materiais obtidos. Assim, a combinação dessas variáveis projeta para o futuro, a possibilidade de se arquitetar materiais com características específicas tais como: área superficial, grau de incorporação orgânica, forma e tamanho de poros, tipo de interface entre as componentes etc.

### 1.1.3 - Etapas do Processo Sol-Gel

Basicamente as etapas envolvidas no processo sol-gel convencional são três: a) gelatinização/polimerização; b) envelhecimento; c) secagem.

#### 1.1.3.1. - Gelatinização/Polimerização

A etapa de gelatinização ou polimerização envolve as reações de hidrólise e condensação, e tem por finalidade formar o gel. Consiste na transformação de uma suspensão coloidal em um gel, pelo estabelecimento de ligações entre as partículas ou entre as espécies moleculares para a formação de uma rede tridimensional. Durante esta transição, o sistema inicialmente viscoso, adquire um caráter elástico. Os aspectos envolvidos nesta transição podem ser descritos a partir da termodinâmica dos fenômenos críticos e dos modelos cinéticos de crescimento e agregação. <sup>3-4,6,12</sup>

A formação do gel se dá a partir dos agregados de partículas formados durante a etapa de hidrólise e condensação, que crescem em tamanho devido as colisões que levam à formação de ligações em ponte entre ligantes oxo, hidroxilo ou alcóxidos residuais. <sup>3-4,6,12</sup>

O ponto de gel, pode ser facilmente observado através do rápido aumento na viscosidade do sol, mas medi-lo com precisão é extremamente difícil.

O tempo de gelatinização normalmente é medido através de valores de viscosidade. Dependendo das condições de síntese, o tempo de gelatinização pode variar de segundos a meses.<sup>12</sup>

### **1.1.3.2 - Envelhecimento**

Define-se o tempo de envelhecimento do gel como sendo o tempo estabelecido entre o ponto de gelatinização e a remoção do solvente. O envelhecimento é uma etapa também muito importante pois permite uma variedade de mudanças no gel. O favorecimento no grau de intensidade destas mudanças pode ser feito a partir do controle da temperatura e do tempo de envelhecimento permitindo, portanto, monitorar propriedades de interesse.<sup>54-56</sup>

Como mudanças passíveis de ocorrerem nesta etapa estão: a) *polimerização*: aumento da conectividade por reações de condensação, ou por hidrólises adicionais e/ou reesterificação; b) *sinerese*: encolhimento ou contração do gel resultando na expulsão de líquidos dos poros; c) *coalescência/crescimento*: aumento do tamanho de poro com decréscimo de área; d) *segregação*: separação de fase ou cristalização.<sup>4,12</sup>

### **1.1.3.3 – Secagem**

A etapa de secagem consiste na remoção do líquido intersticial dos géis. Um problema encontrado no processo sol-gel é o aparecimento de trincas durante a secagem devido ao *stress* causado principalmente pela ação de forças capilares associadas com a interface líquido-vapor presentes nos poros dos géis<sup>4,6,12,58-60</sup>.

Uma das maneiras de atenuar estas forças de capilaridade tem sido o uso de aditivos químicos controladores de secagem (*DCCAs*). Os *DCCAs* como por exemplo, dimetilformamida, modificam a tensão intersticial do líquido e ajudam a aumentar o tamanhos dos poros<sup>61-62</sup>. Podem também atuar como catalisadores, propiciando o crescimento da rede durante o envelhecimento, aumentando assim a resistência mecânica do gel.

A secagem pode ser realizada através da evaporação do solvente à temperatura ambiente ou em condições supercríticas de temperatura e pressão. Nestes dois casos, os materiais resultantes apresentam propriedades distintas.

Em condições normais de temperatura e pressão, o material resultante é denominado de xerogel ou ambigel. Geralmente estes materiais caracterizam-se por serem pouco porosos e de alta densidade.<sup>4,12</sup>

O método de secagem em condições supercríticas, consiste basicamente no tratamento do gel em um autoclave, sob condições críticas em presença de CO<sub>2</sub>, N<sub>2</sub>O, EtOH, etc. Os materiais obtidos por este processo são chamados de aerogéis e são geralmente porosos, com baixa densidade e grandes áreas superficiais.

A secagem supercrítica também serve para evitar o problema das trincas, pois elimina a interface líquido/vapor pelo aquecimento do gel sob pressão acima da pressão e temperatura crítica do solvente. Neste caso, não havendo diferenças entre as interfaces vapor/sólido e líquido/sólido, não há tensões capilares.<sup>4</sup>

## **1.2 - MATERIAIS HÍBRIDOS ORGANO-INORGÂNICOS**

Materiais híbridos organo-inorgânicos têm despertado grande interesse no meio científico nos últimos anos<sup>63</sup>. A ampla potencialidade de aplicação, bem como as inúmeras possibilidades de preparação de materiais multifuncionais com propriedades distintas e em muitos casos superior àquelas obtidas com o material na sua forma pura, tem colocado esta classe de sólidos numa posição de destaque dentro da área da ciência dos materiais<sup>64-65</sup>. Os materiais híbridos surgem como uma alternativa no sentido de suprir às limitações dos materiais convencionais, ou seja, materiais orgânicos e inorgânicos na sua forma pura<sup>66-67</sup>.

Híbridos organo-inorgânicos são formados pela combinação dos componentes orgânico e inorgânico, geralmente através de uma relação de sinergismo, originando um único material com características diferenciadas daquelas que lhe deram origem<sup>68-69</sup>. As propriedades adquiridas pelo material híbrido são resultantes da soma das contribuições individuais de seus constituintes como também da natureza química dos segmentos orgânicos e inorgânicos<sup>69-72</sup>.

Materiais híbridos organo-inorgânicos de um modo geral, podem ser divididos em duas classes principais:

- *Classe I:* Onde a natureza química da interface orgânica-inorgânica é predominantemente interações. Materiais híbridos desta classe, podem ser preparados pela mistura homogênea de uma fase orgânica com precursores inorgânicos em um solvente comum. Durante a hidrólise e

condensação do precursor inorgânico, a fase orgânica permanece dispersa no meio, aprisionando-se nos vazios da rede inorgânica à medida que esta vai crescendo, Figura 1. Neste caso, as interações entre as componentes orgânica e inorgânica dá-se principalmente através interações do tipo van der Waals e ligações de hidrogênio<sup>69-70</sup>.

Uma outra forma de se obter híbridos desta natureza, é através da policondensação da fase inorgânica em presença de orgânicos não hidrolisáveis, ou seja não reativos. A fase orgânica fica aprisionada nos vazios da rede após remoção do solvente. A imobilização de moléculas orgânicas (enzimas, proteínas, corantes etc.), na rede inorgânica, é feita preferencialmente através desse método<sup>73-76</sup>.

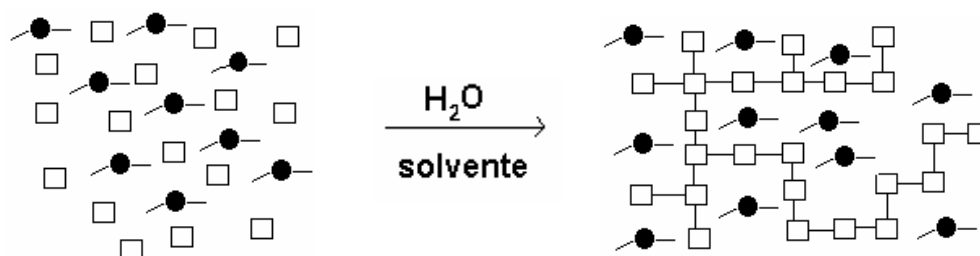


Figura1: Componente orgânico (-●-) imobilizada na rede inorgânica (-λ-λ-λ) preparada via sol gel, a partir de precursores inorgânicos (-λ-)

• *Classe II:* Onde a natureza química da interface é predominantemente covalente. Neste tipo de híbrido, as componente estão ligadas fortemente entre si. Híbridos dessa classe podem ser preparados pela reação entre um precursor inorgânico,  $\text{Si}(\text{OR})_4$ , e um precursor molecular orgânico, contendo grupos hidrolisáveis,  $\text{R}'\text{-Si}(\text{OR})_3$ , conforme Figura 2.<sup>69-70</sup>

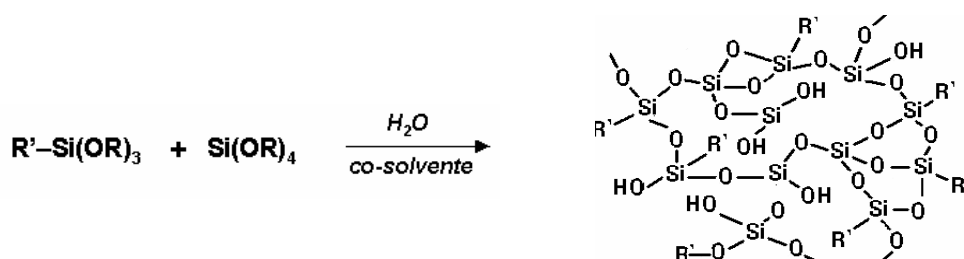


Figura 2: Representação de um material híbrido organo-inorgânico contendo ligações covalentes entre as fases.

Os híbridos sintetizados e estudados no presente trabalho são da Classe II. Existe ainda uma terceira classe de materiais híbridos que são formado pela combinação destas duas classes. Nesse caso, é necessário que o precursor molecular contenha grupos alcoxilanos,  $R'-(\text{SiOR})_3$  hidrolisáveis e grupos aceptores de hidrogênio, como por exemplo,  $R'= \text{RCO}$ . Nessa classe de híbridos existe uma interface covalente como também por pontes de hidrogênio. Abaixo está ilustrado uma híbrido dessa classe <sup>69-70,77</sup>.

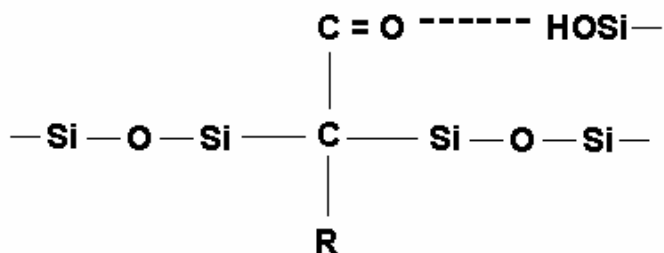


Figura 3. Híbrido orgâno-inorgânico formado por ligações covalentes e de hidrogênio

### 1.2.1 - Aplicações de Materiais Híbridos Organo-Inorgânicos

Conforme já relatado anteriormente, neste texto, materiais híbridos organo-inorgânicos preparados através do processo sol-gel, têm se tornado um atrativo campo de estudos devido principalmente às propriedades destes materiais.

A versatilidade do processo sol-gel permite controlar, nos materiais híbridos, o grau de incorporação orgânica, além das propriedades físicas como área superficial, distribuição do tamanho de poros, tamanho de partículas, etc., o que propicia a estes materiais uma considerável potencialidade de aplicação. Um exemplo disso, é o número crescente de artigos publicados nos últimos anos descrevendo a sua utilização na separação de gases <sup>78</sup>, como carreadores de fármacos <sup>79</sup>, materiais de revestimento <sup>80</sup>, componentes ópticos <sup>81-82</sup>, em fases estacionárias para cromatografia <sup>83-84</sup>, catálise <sup>85-86</sup> adsorventes <sup>87-88</sup>, como sensores <sup>89-90</sup>, em processos eletroquímicos <sup>91</sup> etc.

### 1.3 - MOTIVAÇÃO PARA A REALIZAÇÃO DESSE TRABALHO

A preparação de materiais através do método sol-gel de síntese é simples e conhecido. Entretanto, o mesmo não se pode dizer a respeito dos mecanismos químicos envolvidos no

processo sol-gel. Embora significativos avanços no sentido de melhor compreender a química do processo sol-gel tenha sido possível, questões inerentes ao mecanismo das reações entre as espécies moleculares e os processos cinéticos e termodinâmicos dessas reações não estão totalmente esclarecidas. Isto deve-se às inúmeras possibilidades de ocorrência de reações químicas paralelas, bem como a complexidade dos mecanismos envolvidos durante a transição sol-gel. Como já discutido, a sensibilidade das reações químicas frente a pequenas variações nas condições experimentais de síntese, tem sido um fator motivador da investigação do processo sol-gel. Adicionalmente, na abordagem de materiais híbridos, tem-se uma quantidade maior de constituintes no sistema, o que o torna extremamente rico e fascinante sob o ponto de vista da pesquisa científica básica.

É importante ressaltar que mesmo após decorridos anos de estudos sobre o processo sol-gel, a produção em escala industrial dos materiais oriundos desse processo ainda não tem sido possível, justamente devido às dificuldades na reprodutibilidade das propriedades dos materiais resultantes.

A despeito destes fatos, fica evidente a necessidade de dilatar o conhecimento e o entendimento em todas as etapas envolvidas no processo sol-gel, e isso somente será possível conhecendo-se inicialmente a influência das variáveis de síntese nas propriedades finais desses materiais. É justamente neste contexto que o presente trabalho se insere.

O conhecimento preciso de todas as etapas envolvidas no processo sol-gel, bem como a influência de todas as variáveis de síntese, permitirá talvez, que no futuro possamos teoricamente arquitetar com precisão os processos de síntese visando propriedades finais dos materiais híbridos.

A imobilização de espécies orgânicas como anilina na matriz de sílica, tem se tornado um campo de estudos bastante interessante. Estes sistemas que contêm anéis aromáticos apresentam interações do tipo  $\pi$ - $\pi$ , como também propriedades cromóforas. Portanto, estes materiais podem apresentar importantes propriedades adsorventes e ópticas.

## **1.4. - INTRODUÇÃO ÀS TÉCNICAS DE CARACTERIZAÇÃO UTILIZADAS NESTE TRABALHO**

### **1.4.1 - Medida da Área Superficial pelo Método BET**

O método BET, homenagem a Brunauer, Emmet e Teller <sup>92-93</sup>, consiste na determinação do volume de gás adsorvido em uma monocamada a partir da isoterma de

adsorção física, obtida à temperatura de ebulição desse gás. Geralmente usa-se N<sub>2</sub> como gás sonda.

A isoterma de BET é regida pela equação abaixo:

$$\frac{P}{V (P_0 - P)} = \frac{1}{V_m \cdot C} + \frac{(C - 1) P}{(V_m \cdot C) P_0}$$

onde V é o volume total de gás adsorvido, V<sub>m</sub> é o volume da monocamada, e c é definido como  $\exp(Q-L)/RT$ , onde Q é o calor de adsorção das moléculas da monocamada, L o calor latente de condensação do gás, R é a constante dos gases, T a temperatura absoluta, P<sub>0</sub> é a pressão inicial do gás e P é a pressão de equilíbrio.

Geralmente são obtidos de quatro a cinco pontos entre P/P<sub>0</sub> de 0 até 0,35. O gráfico P/V (P<sub>0</sub>-P) em função de P/P<sub>0</sub> resulta em uma reta. A partir dos valores dos coeficientes linear e angular da reta, a e b, respectivamente, calcula-se a área superficial usando-se a Equação abaixo.

$$S_{\text{BET}} = [1/(a+b)] N a_m$$

onde S<sub>BET</sub> é a área superficial, N o número de Avogadro e a<sub>m</sub> a área da molécula sonda, no caso de N<sub>2</sub>, 0,162 nm<sup>2</sup>.

### 1.4.2 - Espectroscopia no Infravermelho

A espectroscopia no infravermelho ou vibracional é uma importante técnica para identificação molecular. O espectro vibracional envolve: a) *estiramentos*, que são movimentos ao longo do eixo de uma ligação covalente; b) *deformação angular*, que consiste na variação do ângulo de ligações e c) modos de combinações de deformação molecular, que envolvem tanto deformações angulares como estiramentos. Essas últimas especialmente importantes no caso de anéis aromáticos. O espectro vibracional molecular poderá ser observado no infravermelho sempre que a vibração resultar em variação no momento dipolar molecular. A energia da absorção dependerá da natureza da ligação química molecular e das massas reduzidas dos átomos constituintes.



As frequências de absorção ou bandas, são registradas em um gráfico de absorbância vs número de onda ( $1/\lambda$ ). Como determinadas espécies moleculares apresentam bandas características e considerando que a área sob essas bandas são proporcionais à concentração dessas espécies, é possível não apenas identificá-las, como também quantificá-las.<sup>94</sup>

### **1.4.3 - Análise Termogravimétrica (TGA):**

Essa técnica de análise se baseia na perda de massa da amostra em função do aumento planejado de temperatura. Essa técnica permite a visualização de processos endotérmicos que envolvem perda de massa, como dessorção de água da superfície, sinterização e pirólise orgânica.<sup>95</sup>

### **1.4.4 - Análise do Tamanho de Poros**

#### **1.4.4.1 Análise de Poros Totais:**

Duas técnicas foram empregadas na determinação do tamanho de poros dos xerogéis. A técnica de Espalhamento de Raios-x a Baixos Ângulos (SAXS)<sup>96</sup> e a técnica de Espectroscopia de Aniquilação de Pósitrons (PALS)<sup>97-98</sup>. Ambas técnicas estão baseadas no fato de que a matriz porosa apresenta regiões distintas de densidade eletrônica entre os poros e a rede sólida. Na análise por espalhamento de raios-x a baixos ângulos a heterogeneidade na densidade eletrônica da matriz sólida produz um espalhamento de luz que pode ser descrito pela lei de Guinier. Esta lei estabelece que a intensidade de espalhamento  $I(h)$  é descrita por  $\ln I(h) = \ln I_0 - (R_G^2 h^2) / 3$ , onde  $R_G$  é o raio de giro e  $h = (4\pi \sin\theta) / \lambda$ , sendo  $\theta$  ângulo de espalhamento e  $\lambda$  o comprimento de onda usado. O raio de giro pode ser calculado pela equação  $R_G = (3p)^{1/2}$ , onde  $p$  é a inclinação do gráfico de Guinier ( $\ln I(h)$  vs  $h^2$ ).

No caso da espectroscopia de aniquilação de pósitrons o raio de giro é proporcional ao tempo de meia-vida dos pósitrons trapeados nos poros. Quanto maior o tamanho dos poros maior será o tempo de meia-vida.

Se for considerado que os poros são esféricos o raio do poro pode ser calculado aplicando-se a Equação:

$$R_p = (5/3)^{1/2} R_G$$

#### **1.4.4.2 - Análise de Poros Abertos**

Os porosidade devida a poros abertos foi determinada usando-se dados obtidos a partir de isotermas de adsorção e dessorção de nitrogênio<sup>99</sup>. O tratamento de dados foi baseado no método BJH (Barret, Joiner e Halenda)<sup>100</sup> que utiliza a Equação de Kelvin, que no caso de nitrogênio, pode ser escrita como:

$$d = 0,830 / (\log (P_o / P))$$

sendo  $d$  o diâmetro de poros esféricos em nanômetros para uma dada região de  $P/P_o$ . Considerando que a pressão de dessorção é sempre menor que a de adsorção e sendo  $\Delta G$  expresso pela Equação  $\Delta G = RT (\ln P - \ln P_o)$ , onde  $P$  é a pressão de adsorção ou dessorção, tem-se que para uma mesma quantidade de nitrogênio,  $\Delta G$  será sempre menor na dessorção. Assim, a curva de dessorção é mais adequada para o cálculo da distribuição de poros. A equação pode ser aplicada para materiais mesoporosos (diâmetros entre 2 e 50 nm) no intervalo de  $P/P_o$  de 0,5 até 1,0.

#### **1.4.5 - Microscopia Eletrônica de Varredura (SEM)**

A análise por microscopia eletrônica de varredura consiste na varredura de pontos da amostra com um feixe de elétrons de alta energia. Dessa interação surgem os elétrons secundários (choques inelásticos), que são originados abaixo da superfície da amostra a partir das interações do feixe eletrônico com os elétrons das camadas mais externas dos átomos. Esses elétrons apresentam energia menor que 50 eV e portanto, têm dificuldade de sair do material. Por esse motivo, a análise tem uma profundidade máxima de 50 nm. Entretanto, como os elétrons secundários provem de uma zona reduzida (pontual), eles permitem uma boa resolução para imagens de grande aumento.

Todos os elétrons com energia maior que 50 eV são considerados elétrons retroespalhados do feixe original. Como o espalhamento eletrônico depende do número atômico dos elementos constituintes da amostra, é possível efetuar a análise elementar da amostra, a partir da análise dos elétrons retroespalhados. Essa análise é chamada de espectroscopia de elétrons retroespalhados ou *EDS (energy dispersive spectroscopy)*.<sup>101</sup>

## **2. OBJETIVOS**

O presente trabalho tem como objetivo básico contribuir para uma melhor compreensão do processo sol-gel, auxiliando na definição de estratégias que permitam a obtenção de materiais que combinem propriedades que os tornem de interesse científico e tecnológico.

Entre os objetivos gerais deste trabalho estão:

- Obter o híbrido organo-inorgânico anilina-propilsilica através do processo sol-gel;
- Caracterizar o híbrido anilina-propilsilica;
- Estudar a influência de algumas variáveis tais como temperatura de gelatinização, natureza e concentração de catalisador, quantidade de precursor orgânico adicionado, nas características finais do híbrido;
- Investigar a potencialidade de aplicação do híbrido anilina-propilsilica na adsorção de alguns cátions metálicos de interesse ambiental.

### 3. REFERÊNCIAS BIBLIOGRÁFICAS

1. Zarzycki, J.; *J. Sol-Gel Sci Technol.* **1997**, *8*, 17
2. Livage, J.; *Current Opinion in Solid State & Materials Science* **1997**, *2*, 132
3. Hiratsuka, R.S.; Santilli, C.V.; Pulcinelli, S.H.; *Quím. Nova* **1995**, *18*, 171
4. Brinker, C.J.; Scherer, G.W.; *Sol-Gel Science*, Academic Press; London, **1990**
5. Makenzie, J.D.; *Ceramic Trans.* **1995**, *55*, 25
6. Lev, O.; Tsionsky, M.; Rabinovich, L.; Glezer, V.; Sampath, S.; Pankratov, I.; Gun, J.; *Anal. Chem.* **1995**, *67*, 22 A
7. Muller, C.A.; Maciejewski, M.; Mallat, T.; Baiker, A.; *J. Catal.* **1999**, *184*, 280
8. Collinson, M.M.; *Critical Rev. Anal. Chem.* **1999**, *29*, 289
9. Makote, R.; Collison, M.M.; *Anal. Chim. Acta* **1999**, *394*, 195
10. Muñoz-Aguado, M.J.; Gregorkiewitz, M.; *J. Membrane Sci.* **1996**, *111*, 7
11. Livage, J.; Henry, H.; Sanchez, C.; *Progr. Solid State Chem.* **1988**, *18*, 259
12. Hench, L.L.; West, J.K.; *Chem. Rev.* **1990**, *90*, 33
13. Schubert, U., Hüsing, N., Lorenz, A.; *Chem. Mater.* **1999**, *11*, 2796
14. Corriu, R.J.P.; Leclereq, D.; *Angew. Chem. Int. Ed. Engl.* **1996**, *35*, 1421
15. Brinker, C.J.; Scherer, G.W.; *J Non-Cryst. Solids* **1985**, *70*, 304
16. Brinker, C.J.; *J Non-Cryst. Solids* **1988**, *100*, 31
17. Buckley, A. M.; Greenblatt, M.; *J. Chem. Education* **1994**, *71*, 599
18. Tigner, I.C., Fischer, P.; Bohnem, F.M.; Rehage, H.; Maier, W.F.; *Microporous Mater.* **1995**, *5*, 77
19. Cerveau, G.; Corriu, R.J.P.; Framery, E.; *Polyhedron* **2000**, *19*, 313
20. Ballard, R.L.; Tuman, S.J.; Fouquette, D.J.; Stegmiller, W.; Soucek, M.D.; *Chem. Mater.* **1999**, *11*, 726
21. Asomoza, M.; Domínguez, M.P.; Solís, S.; Lara, V.H.; Bosch, P.; López, T.; *Mater. Letters* **1998**, *36*, 249
22. Ro, J.C.; Chung, I.J.; *J. Non-Cryst. Solids* **1991**, *130*, 8
23. Silva, C.R.; Airoidi, C.; *J. Coll. Interf. Sci.* **1997**, *195*, 381
24. Xi, Y.; Liangying, Z.; Sasa, W.; *Sensors Actuators B* **1995**, *24-25*, 347

25. Izutsu, H.; Mizukami, F.; Sashida, T.; Maeda, K.; Kiyozumi, Y.; Akiyama, Y.; *J. Non-Cryst. Solids* **1997**, *212*, 40
26. Nakamura, H.; Matsui, Y.; *J. Am. Chem. Soc.* **1995**, *117*, 2651
27. Vasconcelos, D.C.L.; Campos, W.R.; Vasconcelos, V.; Vasconcelos, W.L.; *Mater. Sci. Eng. A* **2002**, *334*, 53
28. Nassar, E.J.; Neri, C.R.; Calefi, P.S.; Serra, O. A.; *J. Non-Cryst. Solids* **1999**, *247*, 124
29. Yan, Y.; Hoshino, Y.; Duan, Z.; Chaudhuri, S.R.; Sarkar, A.; *Chem. Mater.* **1997**, *9*, 2583
30. Meixner, D.L.; Dyer, P.N.; *J. Sol-Gel Sci Technol.* **1999**, *14*, 223
31. Tian, D.; Blacher, S.; Jerome, R.; *Polymer* **1999**, *40*, 951
32. Cerveau, G.; Corriu, R.J.P.; Framery, E.; *J. Mater. Chem.* **2000**, *10*, 1617
33. Lee, B.I.; Chou, K.; *J. Mater. Sci.* **1996**, *31*, 1367
34. Dubois, G.; Corriu, R.J.P.; Reyé, C.; Brandès, S.; Denat, F.; Guillard, R.; *Chem. Comm.* **1999**, 2283
35. Nakanishi, K.; Soga, N.; *Bull. Chem. Soc. Jpn.* **1997**, *70*, 587
36. Misheva, M.; Djourellov, N.; Margaca, F.M.A.; Salvado, I.M.M.; *J. Non-Cryst. Solids* **2001**, *279*, 196
37. Meixner, D.L.; Gilicinski, A.G.; Dyer, P.N.; *Langmuir* **1998**, *14*, 3202
38. Chu, L.; Tejedor-Tejedor, M.I.; Anderson, M.A.; *Microporous Mater.* **1997**, *8*, 207
39. Muñoz-Aguado, M.J.; Gregorkiewitz, M.; Bermejo, F.J.; *J. Non-Cryst. Solids* **1995**, *189*, 90
40. Korteso, P.; Ahola, M.; Kangas, M.; Jokinen, M.; Leino, T.; Vuorilehto, L.; Laakso, S.; Kiesvaara, J.; Yli-Urpo, A.; Marvola, M.; *Biomaterials* **2002**, *23*, 2795
41. Yin, R.; Ottenbrite, R.M.; Siddiqui, J. A.; *Polymer Bulletin* **1997**, *38*, 23
42. Hüsing, N.; Schubert, U.; Mezei, R.; Fratzl, P.; Riegel, B.; Kiefer, W.; Kohler, D.; Mader, W.; *Chem. Mater.* **1999**, *11*, 451
43. Rodríguez, S.A.; Colón, L.A.; *Chem. Mater.* **1999**, *11*, 754
44. Ben, F.; Boury, B.; Corriu, R.J.P.; Le Strat, V.; *Chem. Mater.* **2000**, *12*, 3249
45. Peeters, M.P.J.; Bernards, T.N.M.; Van Bommel, M. J.; *J. Sol-Gel Sci Technol.* **1998**, *13*, 71
46. Deshpande, R.; Hua, D.W.; Smith, D.M.; Brinker, C.J.; *J. Non-Cryst. Solids* **1992**, *144*, 32
47. Wang, R.; Geiger, C.; Chen, L.; Swanson, B.; Whitten, D.G.; *J. Am. Chem. Soc.* **2000**, *122*, 2399
48. Boury, B.; Corriu, R.J.P.; Nuñez, R.; *Chem. Mater.* **1998**, *10*, 1795

49. Pereira, J.C.G.; Catlow, C.R.A.; Price, G.D.; *J. Phys. Chem. A* **2002**, *106*, 130
50. Xenopolous, C.; Mascia, L.; Shaw, S.J.; *Mater. Sci. Eng. C* **1998**, *6*, 99
51. Valenzuela, M.A.; Téllez, L.; Bosch, P.; Balmori, H.; *Mater. Letters* **2001**, *47*, 252
52. Huang, W.L.; Cui, S.H.; Liang, K.M.; Gu, S.R.; Yuan, Z.F.; *J. Coll. Interf. Sci.* **2002**, *246*, 129
53. Kim, K.; Kim, J., Kim, W.; *J. Mater. Res.* **2001**, *16*, 545
54. Deng, G.; Markowitz, M.A.; Kust, P.R., Gaber, B.P.; *Mater. Sci. Eng. C* **2000**, *11*, 165
55. Takahashi, R.; Nakanishi, K.; Soga, N.; *J. Non-Cryst. Solids* **1995**, *189*, 66
56. Scherer, G.W.; Haereid, S.; Nielsen, E.; Einarsrud, M.; *J. Non-Cryst. Solids* **1996**, *202*,42
57. Cerveau, G.; Corriu, R.J.P.; Framery, E.; *J. Mater. Chem.* **2001**, *11*, 713
58. Smith, D.M.; Scherer, G.W.; Anderson, J.M.; *J. Non-Cryst. Solids* **1995**, *188*, 191
59. Scherer, G.W.; *J. Non-Cryst. Solids* **1997**, *215*, 155
60. Caddock, B.D.; Hull, D.; *J. Mater. Sci.* **2002**, *37*, 825
61. Viart, N.; Niznansky, N.; Rehspringer, J.L.; *J. Sol-Gel Sci. Technol.* **1997**, *8*, 103
62. Lenza, R.F.S.; Vasconcelos, W.L.; *Quím. Nova* **2002**, *25*, 893
63. Judeinstein, P.; Sanchez, C.; *J. Mater. Chem.* **1996**, *6*, 511
64. Chujo, Y.; *Current Opinion in Solid State & Mater. Sci.* **1996**, *1*, 806
65. Schottner, G.; *Chem. Mater.* **2001**, *13*, 3422
66. Yamada, N.; *J. Mater. Sci.* **2002**, *37*
67. Sarwar, M.I.; Ahmad, Z.; *European Polym. J.* **2000**, *36*, 89
68. Schmidt, H.; *J. Sol-Gel Sci. Technol.* **1994**, *1*, 217
69. Kickelbick, G. Ben, F.; Boury, B.; Corriu, R.J.P.; Le Strat, V.; *Chem. Mater.* **2000**, *12*, 3249
70. Novak, B.M.; *Adv. Mater.* **1993**, *6*, 422
71. Loy, D.A.; Shea, K.J.; *Chem. Rev.* **1995**, *95*, 1431
72. Cerveau, G.; Corriu, R.J.P.; Framery, E.; *Chem. Mater* **2001**, *13*, 3373
73. Altstein, M.; Bronshtein, A.; Glatstein, B.; Zeichner, A.; TamirI, T.; Almong. J.; *Anal. Chem.* **2001**, *73*, 2461
74. Dunn, B.; Miller, J.M.; Dave, B.C.; Valentine, J.S.; Zink, J.I.; *Acta Mater* **1998**, *46*, 737
75. Levy, D.; *Chem. Mater.* **1997**, *9*, 2666
76. Avnir, D.; Braun, S.; Lev, O.; Ottolenghi, M.; *Chem. Mater.* **1994**, *6*,1605
77. Chan, C.; Peng, S.; Chu, I.; NI, S.; *Polymer* **2001**, *42*, 4189

78. Okui, T.; Soito, Y.; Okubo, T.; Sadakata, M.; *J. Sol-Gel Sci Technol* **1995**, 5, 127
79. Kortesuo, P.; Ahola, M.; Karlsson, S.; Kangasniemi, I.; Yli-Urpo, A.; Kiesvaara, J.; *Biomaterials* **2000**, 21, 193
80. Choy, T.P.; Chandrasekaran, C.; Limmer, S.J.; Seraji, S.; Wu, Y.; Forbess, M.J.; Nguyen, C.; Cao, G.Z.; *J. Non-Cryst. Solids* **2001**, 290, 153
81. Levy, D.; Esquivias, L.; *Adv. Mater.* **1995**, 7, 120
82. Corriu, R.J.P.; Hesemann, P.; Lanneau, G.F.; *Chem. Comm.* **1996**, 1845
83. Guo, Y.; Colón, L.A.; *Anal. Chem.* **1995**, 67, 2511
84. Cichna, M.; Knopp, D.; Niessner, R.; *Anal. Chim. Acta* **1997**, 339 241
85. Wight, A. P.; Davis, M.E.; *Chem. Rev.* **2002**, 102, 3589
86. Lu, Z.; Lindner, E.; MAYER, H.; *Chem. Rev.* **2002**, 102, 3543
87. Brown, J.; Mercier, L.; Pinnavaia, T.J.; *Chem. Comm* **1999**, 69
88. Farias, R.F.; Souza, A. G.; Nunes, L.M.; Cardoso, V. DE A.; *Coll. and Surf. A: Physicochem. Eng. Aspects* **2002**, 1-4
89. Bescher, E.; Mackenzie, J.D.; *Mater. Sci. and Eng. C* **1998**, 6, 145
90. Wang, J.; *Anal. Chim. Acta* **1999**, 399, 21
91. Walcarius, A.; *Chem. Mater.* **2001**, 13, 3351
92. Sink, K.S.W, Everett, D.H.; Haul, R.A.W.; Moscou, L.; Pierotti, R. A.; Rouquérol, J.; Siemieniewska, T.; *Pure & Appl. Chem.* **1985**, 57, 603
93. Sing, K.S.W.; *Adv. Coll. Interf. Sci.* **1998**, 76, 3
94. Barbara Stuart, Bill George And Peter McIntyre, *Modern Infrared Spectroscopy* , John Wiley & Sons Ltda, **1998**
95. Charles M. Earnest, *Compositional Analysis by Thermogravimetry*, ASTM, **1988**
96. O. Glater And O Kratky, *Small Angle X-Ray Scattering*, Academic Press, **1982**
97. Dull, T.L.; Frieze, W.E.; Gidley, D.W.; *J. Phys. Chem. B* **2001**, 105, 4657
98. Barros De Souza, E.M.; Magalhães, W.F.; Mohallem, N.D.S.; *J. Phys. Chem. Solids* **1999**, 60, 211
99. S.J. Gregg, K.S.W. Sing, *Adsorption Surface Area and Porosity*, Academic Press, New York, **1982**
100. Barret, E.P.; Joyner, L.G.; Halenda, P.P.; *J. Am. Chem. Soc.* **1951**, 73, 373
101. H. Kesttembach, W.J.B Filho, *Microscopia Eletrônica de Transmissão e Varredura*. Associação Brasileira de Metais **1994**.

## **4. ARTIGOS**

### **ANEXO 1**

**4.1- F. A. Pavan, S. Leal, T. M. H. Costa, Y. Gushiken and E. V. Benvenuti.**  
**A Sol-Gel Synthesis for Thermally Stable Aniline/ Silica Material. *Journal of Sol-Gel Science and Technology* 23, 129-133, 2002**



## **A Sol-Gel Synthesis for Thermally Stable Aniline/Silica Material.**

Flávio A. Pavan, Sheila Leal, Tania M. H. Costa,\* Edilson V. Benvenutti\*  
LSS, Instituto de Química, UFRGS, CP 15003, 91501-970, Porto Alegre, RS,  
Brazil.

Yoshitaka Gushikem

Instituto de Química, Unicamp, CP 6154, 13083-970 Campinas, SP, Brazil

## **Abstract**

Aniline/silica sol-gel material was obtained. The aniline was immobilized on the silica surface using Chloropropyltrimethoxysilane as bridge reagent. The base activator NaH was used to produce a fast  $SN_2$  reaction between the base and the alkylorganosilane. The resulting modified silica was characterized by elemental analysis and infrared spectroscopy using an oven cell. The organic coverage on the surface was proportional to the organic precursor concentration. The aniline/silica materials are thermally stable up to 300 °C, in high vacuum.

## Introduction

In recent years, organic modification of silica surfaces has been an important method to obtain solids that can be used as sorbent materials for SPE (solid phase extraction) stationary phase and also for chromatographic techniques.[1-4] The growing interest in the modification of silica with organic groups is due to the final properties of these materials. The organic functionalization of silica materials produces mechanical and morphological properties on the silica support, and addition to changing the chemical properties of the organic attached groups. As a result, the chemical behavior can be determined by choosing the organic group that will be immobilized on the silica surface.

Grafting synthesis is a common method used for immobilization of organic groups on the silica surface. This process involves the immobilization of an organic functional group using an organosilane as an intermediate reagent.[3-5] Organosilanes  $Y_3Si-R-X$  are very common agents used in the grafting process,[6-7] Y is usually a halide or alkoxy group, R a linear chain and X a halide group. Using a  $SN_2$  reaction, the immobilization of several amine organic groups, can be achieved and the resulting materials are thermally stable.[1,2,7] However, in this reaction step a very long reaction time is necessary.[7,8] Furthermore, the grafting method has an organic coverage limitation due to the steric effect that is related to the morphological properties of the silica support.

The other possibility to obtain functionalized silicas is the sol-gel method. Over the decade, sol-gel synthesis has been used to obtain inorganic oxide networks,[9-11] More recently, the sol-gel method has been used to make organo-inorganic hybrid materials.[12-15]

This process shows some advantages when compared to the grafting technique since the surface area, particle size and the organic coverage can be controlled. In this work we propose an easy procedure to obtain a thermally stable organic phase attached to the silica gel surface. The aniline immobilization follows the same procedure used in the grafting process. However, the  $\text{SN}_2$  reaction was optimized using NaH as a base activator. The sol-gel material obtained was very thermally stable up to 300 °C, in vacuum.

## **Experimental**

### ***Reagents and Solutions used are:***

Sodium hydride (NaH; Merck 60%), tetraethylorthosilicate (TEOS; Merck 99.8%), 3-Chloropropyltrimethoxysilane ( $(\text{CH}_3\text{O})_3\text{Si}(\text{CH}_2)_3\text{Cl}$ ; Merck), hydrofluoric acid (Merck; 48%), aniline (Merck; 99%). All dried solvents are analytical grade, and twice distilled water was used.

### ***Synthesis of Aniline/silica Materials***

Aniline was activated with sodium hydride in 10 mL of aprotic solvent mixture (toluene : thf) (1:1) for 30 minutes, and the  $(\text{CH}_3\text{O})_3\text{Si}(\text{CH}_2)_3\text{Cl}$  was added. The quantities of aniline, NaH and  $(\text{CH}_3\text{O})_3\text{Si}(\text{CH}_2)_3\text{Cl}$  were stoichiometric at the concentration range from 0.08 to 0.80 mol.L<sup>-1</sup>. The mixture was stirred under argon at solvent-reflux temperature during a period time of 1 to 10 hours. The solution was then centrifuged, to eliminate the byproduct sodium chloride. After that, TEOS (5 mL), ethyl alcohol (5 mL)

and HF (1.7 mL, 6 %) were added, under stirring. The mixture was stored for 5 days, at room temperature, just covered without sealing, for gelation and solvents evaporation. The solids were then extensively washed with toluene, THF, acetone, ethyl alcohol and distilled water. Finally the materials were dried for 30 minutes in an oven at 100 °C. The dried gel was comminuted in an agate mortar for subsequent analysis.

### ***Infrared analysis***

Self-supporting disks of the material (100 mg) were prepared, with an area of 5 cm<sup>2</sup>, weighing *ca.* 100 mg. The disks were heated to temperatures ranging from 100 to 400 °C, under vacuum (10<sup>-3</sup> Torr), for 1 hour, using an IR cell.[7] An additional analysis was made heating the disk at 400 °C for 6 hours. The self-supporting disks were analyzed in the infrared region using a Shimadzu FTIR, model 8300. The spectra were obtained with a resolution of 4 cm<sup>-1</sup>, with 100 scans.

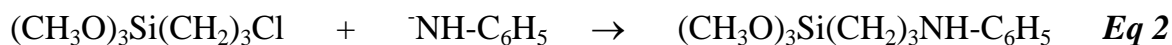
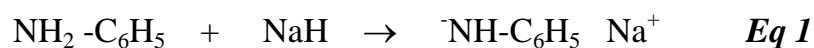
### ***Elemental Analysis***

The organic groups grafted on the silica gel surface were analyzed, in triplicate, using a CHN Perkin Elmer M CHNS/O Analyzer, 2400. The samples were previously heated at 200 °C for 1 hour, in vacuum.

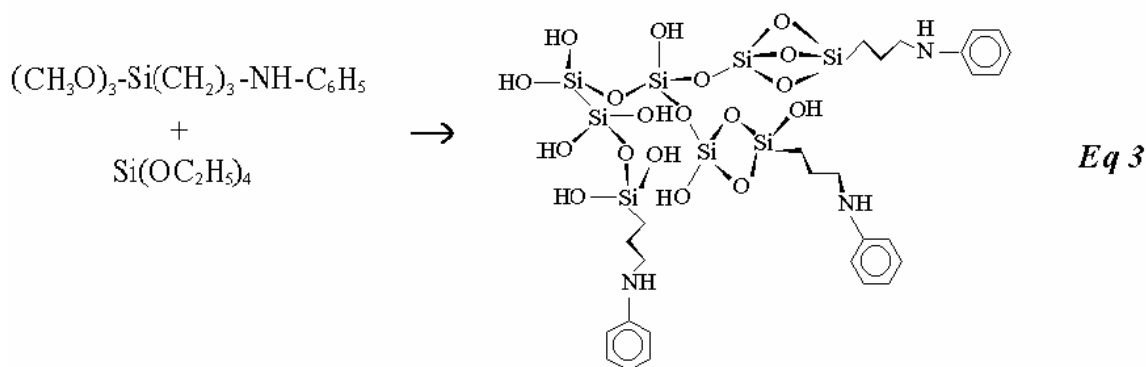
## Results and Discussions

### Synthesis

In the first synthesis step, the  $\text{SN}_2$  reaction between the aniline and  $(\text{CH}_3\text{O})_3\text{Si}(\text{CH}_2)_3\text{Cl}$  was carried out in aprotic solvent mixture toluene-THF, using NaH as base activator as illustrated in Equations 1 and 2.



After the  $\text{SN}_2$  reaction (Equation 2) gelation takes place by the addition of TEOS. The gelation process for aniline/silica material can be described by Equation 3



The influence of the NaH in the kinetics of the  $\text{SN}_2$  reaction was monitored by the analysis of the final organic content of the materials. Although NaH has been used for silica surface activation,[16] to our knowledge, this was the first time it was used as base activator in the  $\text{SN}_2$  reaction for sol-gel synthesis. The use of sodium hydride results in a drastic reduction in the reaction time. The aniline content on the surface is presented

in the Table 1, for materials using NaH in the first step of SN<sub>2</sub> reactions and for materials obtained without NaH. Five hours of reaction with NaH produced higher organic phase content (0.95 mmol.g<sup>-1</sup>) than 50 hours without NaH (0.82 mmol.g<sup>-1</sup>), for precursor concentration of 0.45 mmol.mL<sup>-1</sup>, under the same gelation conditions. The kinetics of this same SN<sub>2</sub> reaction are shown graphically in Figure 1. When NaH was used, the highest organic content was reached after 5 hours. Increasing the precursor concentration to 0.80 mmol.mL<sup>-1</sup>, and assuming the same reaction conditions, we obtain a higher organic content of 1.2 mmol.g<sup>-1</sup> (Table 1). Another advantage of using NaH as a base activator is that the insoluble byproduct NaCl is separated from the organic medium by centrifugation. In the absence of NaH there is a formation of HCl, that reacts with the aniline, resulting in the organic anilinium salt, which is more difficult to separate from the organic medium.[7]

Table 1 and Figure 1

### ***Infrared Analysis***

In this work, *in situ* infrared spectroscopy is a useful tool to clarify how the organic phase is attached. The vibrational modes of aniline aromatic ring at *ca.* 1600 and 1500 cm<sup>-1</sup> are very strong in the spectra (Figure 2). The band area of these absorption modes, for the spectra obtained after thermal treatments at several temperatures, were used to estimate the thermal stability of immobilized aniline on materials, with four different organic contents, and using NaH as base activator. The overtone band of silica at *ca.*1870 cm<sup>-1</sup> was used as a reference band. This normalization was necessary, considering the

heterogeneity in the disks thickness and taking into account the position changes of the infrared beam. The band areas are summarized in Table 2.

Figure 2 and Table 2

For the materials with low organic content (up to  $0.34 \text{ mmol.g}^{-1}$ ), the band areas remain constant up to  $400 \text{ }^\circ\text{C}$  in vacuum, even after 6 hours of treatment (see Table 2). This shows that the aniline groups present in the silica are stable in this temperature range. This fact can be explained by the retention of organic phase in closed silica pores formed during the gelation and drying. However, for the high organic content samples, the band areas remain constant up to  $300 \text{ }^\circ\text{C}$  and decrease significantly after heat treatment at  $400 \text{ }^\circ\text{C}$ . This decreasing is *ca.* 50 % for the sample with  $0.95 \text{ mmol.g}^{-1}$  of organic content and *ca.* 30 % for the sample with  $1.2 \text{ mmol.g}^{-1}$ . This shows that, for the high organic content samples, some fraction part of the organic groups are strongly bonded on the surface and at the same time there are groups retained in the closed pores.

Figure 3

Another evidence that the aniline is strongly bonded to the silica surface is presented in the spectra in Figure 3. The spectrum 3a was obtained for pure aniline, where there are two bands due to the  $\text{NH}_2$  stretching modes. After 5 hours of the  $\text{SN}_2$  reaction between aniline and  $(\text{CH}_3\text{O})_3\text{Si}(\text{CH}_2)_3\text{Cl}$  ( $0.45 \text{ mmol.L}^{-1}$ ) in the presence of NaH, the spectrum of the product exhibits only a stretching band in this region, indicating the presence of NH species. This is



strong evidence that  $\text{SN}_2$  reactions take place, and that covalent bonds between the aniline and the alkylsilane are established, as illustrated by Equations 2.

In this work, organic coverage of aniline on the surface of silica was very extensive, *ca.* three times larger than that obtained by the grafting process.[7,17] In addition it can be easily controlled by the amount of precursor (see Table 1). The organic coverage is related to the sorbent capacity of the stationary phase in SPE (solid phase extraction) or chromatographic columns. Furthermore, it is known that the most densely covered organic phases show better hydrolytic stability.[18,19]

## Conclusions

The sol-gel process can be used in the synthesis of aniline attached to silica surfaces. The thermal stability of organic groups up to 300 °C, in vacuum, indicates that the aniline is covalently bonded to the surface. The organic coverage could be controlled by the adjusting the precursor concentration in the  $\text{SN}_2$  reaction. The use of NaH as base activator in the  $\text{SN}_2$  reaction reduces by a factor of ten the reaction time, compared to that obtained without NaH.

**Acknowledgment:** F. A. P. and S. L. are indebted to CNPq for research grants.

## References

1. Y. Bereznitski, M. Jaroniec *J. Chromatography A* 828, 51 (1998).
2. F. A. Pavan, L. Franken, C. A. Moreira, Y. Gushikem, T. M. H. Costa, E. V. Benvenuti, *J. Coll. Interf. Sci*, in the press.
3. U. Deschler, P. Kleinschmit, P. Panster *Angew. Chem. Int. Ed. Engl.* 25, 236 (1986).
4. A. Gambero, L. T. Kubota, Y. Gushikem, C. Airoidi, J. M. Granjeiro E. M. Taga, E. F. C. Alcantara. *J. Coll. Interf. Sci.*, 185, 313. (1997).
5. C. Perruchot, M. M. Chehimi, D. Mordenti, M. Briand, M. Delamar, *J. Mater. Chem.* 8, 2185 (1998).
6. N. H. Arakaki, C. Airoidi, *Quim. Nova* 22, 2 (1999).
7. J. L. Foschiera, T. M. Pizolatto, E. V. Benvenuti, *J. Braz. Chem. Soc.* 12, 159 (2001).
8. C. R. Silva, I. C. S. F. Jardim, C. Airoidi *HRC - J. High Resol. Chromat.* 22, 103 (1999).
9. L. L. Hench, J. K. West *Chem. Rev.* 90, 33 (1990)
10. M. Palladino, F. Pirini, M. Beghi, P. Chiurlo, G. Cogliati, L. Costa *J. Non-Cryst. Solids* 147, 335 (1992).
11. T. M. H. Costa, M. R. Gallas, E. V. Benvenuti, J. A. H. da Jornada, *J. Non-Cryst. Solids* 220, 195 (1997).
12. N. I. Maliavski, O. V. Dushkin, E. V. Tchekounova, J. V. Markina, G. Scarinci *J. Sol-Gel Sci. Techn.* 8, 571 (1997).
13. H. K. Kim, S. -J. Kang, S. -K. Choi, Y. -H Min, C. -S. Yoon *Chem. Mater.* 11, 779 (1999).
14. N. Hüsing, U. Schubert, R. Mezei, P. Fratzl, B. Riegel, W. Kiefer, D. Kohler, W. Mader *Chem. Mater.* 11, 451 (1999).

15. B. Riegel, W. Kiefer, S. Hofacker, G. Schottner *J. Sol-Gel Sci. Tech.* 13, 385 (1998).
16. B. Lynch, J. D. Glennon, C. Tröltzsch, U. Menyes, M. Pursch, K. Albert *Anal. Chem.* 69, 1756 (1997).
17. W. C. Moreira, Y. Gushikem, *Colloids and Surfaces* 25, 155, (1987).
18. N. Sagliano, T. R. Floyd, R. A. Hartwick, J. M. Dibussolo, N. T. Miller *J. Chromatography* 443, 155 (1988).
19. J. Nawrocki *J. Chromatography* 779, 29 (1997).

Table 1: Organic content on the surface of the sol-gel materials, obtained by elemental analysis.

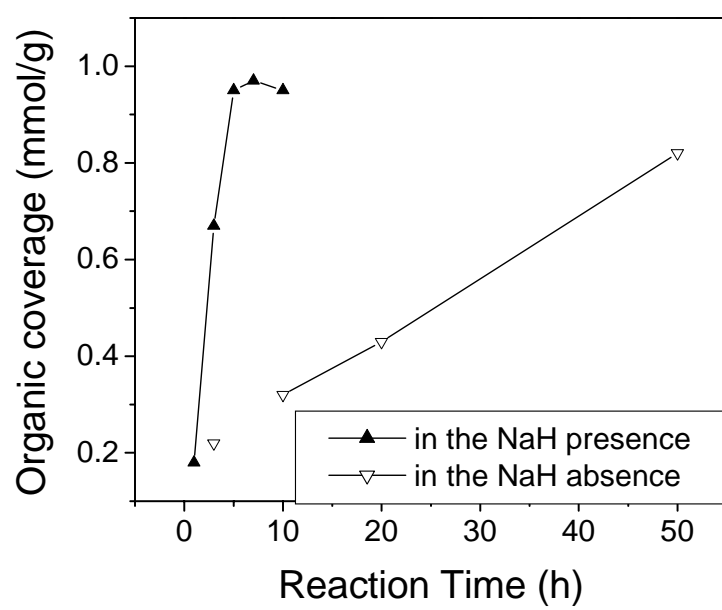
Precursors added (mmol/mL)	SN <sub>2</sub> Reaction Time (h)	Using NaH	Organic content (mmol/g) <sup>a</sup>
0.08	5	yes	0.18
0.15	5	yes	0.34
0.45	1	yes	0.18
0.45	3	yes	0.67
0.45	5	yes	0.95
0.45	7	yes	0.97
0.45	10	yes	0.95
0.80	5	yes	1.2
0.45	3	no	0.22
0.45	10	no	0.32
0.45	20	no	0.43
0.45	50	no	0.82

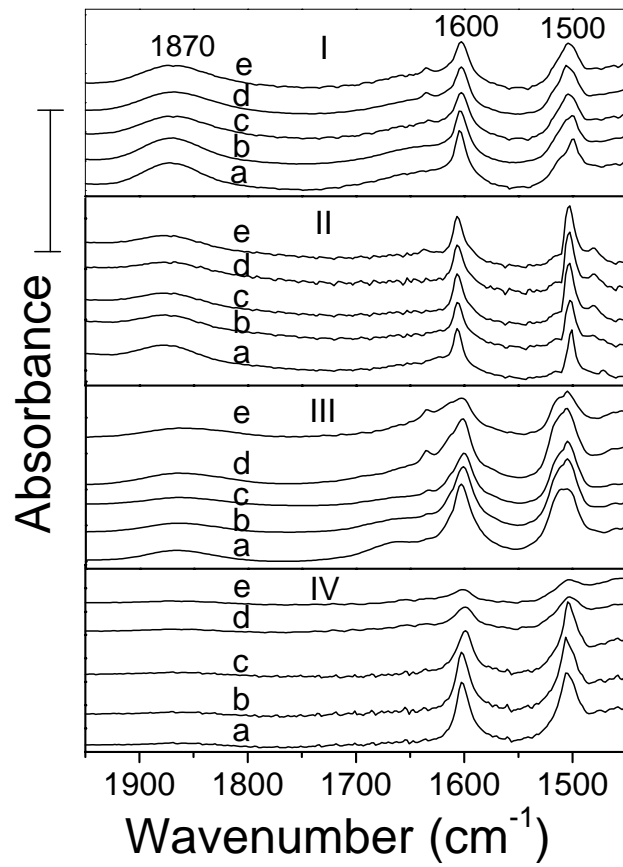
a = mmol of organic groups per gram of solid.

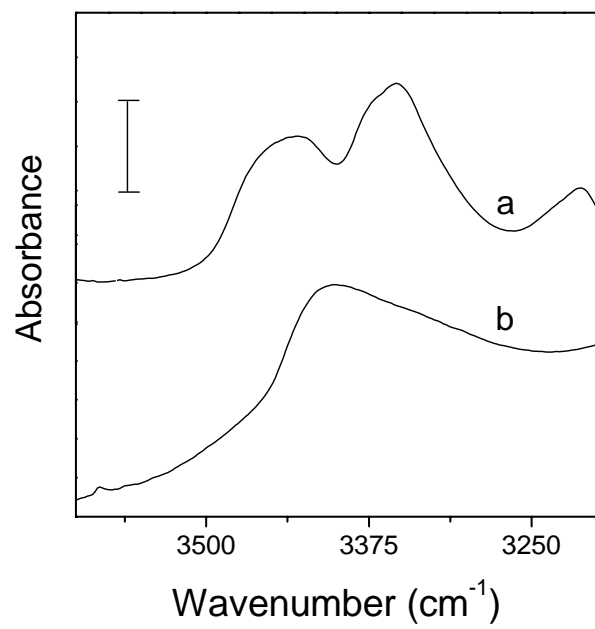
Table 2: Infrared band areas of aniline immobilized on the silica gel surface, heated under vacuum.

Organic content (mmol/g)	Thermal treatment (°C)	Band area ratio <sup>a</sup>
0.18	100	0.44
	200	0.46
	300	0.49
	400	0.45
	400 (6h)	0.45
0.34	100	0.85
	200	0.85
	300	0.88
	400	0.90
	400 (6h)	0.87
0.95	100	2.2
	200	2.1
	300	2.1
	400	1.7
	400 (6h)	1.0
1.2	100	3.9
	200	4.0
	300	3.9
	400	2.5
	400 (6h)	1.1

$$a = \frac{\text{(band area of aniline ring at } 1500 \text{ cm}^{-1}\text{)}}{\text{(silica overtone band area at } 1870 \text{ cm}^{-1}\text{ )}}$$









## Captions of figures

Figure 1:  $\text{SN}_2$  reaction kinetics monitored by the final organic content on the surface of material obtained from  $0.45 \text{ mmol.mL}^{-1}$  of the organic precursor concentration.

Figure 2: Absorbance spectra of aniline/silica sol-gel materials with organic phase content of: I)  $0.18 \text{ mmol.g}^{-1}$ ; II)  $0.34 \text{ mmol.g}^{-1}$ ; III)  $0.95 \text{ mmol.g}^{-1}$ ; IV)  $1.2 \text{ mmol.g}^{-1}$ . The spectra were obtained in vacuum at room temperature after being heated at: a)  $100 \text{ }^\circ\text{C}$ ; b)  $200 \text{ }^\circ\text{C}$ ; c)  $300 \text{ }^\circ\text{C}$ ; d)  $400 \text{ }^\circ\text{C}$ ; e)  $400 \text{ }^\circ\text{C}$  (6 h). The bar value is 1, 1.5, 2 and 3 for Graphics I, II, III and IV, respectively.

Figure 3: Absorbance spectra: a) Pure aniline; b) 3-anilinepropyltrimethoxysilane ( $\text{SN}_2$  reaction product, before gelation). The bar value is 0.1.

**Key Words:** organofunctionalized silica, infrared, aniline, thermal stability, base activator

## **Corresponding author**

Edilson V. Benvenuti

Instituto de Química – UFRGS

CP 15003

91501-970, Porto Alegre, RS, Brazil

Tel +55-51 3316-7209

Fax: +55-51 3316-7304

e-mail: [edilson@iq.ufrgs.br](mailto:edilson@iq.ufrgs.br)

**ANEXO 2**

**4.2 - F. A. Pavan, W. F. Magalhães, M. A. de Luca, C. C. Moro, T. M. H. Costa and E. V. Benvenuti. A characterization study of xerogel silicapropylaniline powders. *Journal of Non-Crystalline Solids* 311 (2002) 54-60**



ELSEVIER

Journal of Non-Crystalline Solids 311 (2002) 54–60

JOURNAL OF  
NON-CRYSTALLINE SOLIDS

www.elsevier.com/locate/jnoncrysol

# A characterization study of xerogel silicapropylaniline powders

Flávio A. Pavan<sup>a</sup>, Wellington F. de Magalhães<sup>b</sup>, Maria A. de Luca<sup>a</sup>,  
Celso C. Moro<sup>a</sup>, Tania M.H. Costa<sup>a,\*</sup>, Edilson V. Benvenutti<sup>a,\*</sup>

<sup>a</sup> LSS—Instituto de Química, UFRGS, CP 15003, 91501-970 Porto Alegre, RS, Brazil

<sup>b</sup> LEAP—ICEX, UFMG, CP 702, 31270-901 Belo Horizonte, MG, Brazil

Received 19 June 2001; received in revised form 25 February 2002

## Abstract

Silicapropylaniline nanometric materials with varying organic content were obtained using a sol–gel synthesis. By increasing the organic load, the scanning electron microscopy technique shows a slight increase in the average size of aggregated particles. N<sub>2</sub> isotherms and positron annihilation lifetime spectroscopy measurements show that the average pore size decreases accompanied by a surface area reduction. FTIR thermal analysis was used to estimate the thermal stability of the organic phase and also to detect the presence of trapped organic groups in closed pores. From the organic coverage and surface area measurements the surface density of the immobilized organic molecules as well as the average intermolecular distance between them could be estimated.

© 2002 Elsevier Science B.V. All rights reserved.

## 1. Introduction

The synthesis and characterization of hybrid organic–inorganic xerogel powdered materials have received great attention in past years [1–3]. These materials present properties related to the matrix as well as the organic phase, which can be combined in order to obtain new materials [4,5]. The sol–gel method is an important route to prepare such materials using alkoxy silanes R–Si(OR)<sub>3</sub> and tetraethylorthosilicate (TEOS) or tetramethylorthosilicate as precursors. The polycondensation of alkoxy silanes can be described in three

steps: (i) hydrolysis; (ii) silanol condensation and; (iii) silanol–alcohol condensation [3,6–8]. The relative simplicity and versatility of the sol–gel process, when compared to covalent-bonding methods to obtain hybrid materials, associated with low cost, are responsible for its extensive utilization. The possibility of obtaining different physico-chemical characteristics like surface area, particle shape and size, porosity and organic functionalization grade, are some advantages of this process [6,9]. Therefore several researchers have been using the sol–gel method to obtain silica chemically modified by organic groups. These new materials present interesting physical and chemical properties allowing their use as sorbents, sensors, electrodes, membranes, etc [1,3,6,10–12]. However a detailed characterization is necessary for a better utilization.

\* Corresponding author. Tel.: +55-51 3316 7209/6279; fax: +55-51 3316 7304.

E-mail address: [edilson@iq.ufrgs.br](mailto:edilson@iq.ufrgs.br) (E.V. Benvenutti).

The adsorption–desorption isotherms are frequently used in xerogels pore size distribution studies [9,12–15], for distinguishing materials with different pore diameters ( $d_p$ ), microporous  $d_p < 2$  nm, mesoporous  $2 < d_p < 50$  nm and macroporous  $d_p > 50$  nm, according to the accepted classification [16,17]. For nanometric xerogel materials, presenting a fraction of micropores or small mesopores, positron annihilation lifetime spectroscopy (PALS) can be used as a complementary technique to monitor the average size of the pores [18,19]. Other techniques like electron microscopy [12,13, 17], nuclear magnetic resonance [15,20], and infrared spectroscopy (FTIR) [13,21–23] have also been used in the characterization of sol–gel materials. A recent paper reports that the infrared band areas of organic phase, obtained by FTIR thermal analysis on hybrid xerogels, could be used to estimate the fraction of trapped organic groups in closed pores [24].

In a previous paper we proposed a synthetic method for obtaining silicaprotylaniline in a satisfactory way, using NaH as a base activator for the synthesis of anilinepropyltrimethoxysilane (APTMS) precursor which reduces the reaction time by a factor of 10 [25]. In this paper, a characterization of this hybrid organic–inorganic xerogel silicaprotylaniline nanometric material is presented. Characterization was carried out using  $N_2$ -isotherms, CHN elemental analysis, scanning electron microscopy (SEM), PALS, and FTIR thermal analysis using an oven cell.

## 2. Experimental procedures

### 2.1. Sol–gel synthesis

The sol–gel method used in this work has already been described elsewhere [25]. Aniline was activated with sodium hydride in 10 ml of aprotic solvents (toluene:THF) (1:1) for 30 min, and  $(CH_3O)_3Si(CH_2)_3Cl$  (CPTMS) was added. Quantities used were stoichiometric CPTMS, aniline and NaH, corresponding to, 1.5, 4.5, 8.0 and 10.0 mmol for synthesis A, B, C and D, respectively. The mixture was stirred under argon at solvent–

reflux temperature for a period of 5 h. The obtained APTMS was then used as sol–gel precursor reagent, in concentrations of 0.15, 0.45, 0.80 and 1.0 mol L<sup>-1</sup> for synthesis A–D, respectively. Afterwards, TEOS (5 ml), ethyl alcohol (5 ml), HF (0.1 ml) and water in stoichiometric ratio with Si  $r = 4/1$  (1.6 ml), were added to the precursor solutions, under stirring. The condensation occurs by a nucleophilic catalytic process using fluoridric acid, [1,22,26] at pH between 7 and 9. The mixtures were stored for 5 days, just covered without sealing, for gelation and solvent evaporation. The gel was then washed with 50 ml of solvents: toluene, THF, acetone, dichloromethane, ethyl alcohol, distilled water and ethyl ether. This process was repeated five times for each solvent. The solid was finally dried for 30 min in an oven at 100 °C. The resulting powders formed were comminuted in an agate mortar for subsequent analysis.

### 2.2. Infrared measurements

Self-supporting disks of the material, with an area of 5 cm<sup>2</sup>, weighing  $\approx 100$  mg, were prepared. The disks were heated for 6 h to temperature ranging from 100 to 400 °C, under vacuum ( $10^{-3}$  Torr), using an IR cell [27]. The self-supporting disks were analyzed in the infrared region using an FTIR spectrometer. The spectra were obtained with a resolution of 4 cm<sup>-1</sup>, with 100 scans.

### 2.3. Elemental analysis

The organic groups present were analyzed using a CHN/CHNS/O analyzer, in triplicate, after heating at 100 °C, under vacuum, for 1 h.

### 2.4. $N_2$ -isotherms

The nitrogen adsorption–desorption isotherms of previous degassed solids, at 150 °C, were determined at liquid nitrogen boiling point in a volumetric apparatus, using nitrogen as probe. The specific surface areas of xerogels were determined from the  $t$ -plot analysis and pore size distribution was obtained using BJH method [28].

### 2.5. Scanning electron microscopy

The materials were analyzed by SEM with 20 kV and  $60\,000\times$  of magnification. The average particle sizes were obtained by choosing and manually marking the diameter of a minimum of a hundred spherical particles in each image. The average diameters and the standard deviations were determined by using the Quantikov software [29].

### 2.6. Positrons annihilation measurements

The positron annihilation lifetime spectrometer was a standard fast-fast coincidence apparatus based on plastic scintillator mounted on photomultipliers powered by a high voltage supplier at 2300 V. It provides a time resolution  $\approx 280$  ps full width at half maximum, using a  $^{22}\text{Na}$  positron source with  $\approx 4.0 \times 10^5$  Bq of activity. The radioisotope was sandwiched between two  $7\ \mu\text{m}$  thick foils of Kapton polymer. The channel width of

multi-channel analyzer was 46 ps/channel. Each lifetime spectrum contains  $\approx 1.3 \times 10^6$  counts. The resulting pore diameters were calculated from the lifetime of trapped positrons, obtained by using the positronfit-extended program [30]. Three spectra were recorded for each sample. The experimental uncertainty for the PAL parameters was found to be around  $\pm 0.05$  ns for  $\tau_3$  and between  $\pm 0.6\%$  and  $\pm 1.1\%$  for  $I_3$ .

### 3. Results

Images obtained by SEM show very similar spherical particles. It was possible to observe that the average size of aggregated particles undergoes a slight increase from sample A to D. The average diameter increases from 99 nm for the synthesis A to 129 nm for synthesis D, with a standard deviation of 17 and 24 nm, respectively (Fig. 1). These average diameters and standard deviations were calculated using the Quantikov software [29].

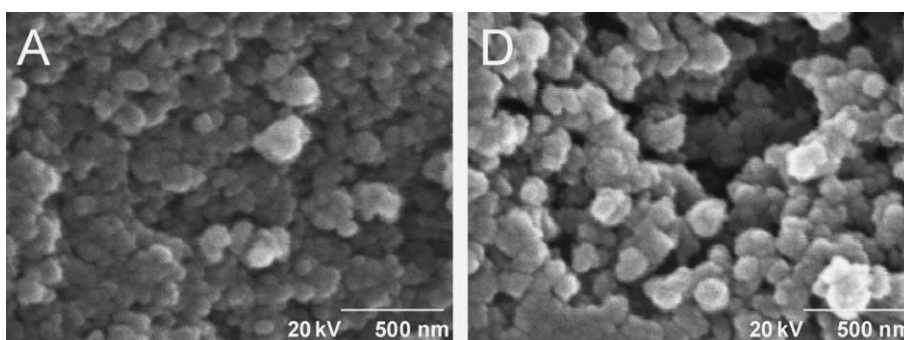


Fig. 1. SEM images of silicopropylaniline xerogels obtained from the synthesis A and D, with  $60\,000\times$  magnification.

Table 1  
SEM, positron annihilation and surface area results

Samples <sup>a</sup>	Organic precursor added (mmol) <sup>b</sup>	Aniline/Si ratio <sup>c</sup>	Positron lifetime <sup>d</sup> ( $\pm 0.05$ ns)	Pore diameters average <sup>d</sup> ( $\pm 0.05$ nm)	Surface area ( $\text{m}^2\ \text{g}^{-1}$ ) ( $\pm 5\%$ )
A	1.5	0.06	60.86	3.36	175
B	4.5	0.17	58.08	3.26	160
C	8.0	0.27	25.65	2.10	154
D	10.0	0.31	17.90	1.82	143

<sup>a</sup> Samples obtained from synthesis A, B, C and D.

<sup>b</sup> Volume of precursor solution added was 10 ml.

<sup>c</sup> Considering total silicon.

<sup>d</sup> Obtained from PALS.

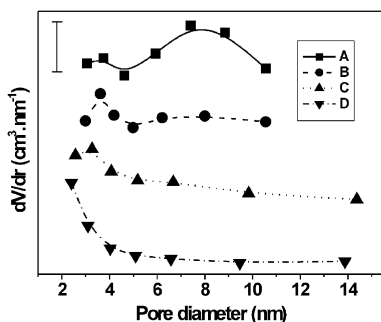


Fig. 2. Pore size distribution for anilinepropylsilica xerogels obtained by BJH method. The bar value is 0.01.

Surface area results are shown in the Table 1. It can be observed a surface area decrease by increasing the organic precursor. The pore size distribution is showed in the Fig. 2. In the sample A with a lower organic loading two distinct pore diameter regions were observed, with the maximum in  $\approx 3.5$  and 7.5 nm. By increasing the organic loading there is an evident decrease in the proportion of the pores with higher size. In the region of small pores (maximum  $\approx 3.5$  nm) the organic loading causes a shift to lower diameters.

For evaluation of small size pores, PALS was also used. The average pore diameters obtained from PALS are shown in Table 1. The average pore diameter undergo a decrease from materials obtained from synthesis A to D, i.e. the pore diameter decreases with the increasing of the organic precursor added, in the sol–gel synthesis.

Infrared spectroscopy allows the coverage of the silica surface by aromatic aniline groups to be verified. The modes of aniline aromatic ring at  $\approx 1600$  and  $1500\text{ cm}^{-1}$  are very strong (Fig. 3), therefore the band area of these absorption modes was used to estimate the thermal stability of organic groups present on the silica surface and the trapped organic fraction in the closed pores could also be estimated (Table 2). The infrared band areas were almost constant up to  $300\text{ }^{\circ}\text{C}$ , although further thermal treatment ( $400\text{ }^{\circ}\text{C}$ ) results in a band area decrease. These band decreases were used to monitor the aniline desorption from the silica surface. The overtone band of silica at  $\approx 1870\text{ cm}^{-1}$  was used as a reference band. This normalization was necessary, considering the heterogeneity

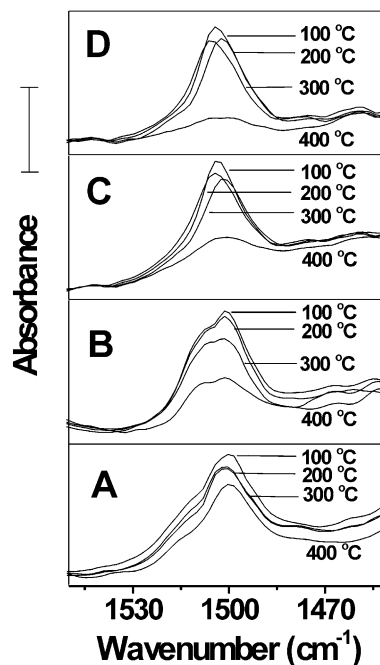


Fig. 3. FTIR absorbance spectra for xerogel materials, obtained at room temperature, from synthesis A, B, C, and D, after heating in vacuum, for 6 h. The bar value was 0.17, 0.7, 1 and 1, for spectra A, B, C and D, respectively.

Table 2  
Infrared band areas of aromatic anile ring band on silicaproylaniline materials, heated under vacuum

Synthesis	Thermal treatment ( $^{\circ}\text{C}$ )	Band area ratio <sup>a</sup> ( $\pm 5\%$ )	Remaining band area percent ( $\pm 5\%$ )
A	100	0.44	100
	200	0.40	91
	300	0.40	91
	400	0.34	77
B	100	2.1	100
	200	2.1	100
	300	2.0	95
	400	1.0	47
C	100	3.9	100
	200	3.8	97
	300	3.8	97
	400	1.3	33
D	100	2.6	100
	200	2.5	96
	300	2.5	96
	400	0.63	24

<sup>a</sup> Band area of aniline ring at  $1500\text{ cm}^{-1}$ /silica overtone band area at  $1870\text{ cm}^{-1}$ .



in disk thickness and taking into account the position changes of the infrared beam.

#### 4. Discussion

Since SEM shows a little change in the size of the aggregated particles size for samples obtained from different organic concentrations (Fig. 1). Nucleation effects that cause notable variation in particle size and consequently changes in the surface area were not too significant. However the surface areas of samples with high organic content were significantly lower than those of sample A, indicating a low organic content (Table 1), as already reported in the literature [21].

The surface area decrease with the increasing concentration of organic precursor was accompanied by an average pore size reduction, which was determined by N<sub>2</sub> adsorption–desorption isotherms (BJH calculations) [28] as well as by PALS [30] (Table 1). The observed average pore diameter decrease with the organic loading could be due to surface organic coverage of the pores resulting in a partial reduction in the pore free volume [31,32], and according to the literature the pore-blocking effect occurs preferentially in the larger pores [33]. From the pore size distribution obtained from N<sub>2</sub> isotherms (Fig. 2) it was also observed that the coverage occurs preferentially in larger pores, since a drastic reduction in the pore fraction was evident from sample A to D. However the organic pore coverage occurs also in the small pores, because there is a shift in average pore size for smaller values (Fig. 2) which was confirmed by PALS (Table 1). This hypothesis could explain the surface area reduction. It is important to note that the

positron annihilation spectroscopy technique provides only the average pore diameters, and is sensitive to both, open and closed pores [18,19]. On the other hand, the N<sub>2</sub> adsorption–desorption measurements are only related to open pores and the BJH method allows the calculation of the pore size distribution for the mesopore size range [28].

From infrared spectroscopy, it can be observed (Fig. 3 and Table 2) that the organic groups are stable up to 300 °C, in high vacuum, for all samples, indicating that organic groups are strongly bonded to the surface, in the covalent form. After further treatment (400 °C) the aniline band areas undergo an evident decrease, indicating that at this temperature the organic phase desorbed from the surface. However even after heating up to 400 °C the spectra show a residual aniline band, interpreted by taking into account the presence of encapsulated organic phase in closed pores. This residual fraction of trapped aniline could be estimated from the band area values, for all samples (Table 2) and was higher for synthesis A and lower for synthesis D, i.e. the remaining organic phase percent, trapped in close pores, decreases with the increase of organic precursor added, once the precursor APTMS concentration increases from A to D. These results could be explained considering that for lower APTMS/TEOS mol ratio i.e. for the samples with low organic loading, a more cross-linked inorganic silica structure is formed [34,35], resulting in a larger fraction of organic entrapped groups in closed pores. It is important to reinforce that in sample A, the organic content is very low, in absolute value (see band area values in Table 2 and CHN analysis in Table 3), and these data are not related to the porosity of the inorganic matrix as a whole.

Table 3  
Organic groups distribution on silica surface

Synthesis	Organic content <sup>a</sup> (mmol g <sup>-1</sup> ) (±6 %)	Nf organic coverage (mmol g <sup>-1</sup> ) (±8 %)	Surface area (m <sup>2</sup> g <sup>-1</sup> ) (±5%)	<i>d</i> (groups/nm <sup>2</sup> ) (±5 %)	<i>l</i> (nm) (±5 %)
A	0.26	0.04	175	0.138	2.69
B	0.71	0.35	160	1.79	1.31
C	1.10	0.74	157	2.84	0.59
D	0.80	0.61	143	2.57	0.62

*d*, surface density of the attached molecules; *l*, average intermolecular distance.

<sup>a</sup> Obtained from CHN elemental analysis.

In Fig. 3, the spectra I and II corresponding to the samples obtained from synthesis A and B, show a broadening in the infrared absorption bands. This broadening could be interpreted taking into account the presence and/or proximity of trapped species, like propylaniline immobilized, unreacted aniline and toluene solvent used in the APTMS synthesis, remaining in closed pores.

FTIR spectra allows the calculation of the organic coverage i.e. organic groups which are really on the surface, in opened pores [24], and these results are summarized in Table 3. Assuming that organic groups cover the surface uniformly, the surface density of attached molecules,  $d$ , can be defined as [24]

$$d = (NfN)/S,$$

where  $Nf$  is the organic coverage ( $\text{mol g}^{-1}$ ),  $N$  is the Avogadro number and  $S$  is the specific surface area.  $Nf$  was obtained by subtracting the organic trapped groups fraction from the total organic content.

The average intermolecular distance  $l$ , is defined by

$$l = (1/d)^{1/2}$$

These distances were calculated using the coverage organic values, since surface area measurements are related only to opened pores. As the surface density of the attached molecules increases for materials obtained from synthesis A to C, the intermolecular distance decreases achieving the value of  $\approx 0.60$  nm for synthesis C and D with molecular loading of 1.10 and 0.80  $\text{mmol g}^{-1}$ , respectively (Table 3). This is an evidence that the saturation condition in the opened pores surface was attained [24]. Possible errors in FTIR analysis, caused by heating of the inorganic matrix, like sintering, were neglected, since these errors should decrease with increasing organic loading.

## 5. Conclusions

Silicapropylaniline xerogels were prepared. Increasing the organic loading results in a slight increase in average aggregated particles size. A decrease in average pore diameter and a surface

area reduction with the organic content were observed. These results were explained by pore volume decrease caused by an increase in organic group density in the pores. The FTIR results show that the organic phase is thermally stable up to 300 °C indicating that the aniline groups are chemically bonded on the surface in the covalent form. The xerogel materials present closed pores, and the fraction of the trapped organic phase in closed pores decreases with increasing the organic precursor concentration. The propylaniline coverage saturation is reached for an intermolecular distance of  $\approx 0.6$  nm.

## Acknowledgement

F.A.P thanks CNPq for his grant.

## References

- [1] R.J.P. Corriu, D. Leclercq, *Angew. Chem., Int. Ed. Engl.* 35 (1996) 1421.
- [2] D. Avnir, *Acc. Chem. Rev.* 28 (1995) 328.
- [3] O. Lev, M. Tsionsky, L. Rabinovich, V. Glazer, S. Sampath, I. Pankratov, J. Gun, *Anal. Chem.* 67 (1995) 22A.
- [4] C.A. Muller, M. Maciejewski, T. Mallat, A. Baiker, *J. Catal.* 184 (1999) 280M.
- [5] T.M.H. Costa, V. Stefani, M.R. Gallas, N.M. Balzaretti, J.A.H. de Jornada, *J. Mater. Chem.* 11 (2001) 3377.
- [6] M.M. Collinson, *Critical Rev. Anal. Chem.* 29 (1999) 289.
- [7] C.J. Brinker, G.W. Scherer, *Sol-Gel Science*, Academic Press, London, 1990.
- [8] L.L. Hench, J.K. West, *Chem. Rev.* 90 (1990) 33.
- [9] G. Dubois, R.J.P. Corriu, C. Reye, S. Brandes, F. Denat, R. Guillard, *Chem. Commun.* (1999) 2283.
- [10] O. Lev, Z. Wu, S. Bharathi, V. Glezer, A. Modestov, J. Gun, L. Rabinovich, S. Sampath, *Chem. Mater.* 9 (1997) 2354.
- [11] R. Makote, M.M. Collinson, *Anal. Chim. Acta* 394 (1999) 195.
- [12] M.J. Muñoz-Aguado, M. Gregorkiewitz, *J. Membr. Sci.* 111 (1996) 7.
- [13] J.C. Ro, I.J. Chung, *J. Non-Cryst. Solids* 130 (1991) 8.
- [14] D.L. Meixner, A.G. Gilicinski, P.N. Dyer, *Langmuir* 14 (1998) 3202.
- [15] M.H. Lim, A. Stein, *Chem. Mater.* 11 (1999) 3285.
- [16] J. Rouquerol, D. Avnir, C.W. Fairbridge, D.H. Everett, J.M. Haynes, N. Pernicone, J.D.F. Ramsay, K.S.W. Sing, K.K. Unger, *Pure Appl. Chem.* 66 (1994) 1739.
- [17] D.A. Loy, K.J. Shea, *Chem. Rev.* 95 (1995) 1431.
- [18] M. Misheva, N. Djourellov, F.M.A. Margaca, I.M.M. Salvado, *J. Non-Cryst. Solids* 279 (2001) 196.

- [19] D.W. Gidley, W.E. Frieze, T.L. Dull, E.T. Ryan, H.M. Ho, *Phys. Rev. B* 60 (1999) R5157.
- [20] B. Boury, P. Chevalier, R.J.P. Corriu, P. Delord, J.J.E. Moreau, M.W. Chiman, *Chem. Mater.* 11 (1999) 281.
- [21] N. Hüsing, U. Schubert, R. Mezei, P. Fratzl, B. Riegel, W. Kiefer, D. Kohler, W. Mader, *Chem. Mater.* 11 (1999) 451.
- [22] T.N.M. Bernardis, M.J. Van Bommel, J.A.J. Jansen, *J. Sol-Gel Sci. Technol.* 13 (1998) 749.
- [23] T.M.H. Costa, M.R. Gallas, E.V. Benvenutti, J.A.H. da Jornada, *J. Non-Cryst. Solids* 220 (1997) 195.
- [24] F.A. Pavan, L. Franken, C.A. Moreira, T.M.H. Costa, E.V. Benvenutti, Y. Gushikem, *J. Colloid Interf. Sci.* 241 (2001) 413.
- [25] F.A. Pavan, S. Leal, T.M.H. Costa, E.V. Benvenutti, Y. Gushikem, *J. Sol-Gel Sci. Technol.* 23 (2002) 129.
- [26] P. Feng, Y. Xia, J. Feng, X. Bu, G.D. Stucky, *Chem. Commun.* (1997) 949.
- [27] J.L. Foschiera, T.M. Pizzolato, E.V. Benvenutti, *J. Braz. Chem. Soc.* 12 (2001) 159.
- [28] E.P. Barret, L.G. Joyner, P.P. Halenda, *J. Am. Chem. Soc.* 73 (1951) 373.
- [29] L.C.M. Pinto, PhD Thesis, Universidade de São Paulo, IPEN, 1996.
- [30] P. Kirkeggard, M. Eldrup, O.E. Mogensen, N.J. Pedersen, *Comput. Phys. Commun.* 23 (1981) 307.
- [31] S. Kitahara, K. Takada, T.T. Sakata, H. Muraishi, *J. Colloid Interf. Sci.* 84 (1981) 519.
- [32] R. Ryoo, C.H. Ko, M. Kruk, V. Antochshuk, M. Jaroniec, *J. Phys. Chem. B* 104 (2000) 11465.
- [33] B. Boury, R.J.P. Corriu, V. Le Strat, *Chem. Mater.* 11 (1999) 2796.
- [34] U. Schubert, N. Hüsing, A. Lorenz, *Chem. Mater.* 7 (1995) 2010.
- [35] H.K. Kim, S.J. Kang, S.K. Choi, Y.H. Min, C.S. Yoon, *Chem. Mater.* 11 (1999) 779.

**ANEXO 3**

**4.3 - F. A. Pavan, Y. Gushiken, C. Moro, T. M. H. Costa and E. V. Benvenuti. The influence of Na<sup>+</sup> on the aniliepropylsilica xerogel synthesis by using the fluoride nucleophilic catalyst. *Colloid Polym Sci* (2003) 281: 173- 177**

## Original Contribution

# The influence of Na<sup>+</sup> on the anilinepropylsilica xerogel synthesis by using the fluoride nucleophilic catalyst

Flávio A. Pavan · Yoshitaka Gushikem · Celso C. Moro · Tania M. H. Costa · Edilson V. Benvenuti(✉)

---

F.A. Pavan · C.C. Moro · T.M.H. Costa · E.V. Benvenuti  
LSS, Instituto de Química - UFRGS, CP 15003, 91501-970 Porto Alegre, RS, Brazil

Y. Gushikem  
Instituto de Química, Unicamp, CP 6154, 13083-970 Campinas, SP, Brazil

---

✉ E-mail: edilson@iq.ufrgs.br  
Phone: +55-51-33167209  
Fax: +55-51-33167304

---

**Received:** 18 March 2002 / **Accepted:** 2 July 2002 / **Published online:**

---

**Abstract.** Anilinepropylsilica xerogel was obtained by using an appropriate organosilane and tetraethyl orthosilicate as precursor reagents. The gelation was carried out using HF and NaF as catalysts. The presence of Na<sup>+</sup> (when NaF was used) resulted in a decrease in the final organic content of the materials. This effect was interpreted as an inhibition of the organosilane polycondensation possibly due to the Na<sup>+</sup> interaction with the SiO<sup>-</sup> groups of the hydrolyzed organosilane. The presence of Na<sup>+</sup> also results in morphological changes in the xerogels.

**Keywords.** Xerogel - Sodium fluoride - Hybrid powders - Nanometric materials - Sol-gel

## Introduction

Nanoparticles have unique electronic, optical and magnetic properties because of their small size and large surface areas. Owing to these characteristics, the nanometric materials present great potential applications in different areas, like catalysis, microelectronics, nonlinear optics, separation science, etc. [1, 2, 3, 4]. Among these materials, the hybrid organic-inorganic silica xerogels have received great attention in the last few years [3, 4, 5, 6, 7, 8]. The relative simplicity and versatility of the sol-gel process, if compared with other covalent-bonding methods for obtaining hybrid materials, associated with the possibility of controlling the morphological properties, like particle shape and size, surface area, and organic functionalization grade, are some advantages of this process [9, 10, 11]. Thus, the sol-gel method has motivated several researchers to develop new materials, using different

precursors and synthesis conditions. The sol-gel method consists of the hydrolysis (Eq. 1) and condensation of alkoxy silanes in general using acidic, basic or nucleophilic catalysts (Eqs. 2a, b) that results in a cross-linked silica network.



The fluoride ion is a very efficient nucleophilic catalyst [2, 6, 12, 13] and it is used in different forms, like HF, NH<sub>4</sub>F, NaF, etc. When sodium fluoride is used, changes in some properties of the gel have been observed [14, 15, 16, 17, 18]. These changes were attributed to the ion-dipole interactions of the Na<sup>+</sup> with water, that causes an inhibition in the silane hydrolysis [15]. However, the effect of the presence of Na<sup>+</sup> in the xerogel synthesis is not completely understood.

In this work, the influence of Na<sup>+</sup> on the anilinepropylsilica xerogel synthesis was studied. The influence of Na<sup>+</sup> was observed in the organic final content of the xerogel materials using CHN elemental analysis and FTIR spectroscopy. The changes in the xerogel morphological properties were investigated by using N<sub>2</sub> adsorption-desorption isotherms and scanning electron microscopy (SEM) techniques.

## Materials and methods

### Sol-gel synthesis

The sol-gel method used in this work has already been described elsewhere [19]. Aniline was activated with sodium hydride in 10 ml of a mixture of aprotic solvents (toluene/tetrahydrofuran 1:1) for 30 min, and the (CH<sub>3</sub>O)<sub>3</sub>Si(CH<sub>2</sub>)<sub>3</sub>Cl (CPTMS) was added. The quantities used were stoichiometric for CPTMS, aniline and NaH; the values were, 1.0, 4.0 and 9.0 mmol. The mixture was stirred under argon at solvent-reflux temperature for a period of 5 h. The product of the reaction, anilinepropyltrimethoxysilane (APTMS), was used as an organic precursor. The quantities of APTMS were 1.0, 4.0 and 9.0 mmol for syntheses 1, 2 and 3, respectively. Tetraethyl orthosilicate (TEOS) (5 ml), ethyl alcohol (5 ml), HF or NaF (3.0 or 8.0 mmol) and water (1.6 ml), in stoichiometric ratio H<sub>2</sub>O/Si of 4:1, were added to the precursor solutions, under stirring. The condensation occurs in a basic environment at a pH between 7 and 9 (Table 1). The pH of the solutions was determined using universal indicator papers, supplied by Merck, pH range 0-14. Fluoridric acid was added owing to the catalytic properties of the fluoride [2, 12, 13]. The mixtures were stored for 5 days, and were just covered without sealing, for gelation and evaporation of the solvents. The gel was then washed with toluene, tetrahydrofuran, methyl alcohol, water and ethyl ether, and finally dried for 30 min in an oven at 100 °C.

**Table 1.** Synthesis conditions, CHN and electron dispersive spectroscopy (EDS) elemental analysis, and surface area results

Sample	Anilinepropyltrimethoxysilane added (mmol)	Catalyst added (mmol)	Gelation pH( $\pm 1$ )	CHN analysis (mmol g <sup>-1</sup> ) <sup>a</sup>	EDS analysis Na atom (%)	Surface area (m <sup>2</sup> g <sup>-1</sup> )
H1	1.0	HF (3.0)	7	0.26	-	363
Na1	1.0	NaF (3.0)	9	-	0.63	470
H4	4.0	HF (3.0)	7	0.71	-	339
Na4	4.0	NaF (3.0)	9	0.50	0.99	378
H9	9.0	HF (3.0)	9	1.10	-	232
Na9	9.0	NaF (3.0)	9	1.18	1.72	224
Na9b	9.0	NaF (8.0)	9	0.75	2.02	413

<sup>a</sup> Millimoles of aniline groups per gram of xerogel

## FTIR analysis

Self-supporting disks of the material, with an area of 5 cm<sup>2</sup>, weighing 100 mg, were prepared. The disks were heated for 1 h at 200 °C, under vacuum (10<sup>-3</sup> torr), using an IR cell [17, 20]. The self-supporting disks were analyzed in the IR region using a Shimadzu FTIR, model 8300. The spectra were obtained with a resolution of 4 cm<sup>-1</sup>, with 100 cumulative scans.

## CHN elemental analysis

The organic phase present on the xerogels was analyzed using a CHN elemental PerkinElmer M CHNS/O analyzer, model 400. Triplicate analysis of the samples, previously heated at 100 °C under vacuum for 1 h, was carried out.

## Scanning electron microscopy

The materials were analyzed by SEM using a JEOL model JSM 5800, with 20 kV and  $\times 60,000$  magnification.

## Electron dispersive spectroscopy elemental analysis

The electron dispersive spectroscopy (EDS) analysis was made using a Noran detector with a JEOL model JSM 5800, with 20 kV and acquisition time of 100 s and  $\times 60$  magnification.

## Surface area

The specific surface areas of the previous degassed solids at 150 °C, under vacuum, were determined by the Brunauer-Emmett-Teller [21] multipoint technique on a volumetric apparatus, using nitrogen as a probe [22]. Homemade equipment with a vacuum line system employing a turbomolecular Edwards vacuum pump was used. The pressure measurements were made using a capillary Hg barometer and also an active Pirani gauge. The results were frequently compared with an alumina standard reference.

## Pore size distribution

The pore size distribution was obtained from the nitrogen adsorption-desorption isotherms, determined at the boiling point of liquid nitrogen, using the volumetric apparatus already described [22]. The xerogel materials were previously degassed at 150 °C in a vacuum. The data analysis was made using the Barret-Joyner-Halenda (BJH) method [23].

## Results

The CHN technique was very important in this work because it allowed the determination of the organic grade of the xerogel materials. It was observed by CHN analysis (Table 1) that for sample Na1, prepared with a low amount of organic precursor and 3 mmol NaF, the organic groups were not incorporated in the gel, but for the sample H1, prepared without NaF, 0.26 mmolg<sup>-1</sup> was incorporated. An increase in the organic content for the samples obtained by addition of a greater amount of the organic precursor was also observed (Table 1). However, for the sample Na4, for which NaF (3 mmol) was used as a catalyst, a lower organic content was observed (0.50 mmolg<sup>-1</sup>) when compared with sample H4 catalyzed with 3 mmol HF (0.71 mmolg<sup>-1</sup>). In the Na9 and H9 samples, the decrease in the organic incorporation, produced by the Na<sup>+</sup> present, is not observed (Table 1). Comparing samples Na9 and Na9b, the organic final content is lower for sample Na9b, catalyzed with a greater amount of NaF (8 mmol) (Table 1).

It was demonstrated recently [10, 17] that FTIR spectroscopy could be used to estimate the content of organic groups present in hybrid xerogels. This technique was also used in this work and the IR spectra of the xerogels, previously heat-treated at 200 °C, are shown in Fig. 1. The aniline ring vibrational mode intensities at 1,600 and 1,500 cm<sup>-1</sup> were used as additional evidence of the incorporation of organic groups. In general, the aniline band intensities increase with the organic loading. However, it was observed that Na<sup>+</sup> causes a decrease in the aniline band intensities when comparing samples with the same quantity of APTMS precursor added (Fig. 1). For sample Na1, with a lower quantity of organic precursor added, these bands were not observed, confirming that the organic groups were not incorporated, in accordance with the CHN results.



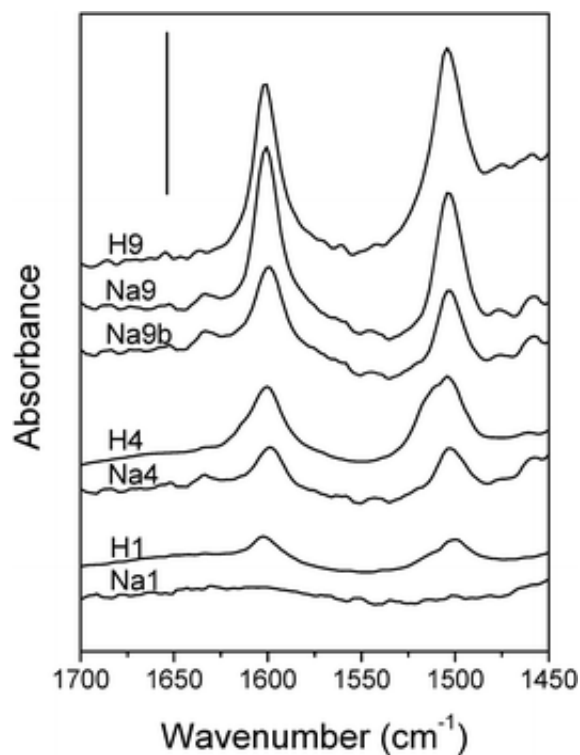


**Fig. 1.** Absorbance IR spectra of the anilinepropylsilica xerogel samples, obtained at room temperature: *a* H1; *b* Na1; *c* Na4; *d* Na9. The *bar* value is 0.5

The pore size distribution of the xerogels obtained by the BJH method [23] is presented in Fig. 2. No significant changes in the pore radii can be observed for the samples where NaF was used as a catalyst and the pore radius was smaller than 2 nm. However, when HF was used as a catalyst, the sample with a lower organic loading (sample H1) showed two distinct pore radius regions with the maximum near 2 and 4 nm (Fig. 2). By increasing the organic loading, there is an evident decrease in the proportion of larger pores. In the region of small pores (maximum near 2 nm) the organic loading causes a shift to lower radii. The surface area results are presented in Table 1. In general, there is a surface area reduction with increasing organic loading.

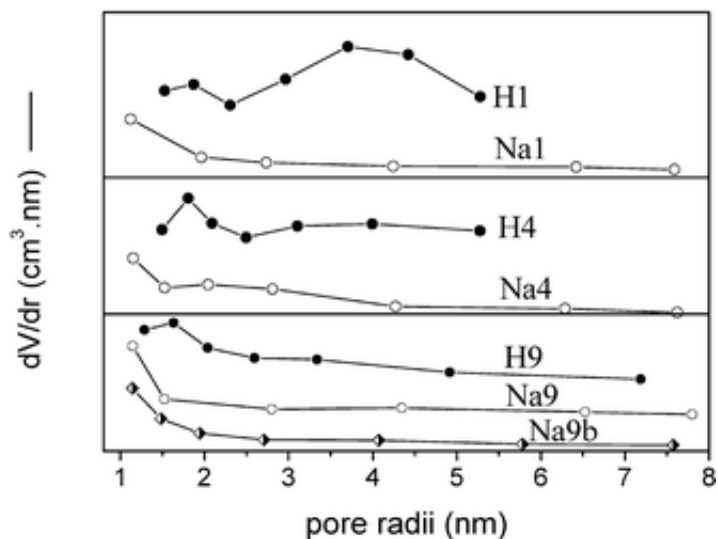


**Fig. 2.** Pore size distribution for anilinepropylsilica xerogels obtained by the Barret-Joyner-Halenda method. The *bar* value is 0.01

The SEM images reveal morphological differences between the samples obtained with different catalysts, HF or NaF. The xerogels obtained using HF as a catalyst have spherical particles, even regarding some pH deviation between 7 and 9 (Table 1); however, for the samples with NaF as a catalyst, the images are different and the particles shape is not defined. The images obtained for samples H4 and Na4 are shown in Fig. 3; the particle shape differences are evident. In both kinds of samples, no significant changes were observed when a high organic precursor concentration was used.

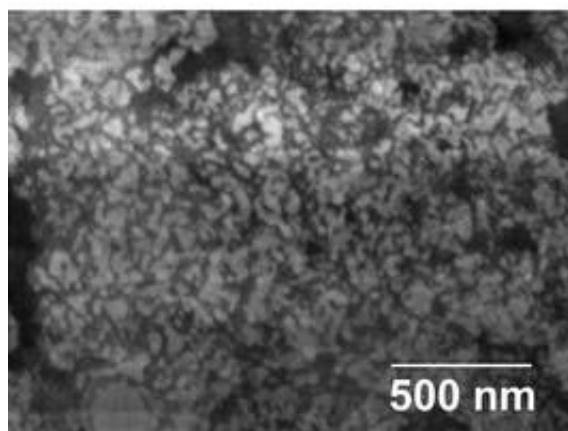
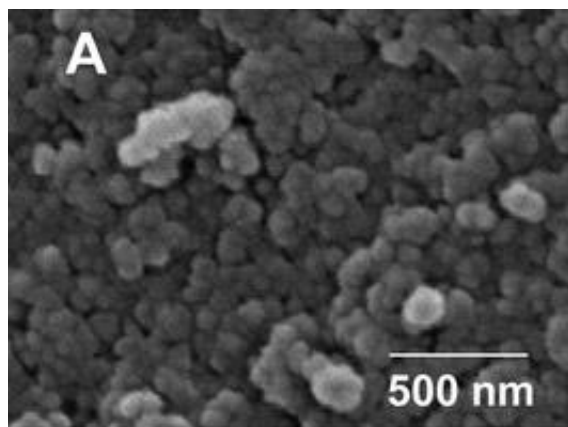


**Fig. 3.** Scanning electron microscopy images of anilinepropylsilica xerogels obtained with  $\times 60,000$  magnification: **a** H4; **b** Na4

## Discussion

A hypothesis found in the literature to explain the influence of  $\text{Na}^+$  in sol-gel synthesis is to consider the ion-dipole interaction of  $\text{Na}^+$  with water that could be responsible for the hindering the TEOS hydrolysis reaction [15]. In the present work this fact does not seem to be significant, because the quantity of  $\text{Na}^+$  ion added is 7 times lower than TEOS and 30 times lower than water. It is improbable that the ion-dipole interaction produces a significant change in the hydrolysis process in these conditions. If we consider an average of six water molecules in the  $\text{Na}^+$  ion-dipole interaction sphere, as has been proposed [15, 24, 25] about 70 mmol water molecules, corresponding to 80% of the water added, remain outside this domain, and they are able to promote the hydrolysis reaction.

In this work we propose that the  $\text{Na}^+$  should interact with the hydrolyzed  $\text{SiO}^-$  species [26, 27] preferentially with the organosilane. For instance, in the H1 and Na1 samples, where the same APTMS precursor quantity was added (1.0 mmol), a marked influence of the  $\text{Na}^+$  on the final organic content of the xerogel was observed (Table 1). Considering the quantity of NaF added (3.0 mmol) and that there are three  $\text{SiO}^-$  species for each APTMS, sample Na1 has a  $\text{SiO}^-/\text{Na}^+$  ratio of 1.0; thus, the APTMS  $\text{SiO}^-$  groups are not available to produce a cross-linked framework with the TEOS. Therefore no organic groups were incorporated (Table 1) and no aniline IR band could be observed (Fig. 1). Nevertheless, for sample H1, with the same amount of APTMS added, but without  $\text{Na}^+$ , an organic

phase was incorporated in the matrix (Table 1, Fig. 1). For the Na4 and Na9 samples, the  $\text{SiO}^-/\text{Na}^+$  ratios were 4.0 and 9.0, respectively. Thus, for these samples,  $\text{SiO}^-$  groups are available to produce the polycondensation with the TEOS and an increase in the organic loading with the  $\text{SiO}^-/\text{Na}^+$  ratio was observed. For samples Na9 and Na9b, where the  $\text{SiO}^-/\text{Na}^+$  ratio was decreased from 9.0 to 3.4 by  $\text{Na}^+$  addition, similar behavior, i.e. a decrease in the organic loading, was observed (Table 1, Fig. 1). If the  $\text{Na}^+$  is bonded to the  $\text{SiO}^-$  groups of the hydrolyzed APTMS, the increase in the organic content also results in an increase in the metal loading, as observed by the EDS technique (Table 1).

The preference of  $\text{Na}^+$  for organosilane instead of TEOS can be explained by considering the nucleophilic character of these species. The hydrolyzed APTMS should be more nucleophilic than the hydrolyzed TEOS, since the organic *R* group can produce an inductive donator effect.

The differences in the pore radii observed from the BJH analysis are evidence that the  $\text{Na}^+$  ion also produces some morphological effect, and they are also supported by the SEM analysis where the images obtained show different particle shapes for samples that use different fluoride catalyst precursors. These morphological differences are probably due to a particle growth inhibition in the gelation process, produced by the  $\text{SiO}^- \text{Na}^+$  interaction, in agreement with the mechanism already proposed.

The surface area data seem just to be influenced by the organic content, for the majority of the experiments, where the same quantity of catalyst was added (3.0 mmol). The decrease in the surface area with the organic loading could be due to the surface organic coverage of the pores that results in a partial reduction in the accessibility to the pores [10, 17]; however, when a greater amount of NaF catalyst was added (sample Na9b), a higher surface area value was observed. Thus, the surface area is also influenced by the presence of  $\text{Na}^+$ . This result is additional evidence of the influence of  $\text{Na}^+$  on the morphological properties of the xerogels. Additionally, the greater amount of fluoride ion added in the Na9b sample could not be discarded as another influence in the increase in the surface area observed [14, 28]

## Summary

We propose that the presence of  $\text{Na}^+$  in the xerogel gelation process produces an inhibition in the polycondensation of organosilane precursors, that results in a lower organic loading in the xerogel material. This effect is possibly due to a preferential interaction of the metal with the hydrolyzed organosilane group instead of the hydrolyzed TEOS. The presence of  $\text{Na}^+$  also has a morphological influence on the xerogels.

**Acknowledgement./thead1> F.A.P. thanks CNPq for his grant.**

## References

1. Levy D, Esquivias L (1995) Adv Mater 7:120
2. Corriu RJP, Leclercq D (1996) Angew Chem Int Ed Engl 35:1420
3. Loy DA, Shea KJ (1995) Chem Rev 95:1431
4. Schubert U, Hüsing N, Lorenz A (1995) Chem Mater 7:2010

5. Aznar AJ, Sanz J, Ruizhitzky E (1992) *Colloid Polym Sci* 270:165
6. Cerveau G, Corriu RJP, Fischmeister-Lepeytre C (1999) *J Mater Chem* 9:1149
7. Pedroso MAS, Dias ML, Azuma C, Mothé CG (2000) *Colloid Polym Sci* 278:1180
8. Ogasawara T, Izawa K, Hattori N, Okabayashi H, O'Connor CJ (2000) *Colloid Polym Sci* 278:293
9. Collinson MM (1999) *Crit Rev Anal Chem* 29:289
10. Pavan FA, Franken L, Moreira CA, Costa TMH, Benvenuti EV, Gushikem Y (2001) *J Colloid Interface Sci* 241:143
11. Pavan FA, Hoffmann HS, Gushikem Y, Costa TMH, Benvenuti EV (2002) *Mater Lett* (in press)
12. Feng P, Xia Y, Feng J, Bu X, Stucky GD (1997) *Chem Commun* 949
13. Bernardis TNM, Van Bommel MJ, Jansen JAJ (1998) *J Sol-Gel Sci Technol* 13:749
14. Wijnen PWJG, Beelen TPM, Rummens KPI, Saeijs HCPL, Haan JW, van de Ven LJM, van Santen RA (1991) *J Colloid Interface Sci* 145:17
15. Arriagada FJ, Osseo-Asare K (1995) *J Colloid Interface Sci* 170:8
16. Guo X, Ding W, Wang X, Yan Q (2001) *Chem Commun* 709
17. Pavan FA, Gobbi SA, Costa TMH, Benvenuti EV (2002) *J Therm Anal Calorim* (2002) 68:199
18. Prouzet E, Pinnavaia TJ (1997) *Angew Chem Int Ed Engl* 36:516
19. Pavan FA, Leal S, Costa TMH, Benvenuti EV, Gushikem Y (2002) *J Sol-Gel Sci Technol* 23:129
20. Foschiera JL, Pizzolato TM, Benvenuti EV (2001) *J Braz Chem Soc* 12:159
21. Brunauer S, Emmett PH, Teller E (1938) *J Am Chem Soc* 60:309
22. Sing KSW, Everett DH, Haul RAW, Moscou L, Pierotti RA, Rouquérol J, Siemieniewska T, (1985) *Pure Appl Chem* 57:603
23. Barret EP, Joyner LG, Halenda PP (1951) *J Am Chem Soc* 73:373
24. Nielsen SB, Masella M, Kebarle P (1999) *J Phys Chem A* 103:9891
25. Tsurusawa T, Iwata S (1999) *J Phys Chem A* 103:6134
26. Hoyau S, Norrman K, Ohanessian G (1999) *J Am Chem Soc* 121:8864
27. Sonnefeld J (1996) *Colloid Polym Sci* 274:1137
28. Brinker CJ, Scherer GW (1990) *Sol-gel science*. Academic, London

**ANEXO 4**

**4.4 - F. A. Pavan, S. A. Gobbi, T. M. H. Costa and E. V. Benvenuti. FTIR Thermal analysis on anilinepropylsilica xerogel. *Journal of Thermal Analysis and Calorimetry*, 68 (2002) 199-206**

## **FTIR Thermal Analysis on Anilinepropylsilica Xerogel**

Flavio A. Pavan, Sidinei A. Gobbi, Tania M. H. Costa, and Edilson V. Benvenutti\*

LSS – Laboratório de Sólidos e Superfícies, Instituto de Química, UFRGS, CP 15003, 91501-970, Porto Alegre, RS, Brazil

### **Abstract**

A FTIR thermal analysis was used for hybrid anilinepropylsilica xerogel obtained from three different organic precursor amount, using HF and NaF as catalyst in the sol-gel process. The aniline ring vibrational mode at  $1500\text{ cm}^{-1}$  of attached aniline groups was used to obtaining the relative aniline content in the xerogel materials after been submitted to thermal treatment at temperature range from 100 to 400 °C. This technique allowed to evaluate the thermal stability of organic phase. The organic coverage on the surface and the fraction of trapped organic groups in closed pores can be also evaluated.

**Key words:** infrared thermal analysis, sol-gel, anilinepropylsilica, fluoride catalyst, NaF catalyst

## Introduction

Organofunctionalized silica materials have received a special attention in the last years due to the great potential applications specially in separation science as adsorbents for SPE (solid phase extraction) or stationary phase for chromatography.[1-5] The sol-gel method [6] has been an important route to prepare these materials using alkoxy silanes  $R-Si(OR)_3$  and tetraethylorthosilicate (TEOS) or tetramethylorthosilicate (TMOS) as precursor. The polycondensation of alkoxy silanes can be described in three reactions: i) hydrolysis; ii) silanol-silanol and silanol-alcohol condensation.[7-10] The simplicity and versatility of the sol-gel process for obtaining organofunctionalized silica materials, associated with the possibility of controlling the morphological properties, like surface area, particle shape and size, and organic functionalization grade, are some advantages of this process.(8,11) In the polycondensation reaction, fluoride ion is very used as nucleophilic catalyst [10,12-13] and it can be utilized in different forms like HF,  $NH_4F$ , NaF, etc. When sodium fluoride is used, changes in the morphological properties of the gel have been observed [14-16] and they are not completely understood.

The thermal analysis is a useful tool to study the interaction strength between the attached groups and the surface of matrix.[1,17-23] Among the thermal analyses the TGA (thermal gravimetric analysis) is widely used in these systems because this technique allows also an evaluation of the organic content attached to the surface. However by using TGA is difficult to differentiate between the organic desorbed groups and water mass loss produced by the dehydroxylation reaction of the surface, that take place with the temperature increasing.[24-26] Additionally the fraction of organic groups trapped in closed pores can not be evaluated. For materials containing organic groups that present characteristic infrared absorption bands these difficulties can be overcome. It was already demonstrated in recent paper [11] that the infrared analysis can be used to estimate the comparative organic content in organofunctionalized silica materials because the infrared band areas of the immobilized groups are related to the organic content. In this work, we have used the FTIR thermal analysis that allows the investigation of the organic groups attached to the surface, using their specific infrared band. It is possible to evaluate the thermal stability and also the fraction of trapped organic groups in the closed pores of the



materials. In this work it was studied the anilinepropylsilica xerogel that was synthesized using two different catalyst precursor, HF and NaF.

## **Experimental**

### *Synthesis anilinepropylsilica xerogels [27]*

Aniline was activated with sodium hydride in the 10 mL of the aprotic solvent mixture (toluene:thf) (1:1) for 30 minutes and then the chloropropyltrimethoxysilane (CPTMS) was added. The quantities used were stoichiometric for CPTMS, aniline and NaH. The product of reaction, anilinepropyltrimethoxysilane (APTMS) was used as organic precursor of the xerogel in the concentration of 1.2, 4.0 and 9.0 mmol.L<sup>-1</sup> for the synthesis 1, 2 and 3, respectively. The mixture was stirred under argon at solvent-reflux temperature during a period of 5 hours. After that, 5 mL of tetraethylorthosilicate (TEOS), 5 mL of ethyl alcohol, 1.6 mL of water (stoichiometric ratio H<sub>2</sub>O/Si = 4) and HF or NaF (4 mmol), were added to the precursor solutions, under stirring. The pH values of the mixtures were basic *ca.* 9. The mixture was stored during 5 days at room temperature just covered without sealing, for gelation and evaporation of solvent. The gel was then washed with toluene, thf, methyl alcohol, water and ethyl ether. The resulting material was dried for 30 minutes in an oven at 100 °C and comminuted in an agate mortar for subsequent infrared analysis.

### *Infrared thermal analysis*

Self-supporting disks of the material to be analyzed were prepared, with an area of 5 cm<sup>2</sup>, weighting *ca.* 100 mg. The disks were heated in a temperature range from 100 to 400 °C under vacuum (10<sup>-3</sup> Torr), from 1 to 6 hours. The IR cell used in this work present two sections, an oven that consists of an electrical filament on the external wall of the cell and another section with two KBr windows for submitting the sample to the infrared beam, using a mobile support. The two sections are pressed together using a viton o-ring. The sample can be heated up to 400 °C, under vacuum and then moved to the infrared beam. Thus the sample is not exposed to the external environmental.[28] The equipment used was

a Shimadzu FTIR, model 8300. The spectra were obtained with a resolution of  $4\text{ cm}^{-1}$ , with 100 scans. The materials obtained by using HF and NaF as catalyst precursors were designated XHF $n$  and XNaF $n$ , respectively, where  $n$  specify the synthesis.

## Results

The vibrational mode of aniline ring at  $1500\text{ cm}^{-1}$  is very strong in the spectra, so the band area of this absorption was used to estimate the thermal stability of the immobilized aniline groups on the silica surface. The silica overtone band at *ca.*  $1865\text{ cm}^{-1}$  was used as a reference band.[11] This normalization was necessary, considering the heterogeneity in the disks thickness and taking into account the position changes of the infrared beam.

The FTIR spectra of xerogels obtained at room temperature, previously heat treated for 6 hours, at temperature range from 100 to  $400\text{ }^{\circ}\text{C}$ , are shown in the Figures 1, 2 and 3 for the synthesis 1, 2 and 3, respectively. In the XNaF1 sample, prepared with low amount of organic precursor (synthesis 1) and NaF as catalyst, the organic groups were not incorporated in the gel (Figure 1). For the XHF1 sample, prepared without NaF, the organic phase was incorporated, because the aniline band modes are present in the spectra even after thermal treatment (Figure 1 and Table 1). Since the organic band areas are related to the organic content, for the synthesis 2 and 3, where a greater precursor amount was added, it was observed an increasing in the organic content (Figures 2, 3 and Table 1). However, for the sample XNaF2, which NaF was used as catalyst, a lower organic content was observed when compared with the sample XHF2 catalyzed with HF (see Table 1). In the XNaF3 and XHF3 samples the decreasing in the organic incorporation, produced by  $\text{Na}^+$  presence, is not observed (Table 1).

The relative remaining organic grades obtained using the band area values (Table 1), are presented in the Figure 4. Six values were obtained for each temperature of treatment (1-6 hours) for each sample. All the samples maintain 100 % of the organic content after heat treatment up to  $200\text{ }^{\circ}\text{C}$  for 6 h. The organic grade begins to decrease for samples obtained from synthesis 2 and 3 after thermal treatment at  $300\text{ }^{\circ}\text{C}$  (Table 1). This decreasing was more visible for the XNaF2 and XNaF3 (Figure 2 and 3). All the samples

present a remaining organic grade even after heat treatment up to 400 °C for 6 hours. This remaining organic grade was inversely related to the organic content (Figure 4).

## Discussion

Considering that the organic band areas are related to the organic content of the xerogel materials, we observed that the organic content was related to the amount of the organic precursor added, since the band areas increase from synthesis 1 to 3 (Table 1). It was also observed that the Na<sup>+</sup> presence reduces the organic content for the samples from synthesis 1 and 2, with low amount of organic precursor added (Figures 1,2 and Table 1).

The relative remaining organic grade indicates the thermal stability of the organic attached groups. The great organic thermal stability observed for the samples heat treated up to 300 °C is an evidence that these groups are strongly bonded to the surface in the covalent form. Further thermal treatment up to 400 °C produces a partial organic desorption from the surface, as observed by the area reduction (Table 1 and Figure 4). It was possible to observe that the samples catalyzed with NaF present lower thermal stability than the samples synthesized without sodium. It is more evident for the synthesis 3 where the organic grade decreasing begins at 300 °C for XNaF3 sample while for the XHF3 this decreasing occurs after heating up to 400 °C (Figure 4). Therefore the more stable organic phase was obtained by using HF as catalyst and high organic precursor concentration *ie.* for XHF3 sample. This fact can be explained taking into account that the more concentrated is the APTMS precursor, closer will be the reactive organic methoxysilane groups and easier the linkage process occurs.[11] Therefore for larger concentration of APTMS added, more thermally stable is the organic phase, since a more linked organic structure was formed in the gelation process. The Na<sup>+</sup> influence was interpreted as an inhibitor of the organosilane linkage by avoiding its proximity.[29] This interpretation may explain also the absence of the infrared organic band in the XNaF1 sample, obtained from synthesis 1, with lower organic precursor concentration and catalyzed by NaF.

All the samples present a residual fraction of organic groups even after thermal treatment for six hours at 400 °C (Table 1 and Figure 1-4). This fact can be only explained taking into account the retention of the organic phase in closed silica pores formed during

the polycondensation and drying process. Considering the band area values found for the sample XHF1, after heat treatment at 400 °C, we can deduce that 85 % of the organic groups are trapped in closed pores (Figure 4). The samples obtained from the synthesis 2 present a lower fraction of organic trapped groups, 50 and 41 % for XHF2 and XNaF2, respectively. For the samples with higher organic loading the trapped organic groups fraction was the lowest, 24 and 27 % for XHF3 and XNaF3, respectively (Figure 4 and Table 1). Therefore the increasing in the organic content results in a decreasing in the fraction of organic trapped groups.

From the band areas of the FTIR spectra it was possible calculate the relative organic coverage *ie.* organic groups that are really on the surface, in opened pores. It was obtained subtracting the band area corresponding to the organic trapped groups from band areas of the organic total content. The resulting organic coverage is presented in the Figure 5. As the organic loading increases with the organic precursor concentration added (from synthesis 1 to 3) and simultaneously occurs a decreasing in the occluded porous fraction, the samples that present higher organic coverage are those obtained from the synthesis 3. The crescent organic coverage with the organic loading (Figure 5) was interpreted considering that the increasing in the APTMS/TEOS precursor ratio produces a less cross-linked silica network that results in a larger fraction of opened pores.[30-32]

## **Conclusions**

The FTIR thermal analysis technique was very effective to find the better synthesis conditions for anilinepropylsilica xerogel material, regarding to achieve a higher organic content, organic coverage and thermal stability. These characteristics, that are important for materials with potential applications in separation sciences, were obtained using high organic precursor amount and HF as catalyst.

## **Acknowledgement**

F. A. P and S. A. G. are indebted to CNPq and FAPERGS, respectively, for their grants.

## References

1. C. P. Jaroniec, M. Kruk, M. Jaroniec and A. Sayari, *J. Phys. Chem. B* 102 (1998) 5503.
2. M. Cichna, P. Markl, D. Knopp and R. Niessner, *Chem.Mater.* 9 (1997) 2640.
3. J. J. Kirkland, J. B. Adams, M. A. van Straten and H. A. Claessens, *Anal. Chem.* 70 (1998) 4344.
4. G. Felix and V. Descorps, *Chromatographia* 49 (1999) 595.
5. Y. Bereznitski and M. Jaroniec, *J. Chromatography A* 828 (1998) 51.
6. C. J. Brinker and G. W. Scherer, *Sol-Gel Science*, Academic Press; London, 1990.
7. O. Lev, M. Tsionsky, L. Rabinovich, V. Glazer, S. Sampath, I. Pankratov and J. Gun, *Anal. Chem.* 67 (1995) 22A.
8. M. M. Collinson, *Critical Rev. Anal. Chem.* 29 (1999) 289.
9. L. L. Hench and J. K. West, *Chem Rev.* 90 (1990) 33.
10. D. A. Loy and K. J. Shea, *Chem. Rev.* 95 (1995) 1431.
11. F. A. Pavan, L. Franken, C. A. Moreira, T. M. H. Costa, E. V. Benvenutti and Y. Gushikem, *J. Coll. Interf. Sci.* 241 (2001) 143.
12. G. Cerveau, R. J. P. Corriu, and C. Fischmeister-Lepeytre, *J. Mater. Chem.* 9 (1999) 1149.
13. T. N. M. Bernards, M. J. Van Bommel, and J. A. J. Jansen, *J. Sol-Gel Sci. Technol.* 13 (1998) 749.
14. P. W. J. G. Wijnen, T. P. M. Beelen, K. P. J. Rummens, H. C. P. L. Saeijs, J. W. Haan, L. J. M. van de Ven and R. A. van Santen, *J. Coll. interf. Sci.* 145 (1991) 17.
15. F. J. Arriagada, and K. Osseo-Asare, *J. Coll. Interf. Sci.* 170 (1995) 8.
16. E. Prouzet, and T. J. Pinnavaia, *Angew. Chem. Int. Ed. Engl.* 36 (1997) 516.
17. M. Zaharescu, A. Jitianu, A. Brăileanu, V. Bădescu, G. Pokol, J. Madarász and Cs. Novák, *J. Therm. Anal. Calorim.* 56 (1999) 191.
18. T. Eklund, L. Britcher, J. Bäckman and J. B. Rosenholm, *J. Therm. Anal. Calorim.* 58 (1999) 67.
19. B. R. Guidotti, E. Herzog, F. Bangerter, W. R. Caseri and U. W. Suter, *J. Coll. Interf. Sci.* 191 (1997) 209.
20. T. I. Desinova, *J. Therm. Anal. Calorim.* 62 (2000) 523.

21. P. Staszczuk, R. Nasuto and S. Rudy, *J. Therm. Anal. Calorim.* 62 (2000) 461.
22. V. M. Bogatyr'ov and M. V. Borysenko, *J. Therm. Anal. Calorim.* 62 (2000) 335.
23. T. C. Chang, Y. T. Wang, Y. S. Hong and Y. S. Chiu, *Thermochim. Acta* 372 (2001) 165.
24. J. Y. Ying, J. B. Benziger and A. Navrotsky, *J. Am. Ceram. Soc.* 76 (1993) 2561.
25. T. M. H. Costa, M. R. Gallas, E. V. Benvenutti and J. A. H. da Jornada, *J. Phys. Chem. B* 103 (1999) 4278.
26. T. M. H. Costa, M. R. Gallas, E. V. Benvenutti and J. A. H. da Jornada, *J. Non-Cryst. Solids* 220 (1997) 195.
27. F. A. Pavan, S. Leal, T. M. H. Costa, E. V. Benvenutti and Y. Gushikem, *J. Sol-Gel Sci. Technol.* in the press.
28. J. L. Foschiera, T. M. Pizzolato, E. V. Benvenutti, *J. Braz. Chem. Soc.* 12 (2001) 159.
29. F. A. Pavan, Y. Gushikem, C. C. Moro, T. M. H. Costa and E. V. Benvenutti, submitted to publication in 2001.
30. U. Schubert, N. Hüsing, A. Lorenz, *Chem. Mater.* 7 (1995) 2010
31. H. K. Kim, S. -J. Kang, S. -K. Choi, Y. -H. Min, C. -S. Yoon, *Chem. Mater.* 11 (1999) 779.
32. F. A. Pavan, W. F. de Magalhães, M. A. de Luca, C. C. Moro, T. M. H. Costa and E. V. Benvenutti, submitted to publication in 2001.

Table 1: Infrared band areas of aniline ring mode at 1500 cm<sup>-1</sup> on xerogel materials and the relative remaining organic grade calculated from these band areas.

Temp. (°C)	Time (hour)	Band area of aniline mode at 1500 cm <sup>-1</sup> / Abs.cm <sup>-1</sup> <sup>1</sup> (Relative remaining organic grade / %)				
		XHF1	XHF2	XNaF2	XHF3	XNaF3
100	6	0.34	2.02	0.54	2.54	2.32
200	1	0.40 (100)	2.06 (100)	0.60 (100)	2.61 (100)	2.65 (100)
	2	0.39 (98)	2.06 (100)	0.59 (98)	2.61 (100)	2.63 (99)
	3	0.39 (98)	2.07 (100)	0.60 (100)	2.61 (100)	2.63 (99)
	4	0.40 (100)	2.06 (100)	0.58 (97)	2.63 (101)	2.61 (98)
	5	0.39 (98)	2.04 (99)	0.57 (95)	2.63 (101)	2.61 (98)
	6	0.40 (100)	2.06 (100)	0.57 (95)	2.51 (96)	2.55 (96)
300	1	0.42 (105)	2.03 (99)	0.53 (88)	2.50 (96)	2.48 (94)
	2	0.40 (100)	2.04 (99)	0.52 (87)	2.51 (96)	2.23 (84)
	3	0.42 (105)	2.03 (99)	0.48 (80)	2.51 (96)	2.32 (88)
	4	0.41 (103)	2.02 (98)	0.48 (80)	2.52 (97)	2.14 (81)
	5	0.42 (105)	2.00 (97)	0.48 (80)	2.49 (95)	2.11 (80)
	6	0.41 (103)	1.98 (96)	0.46 (77)	2.46 (94)	2.09 (79)
350	1	0.41 (103)	1.86 (90)	0.46 (77)	2.43 (93)	1.47 (55)
	2	0.38 (95)	1.77 (86)	0.40 (67)	2.41 (92)	1.43 (54)
	3	0.38 (95)	1.67 (81)	0.42 (70)	2.38 (91)	1.16 (44)
	4	0.40 (100)	1.44 (70)	0.40 (67)	2.31 (89)	1.01 (38)
	5	0.40 (100)	1.43 (69)	0.38 (63)	2.17 (83)	0.95 (36)
	6	0.39 (98)	1.41 (68)	0.40 (67)	2.17 (83)	0.89 (34)
400	1	0.37 (93)	1.30 (63)	0.25 (41)	1.80 (69)	0.91 (34)
	2	0.36 (93)	1.31 (64)	0.26 (43)	0.73 (28)	0.85 (32)
	3	0.35 (88)	1.20 (58)	0.24 (40)	0.63 (24)	0.79 (30)
	4	0.35 (88)	1.20 (58)	0.24 (40)	0.64 (25)	0.73 (28)
	5	0.34 (85)	1.03 (50)	0.25 (41)	0.63 (24)	0.71 (27)
	6	0.34 (85)	1.04 (50)	0.25 (41)	0.63 (24)	0.71 (27)

<sup>1</sup> = band areas normalized with the silica overtone band at 1865 cm<sup>-1</sup>

## Captions of Figures

Figure 1: Infrared spectra of xerogel samples obtained by synthesis 1, after heating in vacuum, for 6 hours at: a) 100, b) 200, c) 300, d) 350 and d) 400 °C. The bar value is 0.2 and 0.1 for the spectra of the xerogels XHF1 and XNaF1, respectively.

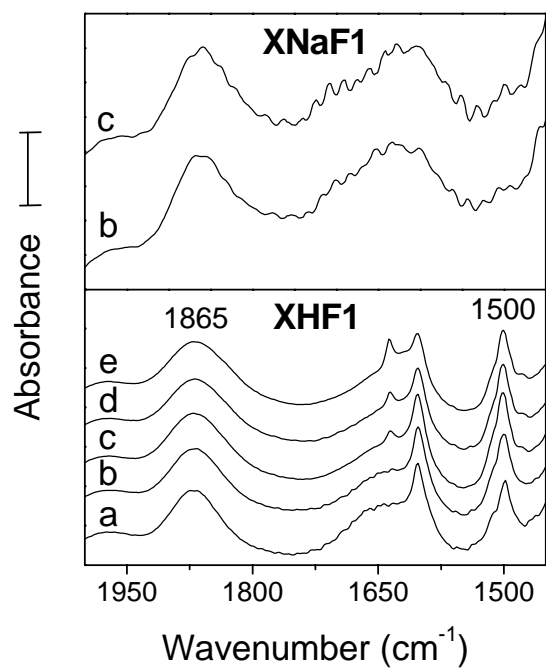
Figure 2: Infrared spectra of xerogel samples obtained by synthesis 2, after heating in vacuum, for 6 hours at: a) 100, b) 200, c) 300, d) 350 and d) 400 °C. The bar value is 1 and 0.4 for the spectra of the xerogels XHF2 and XNaF2, respectively.

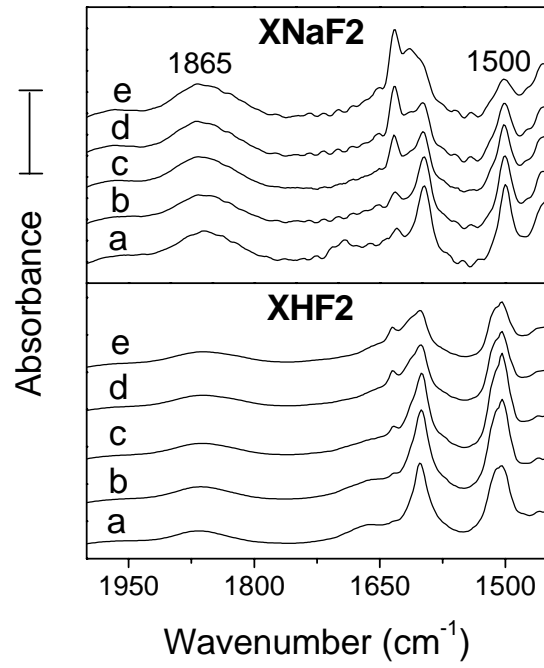
Figure 3: Infrared spectra of xerogel samples obtained by synthesis 3, after heating in vacuum, for 6 hours at: a) 100, b) 200, c) 300, d) 350 and d) 400 °C. The bar value is 1 for the spectra of the xerogels XHF3 and XNaF3.

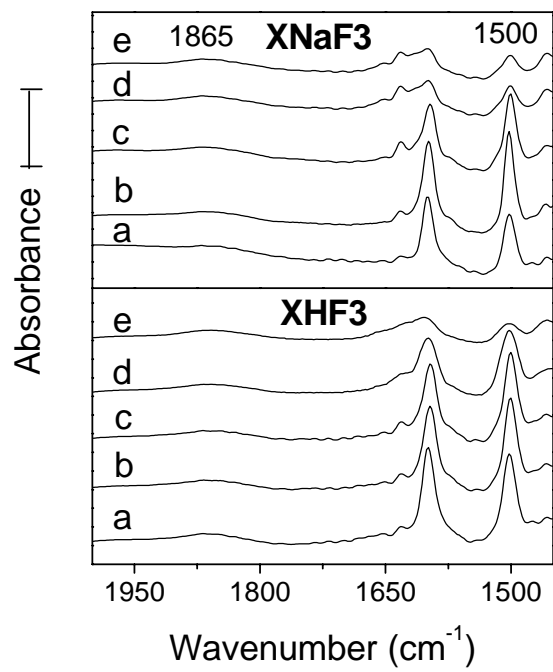
Figure 4: Relative remaining organic grade calculated from the relative band area of the infrared aniline band at  $1500\text{ cm}^{-1}$  in relation to the thermal treatment of the xerogels obtained from synthesis 1-3 using HF and NaF as precursor catalysts. For each temperature of treatment six measurements were made (1-6 h).

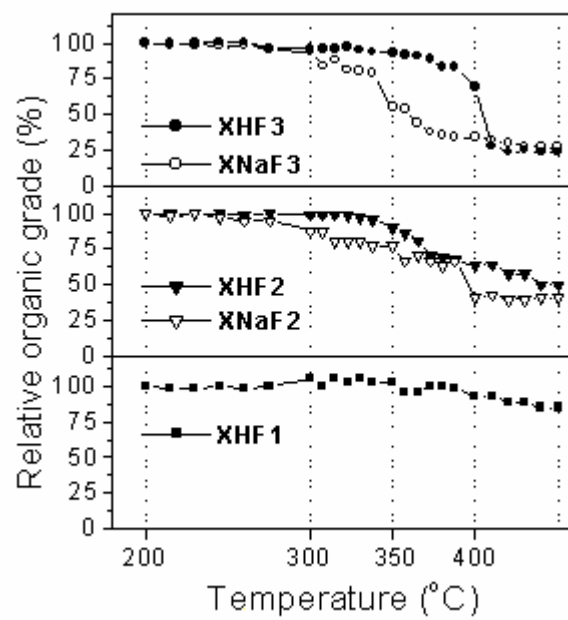
Figure 5: Relative organic content and organic coverage of the xerogel materials calculated from the band areas of the infrared aniline mode at  $1500\text{ cm}^{-1}$ .

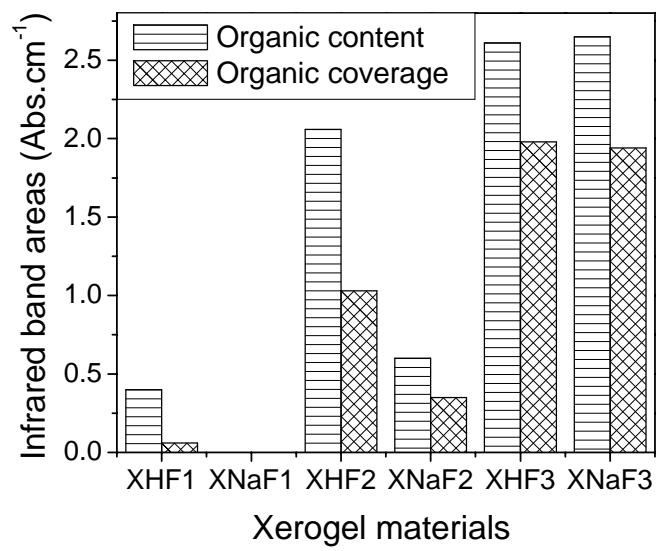












**ANEXO 5**

**4.5 - F. A. Pavan, S. A. Gobbi, C. C. Moro, T. M. H. Costa and E. V. Benvenuti. The Influence of the Amount of Fluoridre Catalyst on the Morphological Properties of the Anilinepropylsilica Xerogel Prepared in Basic Medium. *Journal of Porous Materials* 9: 307-311, 2002**

**The influence of the amount of fluoride catalyst on the morphological properties of the anilinepropylsilica xerogel prepared in basic medium.**

Flávio A. Pavan, Sidinei A. Gobbi, Celso C. Moro, Tania M. H. Costa, Edilson V. Benvenuti\*

LSS – Laboratório de Sólidos e Superfícies, Instituto de Química, UFRGS, CP 15003. 915019-70, Porto Alegre, RS, Brazil.

## **Abstract**

Anilinepropylsilica hybrid powder was synthesized by a sol-gel route in basic medium using HF as catalyst. The effect of the amount of HF catalyst on the morphologies and on organic content was studied. The xerogels were characterized using FTIR, SEM and N<sub>2</sub> adsorption-desorption isotherms. The increase in the HF quantity results in a slight increase in organic content and changes in the particle size, surface area and pore structure.



## Introduction

The sol-gel method is an attractive route to prepare hybrid organic-inorganic silica based materials.(1-4) These materials present interesting properties that provide them applications as sorbents, sensors, catalysts, optical and electrochemical devices.(5-8) The sol-gel synthesis can be performed at room temperature. The resulting materials exhibit good homogeneity and purity. This process consists of hydrolysis and polycondensation of metal alkoxides. In general, acid, basic or nucleophilic catalysts, that influence in the resulting crosslinked silica network are used. (9-11) Among the nucleophilic catalysts the fluoride ion has been often used, mainly in the form of HF.(12-14) However, it is reported that little changes in the parameters of the sol-gel synthesis, can result in great modifications of morphologies of the final materials.(11,14-18) In this context, the study on the synthesis conditions and resulting properties, is very important to understand these systems.

In this work the influence of the fluoride catalyst content on the properties of anilinepropylsilica xerogel was investigated. Infrared spectroscopy was used to identify the presence of the organic and inorganic phases. The organic phase content was obtained from CHN elemental analysis and the morphologies of xerogel were investigated using scanning electron microscopy and N<sub>2</sub> adsorption-desorption isotherms.

## Experimental

### *Synthesis of anilinepropylsilica xerogel*

The sol-gel synthesis used in this work has already been described elsewhere.(19) Firstly the organic precursor anilinepropyltrimethoxysilane (APTMS) was obtained as follows: Aniline was activated, for 30 minutes, with hydride using a mixture of aprotic solvents, toluene (5.0 ml) and THF (5.0 ml), and the 3-chloropropyltrimethoxysilane (CPTMS) was added. The amounts of aniline, NaH and CPTMS added were stoichiometric (8 mmol). The mixtures were stirred for 5 hours under argon at reflux temperature. The solution was centrifuged at 5000 rpm, for 20 minutes, in order to separate the NaCl, and the supernatant containing the APTMS was used as organic precursor in the gelation process.

In a second step, the sol-gel reaction was performed: The follow reagents were added, under stirring, to the solution containing the organic precursor (APTMS): 5 ml of tetraethylorthosilicate (TEOS), 5 ml of ethyl alcohol, 1.6 ml of water and 0.5, 1.0, 1.5, 3.0 and 4.0 mmol of HF for samples A-E, respectively. The gelation occurs on basic environment at pH between 9 and 10 (Table 1). The pH of solutions was measured using Universal indicator papers, supplied by Merck, pH range 0-14. The mixtures were stored for 5 days, just covered without sealing. The gel was then washed with toluene, THF, methanol, water and ethyl ether, and finally dried for 30 minutes in an oven at 100 °C.

#### *Elemental Analysis*

The organic phase content was obtained using a CHN Perkim Elmer M CHNS/O Analyzer, model 2400. The analysis was made in triplicate, after heating the materials at 100 °C, under vacuum, for 1 hour.

#### *Infrared Analysis*

Self-supporting disks of the samples were prepared with 5 cm<sup>2</sup> of area, weighing ca.100 mg. The disks were heated at 200 °C, under vacuum (10<sup>-3</sup> Torr) (1 Torr = 133.3 Pa), for 2 hour, using an IR cell.(20) The self-supporting disks were analyzed in the infrared region using a Shimadzu FTIR, model 8300. The spectra were obtained at room temperature with a resolution of 4 cm<sup>-1</sup>, with 100 scans.

#### *Scanning Electron Microscopy*

The materials were analyzed by scanning electron microscopy (SEM) in a Jeol equipment, model JSM 5800, with 20kV and 60000x of magnification. The average particle sizes were obtained by choosing and manually marking the diameter of a minimum of a hundred spherical particles in each image. The average diameters and the standard deviations were determined by using the Quantikov software.(21)

#### *Pore size distribution*

The pore size distribution was obtained by the nitrogen adsorption-desorption isotherms, determined at liquid nitrogen boiling point, using a homemade volumetric

apparatus, connected to a turbo molecular Edwards vacuum line system, employing a Hg capillary barometer and also an active Pirani gauge. The apparatus is frequently checked with alumina standard reference. The xerogel materials were previously degassed at 150 °C, in vacuum, for 2 hours. The data analysis was made using the BJH (Barret, Joyner, and Halenda) method.(22)

### *Surface Area*

The specific surface areas of the previous degassed solids at 150 °C, under vacuum, were determined by the BET (Brunauer, Emmett and Teller) (23) multipoint technique in the volumetric apparatus, cited above, using nitrogen as probe.

## **Results and Discussion**

The infrared spectroscopy has been an important tool in the hybrid xerogel characterization.(24) Figure.1 shows a typical infrared spectrum of hybrid xerogel materials, obtained at room temperature, after heat treatment at 200 °C, in vacuum. It shows the peaks of both organic and inorganic phases. The organic component can be identified by the bands at 1600 and 1500  $\text{cm}^{-1}$  corresponding to the aniline ring modes,(24) bands at 2930 and 3050  $\text{cm}^{-1}$  attributed to aliphatic and aromatic C-H stretching modes, respectively and the N-H stretching at 1410  $\text{cm}^{-1}$ .(19) The inorganic silica component can be identified from the silanol stretching bands with a maximum near 3615  $\text{cm}^{-1}$ , the Si-O-Si modes observed below 1250  $\text{cm}^{-1}$  and also the typical overtone bands near 1870  $\text{cm}^{-1}$ .(25-27) The presence of the organic phase in the sample heat treated at 200 °C in vacuum is an evidence that it is thermally very stable.(4,24).

Images obtained from scanning electron microscopy show a very similar spherical particles for all the samples, and a typical image are presented in Figure 2. However, it was possible to observe that the average size of aggregated particles undergoes a decrease with the HF quantity added. The average diameter decreases from 155 nm for the sample A, catalyzed with 0.5 mmol of HF, to 125 nm for sample E, catalyzed with 4.0 mmol of HF.

The values obtained for all samples (A-E) are presented in Table 1. The average diameters and the standard deviations were calculated using the Quantikov software.(21)

Table 1 presents some synthesis parameters and morphological data obtained from the N<sub>2</sub> adsorption-desorption isotherms. It was observed that the gelation time is strongly influenced by the presence of the fluoride catalyst (Table 1). The increase in the amount of HF catalyst produces a drastic reduction in the time of gelation. The organic phase content increases with the amount of fluoride added (Table 1).

Figure 3 shows typical type IV N<sub>2</sub> isotherms obtained for the xerogel samples, characteristic of mesopore materials.(28-31) The plateau of each isotherm was reached indicating the complete filling of the pores.(30,31) In general the desorption curves present a hysteresis at high relative pressure. This behavior could be explained considering the micropores presence,(30) or occurrence of a small capillary condensation,(28-30) possibly due to the organics presence. Nevertheless the hysteresis analysis for hybrid material is difficult, due to other network effects like disordered pore structure, presence of bottle shape pores,(32,33) N<sub>2</sub> network-percolation, etc.(31-33)

Figure 4 presents the pore size distribution analysis obtained from the N<sub>2</sub> adsorption-desorption isotherms by using the BJH calculation.(22) It was possible to observe in Figure 4 that the increase in the amount of HF produces some influences in the xerogel pore size distribution. For the materials catalyzed with 0.5, 1.0 and 1.5 mmol of HF, samples A, B and C, respectively, the pore diameters are predominantly lower than 4 nm. However for the samples catalyzed with 3.0 and 4.0 mmol of HF, samples D and E, respectively, the pore size distribution was broader, including pores with larger diameters, up to 6 nm. This larger distribution is more evident for the sample E (Figure 4). The pore size distribution enlargement was accompanied by the increasing pore volume (see Table 1). Therefore the amount of HF added produces an increase in the porosity of materials. The increase in the pore volume by the fluoride action was already reported in silica (34) and aluminosilicate systems.(35) In the present work the changes are not too impressive if compared with these works, possibly due to the large amount of organics present in the xerogels.

BET analysis shows an increase in the surface area from sample A to E. This surface area increasing with the amount of HF catalyst was interpreted considering two

components, the particle size decreasing and also the presence of a larger pore size distribution, as shown in Figure 4, that resulted in an increase in the pore volume of materials (Table 1). The increase in the pore volume by the fluoride action was already reported in silica (34) Nevertheless in the conditions presented in this work, all the property variations caused by HF action, were not so marked if compared with that produced by changing other synthesis parameters like pH medium,(11,14,16) solvent used (36) and gelation temperature.(37)

## **Conclusions**

The anilinepropylsilica xerogel presents spherical aggregated particles and the organic phase are thermally stable up to 200 °C, in vacuum. The increase in the amount of HF catalyst results in an increase in the amount of organics and also in the surface area. This surface area increase was attributed to the particle size decreasing and also the alterations in the pore structure with an increase in the porosity.

## **Acknowledgement**

F. A. P and S. A. G. are indebted to CNPq and FAPERGS, respectively, for their grants.

## References

1. H.K. Kim, S.J. Kang, S.K. Choi, Y.H. Min, and C.S. Yoon, *Chem. Mater.* 11, 779 (1999).
2. D.A. Loy, and K.J. Shea, *Chem. Rev.* 95, 1431 (1995).
3. N. Hüsing, U. Schubert, R. Mezei, P. Fratzl, B. Riegel, W. Kiefer, D. Kohler, and W. Mader, *Chem. Mater.* 11, 451(1999).
4. F.A. Pavan, L. Franken, C.A. Moreira, T.M.H. Costa, E.V. Benvenuti, and Y. Gushikem, *J. Colloid Interface Sci.* 241, 413 (2001).
5. D.R. Uhlmann, and G. Teowee, *J. Sol-Gel Sci. Technol.* 13, 153 (1998).
6. B.S. Bae, O.H. Park, R. Charters, B.L. Davies, and G.R. Atkins, *J. Mater. Res.* 16, 3184 (2001).
7. S.L. Chong, D. Wang, J.D. Hayes, B.W. Wilhite, and A. Malik, *Anal. Chem.* 69, 3889 (1997).
8. O. Lev, Z. Wu, S. Bharathi, V. Glezer, A. Modestov, J. Gun, L. Rabinovich, and S. Sampath, *Chem. Mater.* 9, 2354 (1997).
9. C.J. Brinker, and G.W. Scherer, *Sol-Gel Science* (Academic Press) London, 1990.
10. R.J.P. Corriu, D. Leclercq, *Angew. Chem. Int. Ed. Engl.* 35, 1420 (1996).
11. M.M. Collinson, *Crit. Rev. Anal. Chem.* 29, 289 (1999).
12. T.N.M. Bernards, M.J. Van Bommel, and J.A.J. Jansen, *J. Sol-Gel Sci. Technol.* 13, 749 (1998).
13. F.H.P. Silva, and H.O. Pastore, *Chem. Commun.* 833 (1996).
14. J.M. Kim, Y.J. Han, B.F. Chmelka, and G.D. Stucky, *Chem. Commun.* 2437 (2000).
15. K. Nakanishi, T. Nagakane, and N. Soga, *J. Porous. Mater.* 5, 103 (1998).
16. S. Rajeshkumar, G.M. Anilkumar, S. Ananthakumar, and K.G.K. Warriar, *J. Porous Mater.* 5, 59 (1998).
17. T. Caykara, and O. Guven, *J. Appl. Polym. Sci.* 70, 891 (1998).
18. N. Yamada, I. Yoshinaga, S. Katayama, *J. Porous Mater.* 14, 1720 (1999).
19. F.A. Pavan, S. Leal, T.M.H. Costa, E.V. Benvenuti, and Y. Gushikem, *J. Sol-Gel Sci. Technol.* 23, 129 (2002).

20. J.L. Foschiera, T.M. Pizzolato, and E.V. Benvenuti, *J. Braz. Chem. Soc.* 12, 159 (2001).
21. L.C.M. Pinto, PhD Thesis, Universidade de São Paulo, IPEN, 1996.
22. E.P. Barret, L.G. Joyner, and P.P. Halenda, *J. Am. Chem. Soc.* 73, 373 (1951).
23. S. Brunauer, P.H. Emmett, and E. Teller, *J. Am. Chem. Soc.* 60, 309 (1938).
24. F.A. Pavan, S.A. Gobbi, T.M.H. Costa, and E.V. Benvenuti, *J. Therm. Anal. Calorim.* 68, 199 (2002).
25. D.L. Wood, and E.M. Rabinovich, *Appl. Spectrosc.* 43, 263 (1989).
26. T.M.H. Costa, M.R. Gallas, E.V. Benvenuti, and J.A.H. da Jornada, *J. Non-Cryst. Solids* 220, 195 (1997).
27. R.M. Almeida, and C.G. Pantano, *J. Appl. Phys.* 68, 4225 (1990).
28. S. Brunauer, L.S. Deming, W.S. Deming, and E. Teller, *J. Am. Chem. Soc.* 62, 1723 (1940).
29. K.S.W. Sing, D.H. Everett, R.A.W. Haul, L. Moscou, R.A. Pierotti, J. Rouquérol, and T. Siemieniewska, *Pure Appl. Chem.* 57, 603 (1985).
30. S.J. Gregg, and K.S.W. Sing, *Adsorption, Surface Area and Porosity* (Academic Press) London, 1982..
31. K.S.W. Sing, *Adv. Coll. Interf. Sci.* 76-77, 3 (1998).
32. M.H. Lim, and A. Stein, *Chem. Mater.* 11, 3285 (1999).
33. C.J. Brinker, and G.W. Scherer, *J. Non-Cryst. Solids* 70, 301 (1985).
34. R.F. Silva, and W.L. Vasconcelos, *Mater. Res.* 2, 197 (1999).
35. C. Boissière, A. van der Lee, A.E. Mansouri, A. Larbot, and E. Prouzet, *Chem. Commun.* 2047 (1999).
36. G. Dubois, R.J.P. Corriu, C. Reyé, S. Brandès, F. Denat, and R. Guillard, *Chem. Commun.* 2283 (1999).
37. F.A. Pavan, H.S. Hoffmann, Y. Gushikem, T.M.H. Costa, and E.V. Benvenuti, *Mater. Letters* 55, 378 (2002).

Table 1: Synthesis parameters and morphological properties.

Sample	HF catalyst added mmol	Gelation medium pH $\pm$ 1	Elemental analysis mmol g <sup>-1</sup> <sup>a</sup>	Particle diameter nm <sup>b</sup>	Surface area m <sup>2</sup> g <sup>-1</sup>	Pore volume (cm <sup>3</sup> .g <sup>-1</sup> )	Gelation time hour
A	0.5	10	1,24	155	60	0.10	20
B	1.0	10	1,26	149	70	0.09	18
C	1.5	10	1,38	137	75	0.11	few minutes
D	3.0	10	1,54	129	80	0.13	instantaneous
E	4.0	9	1,54	125	93	0.17	instantaneous

<sup>a</sup> = mmol of aniline per gram of material.

<sup>b</sup> = standard deviation was lower than 30 nm.



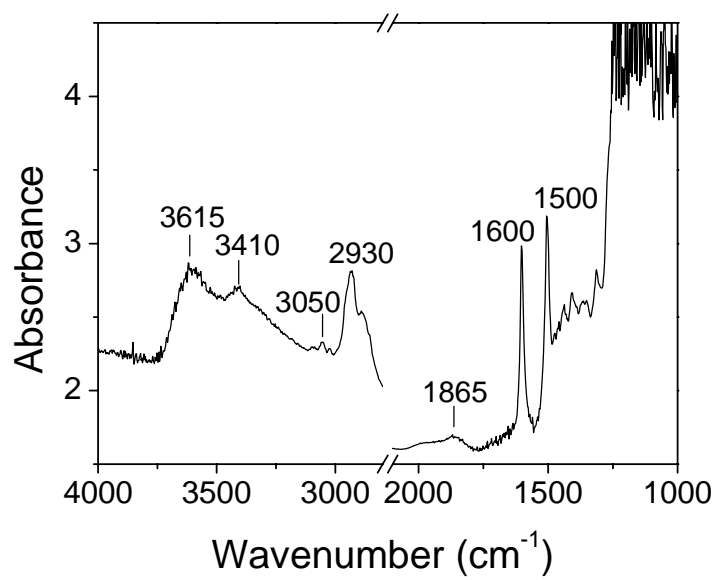
## Caption of Figures

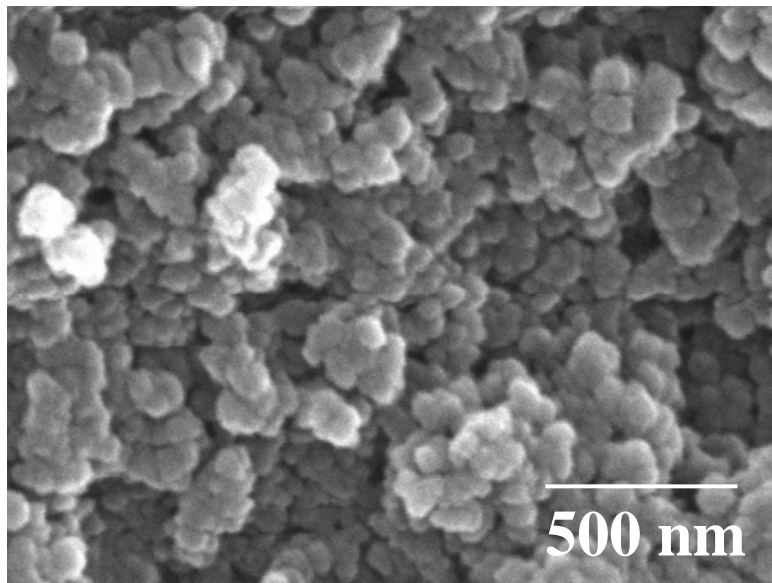
Figure 1: Infrared absorbance spectrum of anilinepropylsilica xerogel (sample E), obtained at room temperature, after heating at 200 °C, in vacuum, for 2 hour.

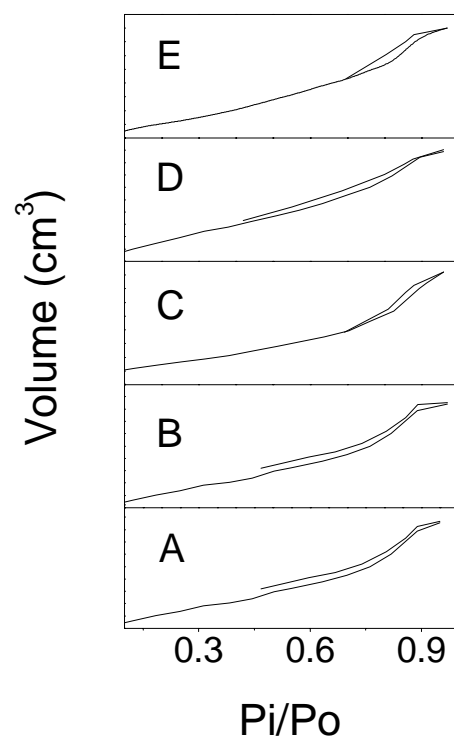
Figure 2: SEM image of anilinepropylsilica xerogel obtained from the synthesis B, with 60000 X magnification and 20 kV.

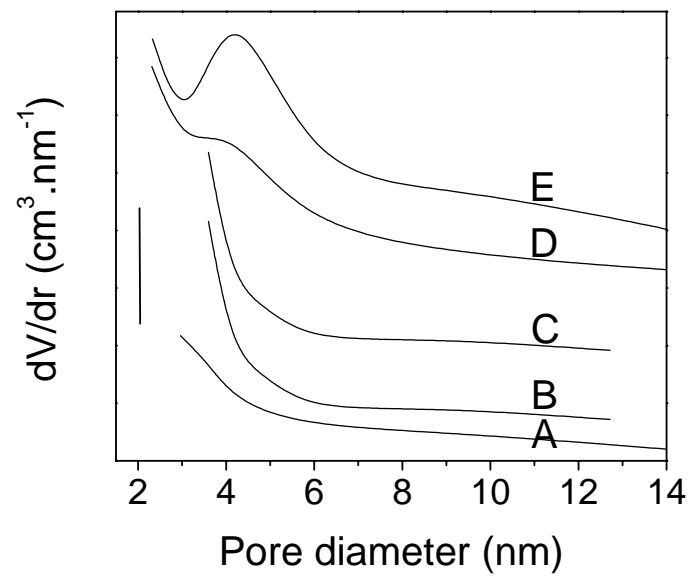
Figure 3: N<sub>2</sub> adsorption-desorption isotherms for anilinepropylsilica xerogel samples A-E.. The amount of HF catalyst added was: A) 0.5 mmol; B) 1.0 mmol; C) 1.5 mmol; D) 3.0 mmol; E) 4.0 mmol.

Figure 4: Pore size distribution of anilinepropylsilica xerogel samples A-E, obtained by using BJH method: The amount of HF catalyst added was: A) 0.5 mmol; B) 1.0 mmol; C) 1.5 mmol; D) 3.0 mmol; E) 4.0 mmol.









\* Corresponding Author: Edilson V. Benvenuti  
Phone: +55 51 3316 7209  
Fax: +55 51 3316 7304  
e-mail: [edilson@iq.ufrgs.br](mailto:edilson@iq.ufrgs.br)

Address: Instituto de Química, UFRGS, CP 15003.  
99501-970, Porto Alegre, RS, Brazil.

**Keywords:** amorphous materials, microporous materials, nanostructures, hybrid xerogels.

**ANEXO 6**

**4.6 - F. A. Pavan, S. A. H. S. Hoffmann, Y. Gushiken, T. M. H. Costa, E. V. Benvenuti. The gelation temperature effects in the anilinepropylsilica xerogel properties. *Materials Letters* 55, (2002) 378-382**



## The gelation temperature effects in the anilinepropylsilica xerogel properties

Flávio A. Pavan<sup>a</sup>, Helena S. Hoffmann<sup>a</sup>, Yoshitaka Gushikem<sup>b</sup>,  
Tania M.H. Costa<sup>a</sup>, Edilson V. Benvenuti<sup>a,\*</sup>

<sup>a</sup>LSS, Instituto de Química, UFRGS, CP 15003, 91501-970, Porto Alegre, RS, Brazil

<sup>b</sup>Instituto de Química, UNICAMP, CP 6154, 13083-970, Campinas, SP, Brazil

Received 14 October 2001; accepted 17 October 2001

### Abstract

The sol–gel method was employed to obtain the hybrid nanometric anilinepropylsilica material, using different temperatures of gelation. The resulting powder materials were studied by FTIR, thermogravimetric analysis (TGA), SAXS and scanning electron microscopy (SEM) techniques. The organic phase incorporated in the material was very thermally stable and the gelation temperature produces morphological effects in the resulting anilinepropylsilica material. © 2002 Elsevier Science B.V. All rights reserved.

PACS: 81.07.-b; 78.66.Vs

Keywords: Xerogel; Aniline; Thermal stability; Particle size; Pore size; Silica; Hybrid materials

### 1. Introduction

Over the decade, hybrid nanometric materials, synthesized by sol–gel method using alkoxysilanes R-Si(OR)<sub>3</sub> and tetraethylorthosilicate (TEOS) have been extensively studied [1–4]. This particled materials present distinct optical, magnetic and electronic properties due to its small size. These characteristics make these material ones very promising in different technological areas. The sol–gel method, described by

two steps, hydrolysis of the alkoxysilanes and polycondensation or gelation of the hydrolyzed silanes, is a very important and attractive synthesis procedure, since it can be performed at low temperatures, with high homogeneity and purity of the resulting materials [4–8]. This method allows to prepare hybrid xerogel nanometric materials, with the control of several physical properties. However, a little change in the parameter conditions of the synthesis, like solvent, catalyst or silane amount, can produce great modifications in the final properties of the materials [9–12]. In this context, the study of the synthesis conditions and the related resulting properties is very important to understand these systems. In this work, the anilinepropylsilica xerogel material was obtained from different temperatures of gelation. The thermal stability of

\* Corresponding author. Tel.: +55-51-3316-7209; fax: 55-51-3316-7304.

E-mail address: edilson@iq.ufrgs.br (E.V. Benvenuti).

the organic phase and some morphological properties of the powder material were investigated.

## 2. Experimental

### 2.1. Synthesis of xerogel materials

The sol–gel method used in this work follows the same procedures already described in details [13]. Aniline was activated with sodium hydride in 10 ml of a mixture of aprotic solvent (toluene/THF) (1:1) for 30 min, and the  $(\text{CH}_3\text{O})_3\text{Si}(\text{CH}_2)_3\text{Cl}$  (CPTMS) was added. The quantity used was stoichiometric for CPTMS, aniline and NaH, the value was 8.0 mmol. The mixture was stirred under argon at solvent-reflux temperature for a period of 5 h. The product of reaction, anilinepropyltrimethoxysilane (APTMS), was then used as sol–gel precursor reagent, in the concentration of  $0.80 \text{ mol l}^{-1}$ . After that, tetraethylorthosilicate (TEOS) (5 ml), ethyl alcohol (5 ml), HF (70  $\mu\text{l}$ ) and water in stoichiometric ratio with Si  $r=4/1$  (1.6 ml), were added to the precursor solutions, under stirring. The condensation occurs by a nucleophilic catalytic process using fluoridric acid, [11,14] at pH 10. The mixture was stored, just covered without sealing, at different controlled temperatures, 20, 30, 40 and  $50 \pm 1$  °C for gelation and evaporation of solvent. The resulting materials were designated A, B, C and D, respectively. The gels were then comminuted and washed exhaustively with various solvents and finally dried for 30 min in an oven at 100 °C.

### 2.2. Infrared measurements

Self-supporting disks of the material, with an area of  $5 \text{ cm}^2$ , weighing ca. 100 mg, were prepared. The disks were heated for 1 h at 300 °C, under vacuum ( $10^{-3}$  Torr), using an IR cell [15]. The self-supporting disks were analyzed in the infrared region using a Shimadzu FTIR, model 8300. The spectra were obtained with a resolution of  $4 \text{ cm}^{-1}$ , with 100 scans.

### 2.3. TGA analysis

The thermogravimetric analysis (TGA) was made using a TA Instruments 5100 analyser. The curves

were recorded at a heating rate of  $10 \text{ }^\circ\text{C min}^{-1}$  in argon atmosphere.

### 2.4. Surface area

The specific surface areas of the previous degassed solids at 150 °C, under vacuum, were determined by the BET multipoint technique on a volumetric apparatus, using nitrogen as probe.

### 2.5. Scanning electron microscopy

The materials were analyzed by scanning electron microscopy (SEM) with 20 kV and  $80,000 \times$  of magnification. The images were processed using the Quantikov software [16].

### 2.6. SAXS analysis

The average pore radii of the samples were obtained by using the Guinier law [17,18]. This law establish that the scattering intensities  $I(h)$  are described as  $\ln I(h) = \ln I_0 - (\text{RG}^2 h^2)/3$ , where RG is the gyration radii and  $h$  is defined as  $h = (4\pi \sin\theta)/\lambda$ , where  $\theta$  is the scattering angle and  $\lambda$  the wavelength of the X-ray used. The gyration radii could be calculated by the equation  $\text{RG} = (3p)^{1/2}$ , where  $p$  is the slope of the Guinier plot, ( $\ln(h)$  vs.  $h^2$ ). Considering spherical pores, the pore radii were obtained by the equation  $R_p = (5/3)^{1/2} \text{RG}$ . The equipment used was a Shimadzu XD3A equipment, with a Cu K $\alpha$  radiation source.

## 3. Results and discussion

Characteristics of the samples A, B, C and D, obtained at 20, 30, 40 and 50 °C of gelation temperatures are presented in Table 1. It was observed that the gelation time is inversely related with the gelation temperature and it is in accordance with other results found in the literature [19,20].

Generally, the nanometric hybrid materials obtained from the sol–gel method present good thermal stability of the organic phase, [12,21–24] and it was also observed in this work. In Fig. 1, shown is the infrared spectra of the materials obtained after heating up to 300 °C, in vacuum, and it was

Table 1  
Synthesis conditions, infrared data and morphological characteristics of the anilinepropylsilica xerogels

Sample	Gelation temperature (°C)	Gelation time (h)	IR band area (Abs cm <sup>-1</sup> ) <sup>a</sup>	Surface area (m <sup>2</sup> g <sup>-1</sup> )	Pore diameter (nm) <sup>b</sup>
A	20	48	0.20	166	3.9
B	30	48	0.21	145	3.7
C	40	30	0.35	120	3.9
D	50	15	0.49	63	3.7

<sup>a</sup> Obtained from the aniline mode at 1500 cm<sup>-1</sup> using the silica overtone band at 1860 cm<sup>-1</sup> as reference band.

<sup>b</sup> Obtained from SAXS measurements.

possible to observe that the infrared aniline absorption modes at 1600 and 1500 cm<sup>-1</sup> are present. These spectra reveal that the organic phase was incorporated in all samples and it is strongly bonded to the silica network, since the organic phase are present after this thermal treatment. The silica overtone band at ca. 1860 cm<sup>-1</sup> can be also visualized in the spectra. The aniline band at 1500 cm<sup>-1</sup> was used to estimate the comparative organic loading in the xerogel materials

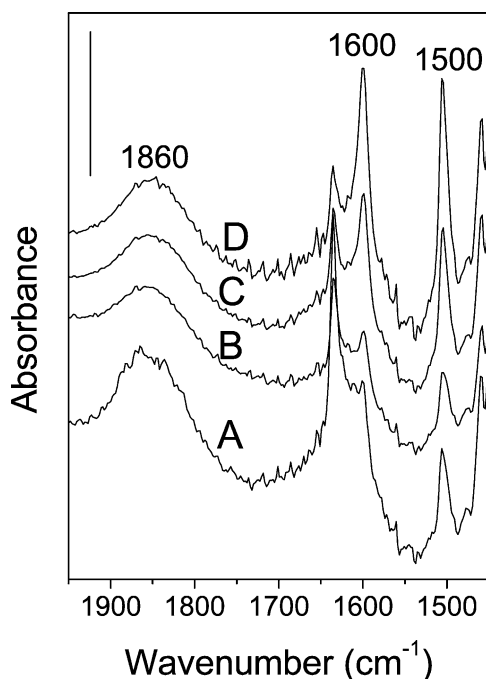


Fig. 1. Infrared absorption spectra of the anilinepropylsilica xerogel after being heat treated at 300 °C, in vacuum, for 1 h. The bar value is 0.5.

and the silica overtone band at ca. 1860 cm<sup>-1</sup> was used as a reference band. This normalization was necessary, considering the heterogeneity in the disks thickness obtained for the different samples. The band areas of the samples A, B, C and D are presented in Table 1. An increase in the band areas from the sample A to D was observed. Considering that the organic band areas are related to the organic content, the increase in the gelation temperature results in a crescent organic loading in the materials.

The great thermal stability of the organic attached groups can be confirmed by the thermogravimetric analysis (TGA), presented in Fig. 2. From the thermogravimetry, it was possible to observe that the organic phase is very stable at least to heat treatment at 400 °C, for the samples obtained in all gelation temperatures and times. In the thermogravimetric curves, from room temperature to 200 °C, there is a weight loss typical of the water desorption very common in silica materials. At 200 °C begins the dehydroxilation, i.e. conversion of silanol in siloxane groups, [25] and the organic phase desorption starting only after heating up to 400 °C.

The images obtained by scanning electron microscopy for the samples obtained in all gelation temper-

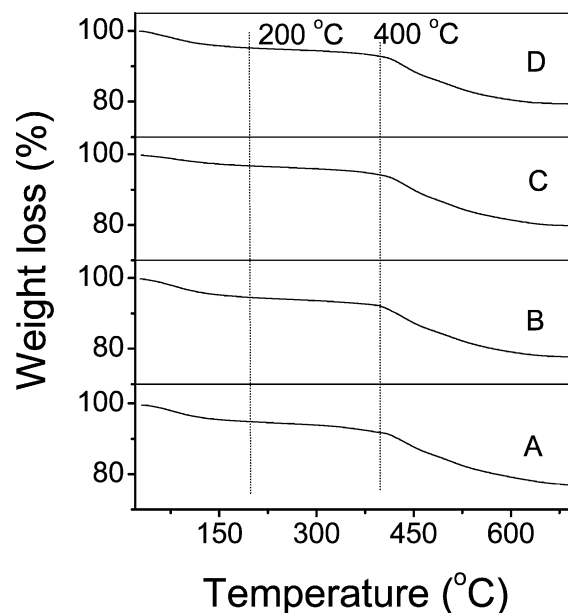


Fig. 2. Thermogravimetric curves for materials obtained from the syntheses A, B, C and D.

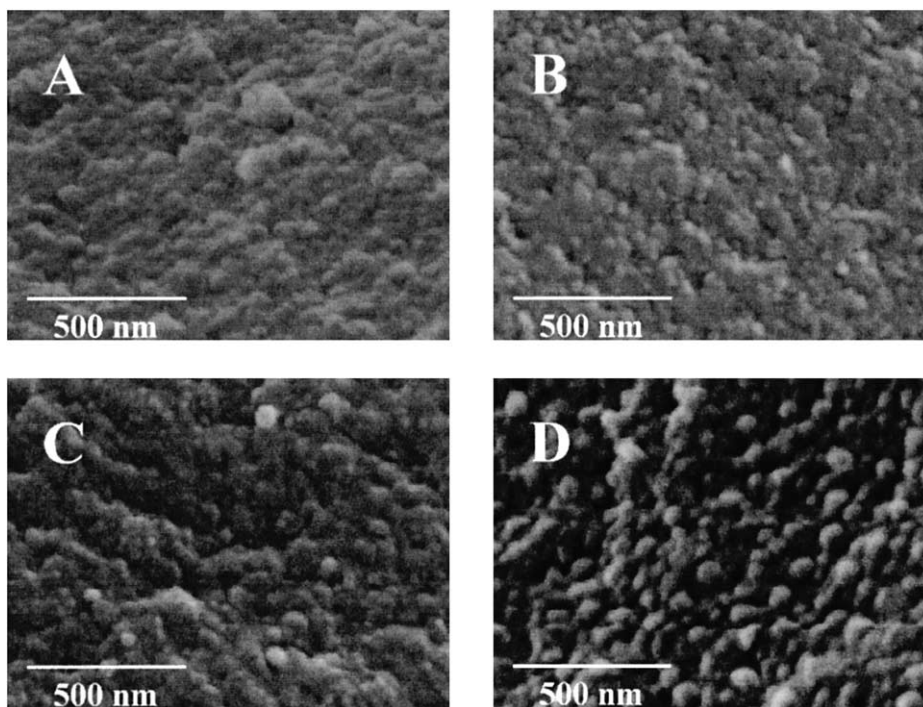


Fig. 3. SEM images of anilinepropylsilica xerogels obtained from the synthesis A, B, C and D, with  $80,000\times$  of magnification and 20 kV.

atures are presented in Fig. 3. In the images of the samples obtained from syntheses A and B, where the gelation process was carried out at 20 and 30 °C, respectively, the aggregated particles are not defined. Nevertheless, for the samples obtained from the synthesis C, at 40 °C of gelation temperature, there are few spherical particles formed and finally for the sample D, obtained at 50 °C of gelation temperature, the SEM image shows defined aggregated of spherical particles (Fig. 3). The average diameter of the spherical particles of the sample D, obtained using the Quantikov software [16], was achieved as 113 nm with a standard deviation of 20.

Another morphological difference observed for the samples synthesized at different gelation temperatures was the BET surface area. It is possible to observe in Table 1 that the increase in the gelation temperature produces a decrease in the surface area. On the other hand, no changes in the average pore diameter were observed from the SAXS analysis (Table 1), and it is in agreement with other papers, where the gelation temperature do not influences the pore size [26–28]. In this case the surface area decreasing with the

organic content could be explained by the surface organic coverage of the pores that results in a partial reduction in the accessibility to the pores. A decrease in the BET surface area produced by the increase of average aggregate particle size can not be discarded.

#### 4. Conclusions

The aniline was incorporated in a silica xerogel and the organic phase is very thermally stable. The increase in the gelation temperature results in a decrease in the gelation time and in an increase in the organic loading. The increase in the gelation temperature produces also morphological changes in the resulting material, such as a decrease in the surface area and the formation of spherical aggregated particles.

#### Acknowledgements

F.A.P. and H.S.H. are indebted to the CNPq for the grants.

## References

- [1] B. Boury, P. Chevalier, R.J.P. Corriu, P. Delord, J.J.E. Moreau, M.W. Chiman, *Chem. Mater.* 11 (1999) 281.
- [2] N. Yamada, I. Yoshinaga, S. Katayama, *J. Sol-Gel Sci. Technol.* 13 (1998) 445.
- [3] O. Lev, Z. Wu, S. Bharathi, V. Glezer, A. Modestov, J. Gun, L. Rabinovich, S. Sampath, *Chem. Mater.* 9 (1997) 2354.
- [4] D.A. Loy, K.J. Shea, *Chem. Rev.* 95 (1995) 1431.
- [5] O. Foussaier, M. Menetrier, J.J. Videau, E. Duguet, *Mater. Lett.* 42 (2000) 305.
- [6] O. Lev, M. Tsionsky, L. Rabinovich, V. Glezer, S. Sampath, I. Pankratov, J. Gun, *Anal. Chem.* 67 (1995) A22.
- [7] L.L. Hench, J.K. West, *Chem. Rev.* 90 (1990) 33.
- [8] U. Schubert, N. Hüsing, A. Lorenz, *Chem. Mater.* 7 (1995) 2010.
- [9] M.M. Collinson, *Crit. Rev. Anal. Chem.* 29 (1999) 289.
- [10] T. Caykara, O. Guven, *J. Appl. Polym. Sci.* 70 (1998) 891.
- [11] R.J.P. Corriu, D. Leclercq, *Angew. Chem., Int. Ed. Engl.* 35 (1996) 1420.
- [12] D.A. Loy, J.V. Beach, B.M. Baugher, R.A. Assink, K.J. Shea, J. Tran, J.H. Small, *Chem. Mater.* 11 (1999) 3333.
- [13] F.A. Pavan, S. Leal, T.M.H. Costa, E.V. Benvenutti, Y. Gushikem, *J. Sol-Gel Sci. Technol.*, in press.
- [14] T.N.M. Bernards, M.J. Van Bommel, J.A.J. Jansen, *J. Sol-Gel Sci. Technol.* 13 (1998) 749.
- [15] J.L. Foschiera, T.M. Pizzolato, E.V. Benvenutti, *J. Braz. Chem. Soc.* 12 (2001) 159.
- [16] L.C.M. Pinto, PhD Thesis, Universidade de São Paulo, IPEN, 1996.
- [17] A. Guinier, G. Fournet, *Small-Angle Scattering of X-Ray*, Wiley, New York, 1955.
- [18] O. Glatter, O. Kratky, *Small Angle X-Ray Scattering*, Academic press, London, 1982.
- [19] M.W. Colby, A. Osaka, J.D. Mackenzie, *J. Non-Cryst. Solids* 82 (1986) 37.
- [20] K.T. Chou, B.I. Lee, *Ceram. Int.* 19 (1993) 315.
- [21] F.A. Pavan, L. Franken, C.A. Moreira, T.M.H. Costa, E.V. Benvenutti, Y. Gushikem, *J. Colloid Interface Sci.* 241 (2001) 143.
- [22] H.K. Kim, S.J. Kang, S.K. Choi, Y.H. Min, C.S. Yoon, *Chem. Mater.* 11 (1999) 779.
- [23] F.A. Pavan, S.A. Gobbi, T.M.H. Costa, E.V. Benvenutti, *J. Therm. Anal. Calorim.*, submitted for publication.
- [24] Y. Wei, D.C. Yang, R. Baktavatchalam, *Mater. Lett.* 13 (1992) 261.
- [25] T.M.H. Costa, M.R. Gallas, E.V. Benvenutti, J.A.H. da Jornada, *J. Non-Cryst. Solids* 220 (1997) 195.
- [26] T.W. Chung, T.S. Yeh, T.C.K. Yang, *J. Non-Cryst. Solids* 279 (2001) 145.
- [27] R.F. Silva, W.L. Vasconcelos, *Mater. Res.* 2 (1999) 197.
- [28] M. Misheva, N. Djourellov, F.M.A. Margaca, I.M.M. Salvato, *J. Non-Cryst. Solids* 279 (2001) 196.

**ANEXO 7**

**4.7 - F. A. Pavan, A. M. S. Lucho, R. S. Gonçalves, T. M. H. Costa and E. V. Benvenuti. Anilinepropylsilica xerogel used as a selective Cu(II) adsorbent in aqueous solution. *Journal Colloid Interface Science* 20003, 668**

Note

# Anilinepropylsilica xerogel used as a selective Cu (II) adsorbent in aqueous solution

Flávio A. Pavan, Alzira M.S. Lucho, Reinaldo S. Gonçalves, Tania M.H. Costa, and Edilson V. Benvenutti \*

*Instituto de Química UFRGS, C.P. 15003, 91501-970, Porto Alegre, RS, Brazil*

Received 25 October 2002; accepted 13 March 2003

## Abstract

The metal ion adsorption properties of the microporous hybrid anilinepropylsilica xerogel were studied using divalent copper, zinc, and cadmium ions in aqueous solutions in concentrations ranging from  $10^{-4}$  up to  $5 \times 10^{-3} \text{ mol l}^{-1}$ . At low concentrations the surface of the solid phase presents selectivity for Cu (II), even in competitive conditions. This preferential sorption ability for copper in relation to zinc and cadmium ions was interpreted by considering the xerogel morphology.

© 2003 Elsevier Inc. All rights reserved.

*Keywords:* Sol–gel; Metal ion adsorption; Anodic stripping voltammetry

## 1. Introduction

Hybrid materials have been obtained by the immobilization of chelating organic groups on silica surfaces by grafting reactions. Among the several potential applications of these materials, the use as a metal adsorbent has been noticed [1–3]. However, the hybrids prepared in this way rarely surpass  $0.3 \text{ mmol g}^{-1}$ , which is very small if compared with organic resins. Furthermore, considerable efforts have been devoted in order to overcome the lack of selectivity presented by these materials [2–6].

In recent years new hybrid materials have been developed using the sol–gel method [6,7]. Although this method has shown attractiveness due to the possibility of controlling the physicochemical properties of the resulting materials, they are not extensively used as metal ion sorbents. There are some reports of using hybrid sol–gel materials containing sulfur or nitrogen as donor atoms to remove metal ions selectively from aqueous solutions [8–10].

In recent papers, we have presented a synthesis procedure to obtain a nanoparticle anilinepropylsilica xerogel [11]. The material presented a microporous structure with the organic phase covalently bonded. In this work, the metal ion ad-

sorption properties of this material, anilinepropylsilica, was investigated using copper, zinc, and cadmium in aqueous solutions. In competitive conditions, the metal adsorption was evaluated using anodic stripping voltammetry.

## 2. Materials and methods

### 2.1. Sol–gel synthesis

The sol–gel synthesis used in this work has already been described elsewhere [11]. Aniline was activated for 30 min with sodium hydride using a mixture of aprotic solvents, toluene (5.0 ml) and THF (5.0 ml), and 3-chloropropyltrimethoxysilane was added. The amounts of aniline, NaH, and 3-chloropropyltrimethoxysilane were stoichiometric (10 mmol). The mixtures were stirred for 5 h under argon at reflux temperature. The solution was centrifuged at 5000 rpm for 20 min, separating the byproduct NaCl, and the supernatant containing the anilinepropyltrimethoxysilane was used as organic precursor in the gelation process. To this solution was added, under stirring, tetraethylorthosilicate (TEOS) (5 ml), ethyl alcohol (5 ml), water (1.6 ml) in stoichiometric ratio,  $\text{H}_2\text{O}/\text{Si} = 4/1$ , and HF (1.5 mmol). The gelation occurs on a basic environment at pH 10. The pH of the solutions was determined using Universal indicator papers, supplied by Merck, pH range 0–14.

\* Corresponding author.

E-mail address: [edilson@iq.ufrgs.br](mailto:edilson@iq.ufrgs.br) (E.V. Benvenutti).

The mixtures were stored for 5 days, just covered without sealing. The resulting material, designated as anilinepropylsilica xerogel, was then washed with toluene, THF, methyl alcohol, water, and ethyl ether and finally dried for 30 min in an oven at 100 °C.

## 2.2. Metal adsorption isotherms

The adsorption isotherms of metal ions were obtained at 25 °C in water solution by a batch technique. About 0.1 g of the anilinepropylsilica xerogel was immersed in 50 ml of metal halide solution with variable concentration. The mixture was shaken for 1 h, considering that in previous experiments the equilibrium was reached after 15 min. The metal ion adsorption capacity of the solid phase ( $N_f$ ), obtained in the saturation plateau, was calculated by applying the equation  $N_f = (N_a - N_s)/m$ , where  $N_a$  is the initial metal quantity added,  $N_s$  is the metal quantity present in the solution, in equilibrium with the solid phase, and  $m$  is the weight of the solid phase. The metal ion quantities in the solution phase were determined by complexometric titration using 0.01 mol l<sup>-1</sup> EDTA standard solution.

## 2.3. Anodic stripping voltammetry

The solution containing the test ions was analyzed in order to determine the amount of the metal ion remaining after the contact with the anilinepropylsilica xerogel. Anodic stripping voltammetry measurements were carried out with a Model 264A polarographic analyzer/stripping voltammeter from EG&G. Current/potential curves were recorded with a Model RE0150 XY recorder from EG&G. The ions were reduced on a Model 303A static mercury electrode (SMDE) from EG&G. The electrochemical cell was adapted to the working electrode system with a saturated calomel electrode as reference and a platinum wire as auxiliary electrode. The aqueous solutions containing the test ions and KCl, 0.10 mol l<sup>-1</sup>, as supporting electrolyte were deaerated with pure nitrogen around 20 min prior to the measurements. The temperature was kept constant at 25 °C.

## 3. Results and discussion

The morphological properties of the hybrid xerogel used in this work have already been reported [12]. The results obtained by using positron annihilation spectroscopy and N<sub>2</sub> adsorption–desorption isotherms showed mainly the presence of micropores, smaller than 3 nm. The average pore diameter was 1.8 nm. The surface area and pore volume were 140 m<sup>2</sup> g<sup>-1</sup> and 0.10 cm<sup>3</sup> g<sup>-1</sup>, respectively. Furthermore, the hybrid xerogel shows a high thermal stability, indicating that the organic groups are bonded in the covalent form [12]. However, in this kind of material there is a fraction of organics trapped in closed pores, near 25% [13]. The elemental CHN analysis confirms the presence of the

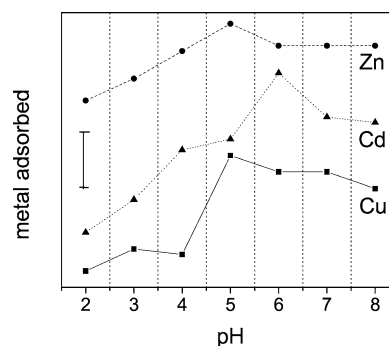


Fig. 1. Anilinepropylsilica xerogel metal ion adsorption capacity from aqueous solution, obtained at 25 °C, at different pH values. The bar value is 0.01 mmol g<sup>-1</sup>.

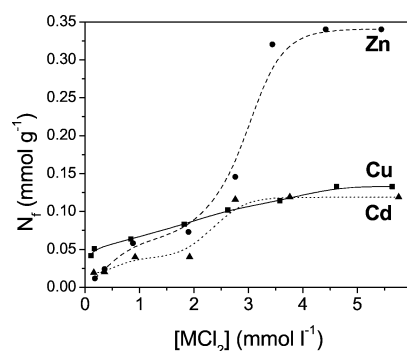


Fig. 2. Metal ion adsorption isotherms from aqueous solution, at 25 °C.

organic phase in this xerogel. The achieved organic content was very extensive, larger than that obtained by the grafting process [3,14], 1.3 mmol of aniline groups per gram of xerogel.

Considering that the pH of the medium is an important factor controlling the limit of extractability of the metal ions by the solid phases, the metal uptake capacity of the hybrid xerogel was first investigated at pH ranging from 2 to 8, using the batch equilibrium method after a shaking time of 1 h. From Fig. 1 we can see that the best pH range for the adsorption of divalent copper, zinc, and cadmium ions was between 5 and 6. Thus, the ability of the hybrid xerogel to adsorb these cations through the complexation process was evaluated by isotherms, using pH 5.5. The results are shown in Fig. 2.

It can be observed in Fig. 2 that the saturation plateau was reached for Zn (II) and Cd (II) isotherms, and the metal ion adsorption capacity values ( $N_f$ ) were 0.34 and 0.11, respectively. The Cu (II) isotherm will be discussed below. The best metal adsorption capacity was observed for zinc; however the value was ca. four times lower than the adsorption capacity estimated from the organic content. This fact can be interpreted by considering that a large fraction of the organics on the surface are not available due to the presence of closed pores containing entrapped organic matter [13]. Additionally, the anilinepropylsilica xerogel used in this work presents a predominantly microporous struc-



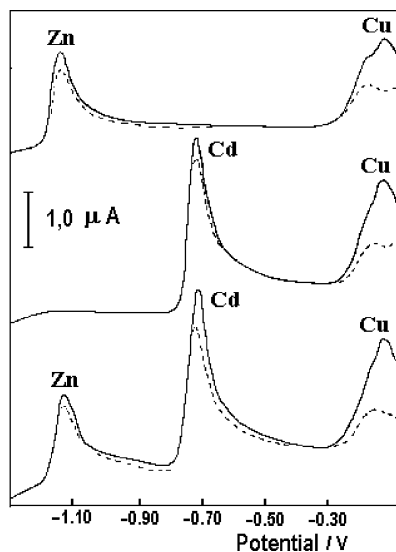


Fig. 3. Current  $\times$  potential curves for the electrooxidation of the metal present in the solution (—) before and (---) after the adsorption equilibrium.

ture [12], so that the sorption process is controlled by the ion diffusion.

Using the Giles classification scheme [15], the isotherm obtained for zinc and cadmium in Fig. 2 was similar to the subgroup 4–L type; however in the copper case, the curve seems be of the subgroup 2–C type. According to Giles, the C type isotherm is not common and occurs when the availability of the sites remains constant for all concentrations up to saturation. This situation can be reproduced in a microporous structure [3,15]. In the present work, the subgroup 2–C-type isotherm was observed only for copper, and this fact can only be interpreted by taking into account its smaller size. The aqueous ionic radii of copper, zinc, and cadmium ions were 0.059, 0.069, and 0.095 nm, respectively [16]. Thus the isotherm behavior was interpreted as a consequence of metal diffusion in the micropores. The copper mobility through the micropores should be higher because its small size.

Another interesting consequence of these results can be obtained when the isotherms are analyzed in the low concentration range. It can be observed in Fig. 2 that below  $1.8 \text{ mmol l}^{-1}$ , the metal uptake was higher for copper than zinc and cadmium. In order to gain a better understanding, diluted mixture solutions of ions, copper, zinc, and cadmium, were analyzed in a competitive situation. The metal ion solutions were submitted to contact with the hybrid xerogel (shaken for 1 h) and were analyzed by anodic stripping voltammetry. The strategy used in this technique was to keep the SMDE electrode polarized at  $-1.20 \text{ V}$  (SCE) for 15 min in order to reduce all metal ions present in the solutions. After that, the potential of the electrode shifted to more positive values at constant sweep rate  $0.10 \text{ mV s}^{-1}$  in order to reoxidize the metals. The obtained voltammetric curves, before and after the adsorption equilibrium, are presented in Fig. 3. The charge associated with the reoxidation of the ions was

Table 1  
Competitive metal ion adsorption selectivity of anilinepropylsilica xerogel obtained by anodic stripping voltammetry

Metal ion solution	Cu (II) selectivity (%)
Cu (II) + Zn (II)	66
Cu (II) + Cd (II)	69
Cu (II) + Zn (II) + Cd (II)	86

calculated directly from the current peaks of each species. The electrooxidation of each metal occurs of an independent and specific potential. Another important result is related to the current values obtained for metal solutions after equilibrium. The amount of the reoxidized metal was clearly lower after the contact with hybrid xerogel than that obtained before the contact. This means that a fraction of the ions were adsorbed by the xerogel. However, it is clear that the amount of remaining copper ion was lower than that of the other ones. In order to visualize this copper affinity with the xerogel surface, the charge values were used to estimate the selectivity,  $S$ , using the equation

$$S (\%) = \frac{Q_T - Q_{Eq}}{Q_T} \times 100, \quad (1)$$

where  $Q_T$  and  $Q_{Eq}$  are the charges of metal reoxidation before and after the adsorption equilibrium, respectively.

The estimated selectivity for copper ion in each solution, obtained from the band area of the voltammetric curves, is presented in the Table 1. A surface selectivity for copper ion is clearly observed in the studied conditions. These results agree with those obtained from adsorption isotherms presented in Fig. 2. Therefore, this hybrid xerogel is a promising material for Cu (II) clean-up from water in the presence of Zn (II) and Cd (II).

## Acknowledgments

F.A.P and A.M.S.L. are indebted to CNPq and Capes for their grants.

## References

- [1] L.N.H. Arakaki, A.N. de Souza, J.G.P. Espinola, S.F. Oliveira, C. Airoidi, J. Colloid Interface Sci. 249 (2002) 290.
- [2] T. Meyer, S. Prause, S. Spange, M. Friedrich, J. Colloid Interface Sci. 236 (2001) 335.
- [3] M.G. Fonseca, J.G.P. Espinola, S.F. Oliveira, L.C.R. dos Santos, A.G. Souza, C. Airoidi, Colloids Surf. A 133 (1998) 205.
- [4] M.E. Mohamed, E.M. Soliman, Talanta 44 (1997) 15.
- [5] A.M. Liu, K. Hidajat, S. Kawi, D.Y. Zhao, Chem. Commun. (2000) 1145.
- [6] Y.L. Zub, H.W. Rocsy, M.M. Malyar, A.A. Chuiko, M. Jaroniec, R. Murugavel, Solid State Sci. 3 (2001) 169.
- [7] F.A. Pavan, L. Franken, C.A. Moreira, T.M.H. Costa, E.V. Benvenutti, Y. Gushikem, J. Colloid Interface Sci. 241 (2001) 413.
- [8] J. Brown, L. Mercier, T.J. Pinnavaia, Chem. Commun. (1999) 69.

- [9] J. Seneviratne, J.A. Cox, *Talanta* 52 (2000) 801.
- [10] M.C. Burleigh, S. Dai, E.W. Hagaman, J.S. Lin, *Chem. Mater.* 13 (2001) 2537.
- [11] F.A. Pavan, S. Leal, Y. Gushikem, T.M.H. Costa, E.V. Benvenuti, *J. Sol–Gel Sci. Technol.* 23 (2002) 129.
- [12] F.A. Pavan, W.F. de Magalhães, M.A. de Luca, C.C. Moro, T.M.H. Costa, E.V. Benvenuti, *J. Non-Cryst. Solids* 311 (2002) 54.
- [13] F.A. Pavan, S.A. Gobbi, T.M.H. Costa, E.V. Benvenuti, *J. Therm. Anal. Calorim.* 68 (2002) 199.
- [14] J.L. Foschiera, T.M. Pizzolato, E.V. Benvenuti, *J. Braz. Chem. Soc.* 12 (2001) 159.
- [15] C.H. Giles, T.H. MacEwan, S.N. Nakhwa, D. Smith, *J. Chem. Soc.* (1960) 3973.
- [16] Y. Marcus, *J. Solution Chem.* 12 (1983) 271.

**ANEXO 8**

**4.8 - F. A. Pavan, T. M. H. Costa, E. V. Benvenuti. Adsorption of  $\text{CoCl}_2$ ,  $\text{ZnCl}_2$  and  $\text{CdCl}_2$  on aniline/silica hybrid material obtained by sol-gel method. *Colloid and Surface A: Physicochemical and Engineering Aspects* (trabalho aceito)**

**Adsorption of CoCl<sub>2</sub>, ZnCl<sub>2</sub> and CdCl<sub>2</sub> on aniline/silica hybrid material obtained by sol-gel method**

Flávio A . Pavan, Tania M. H. Costa, Edilson V. Benvenutti\*

LSS – Laboratório Sólidos e Superfícies, Instituto de Química UFRGS, CP 15003, 91501-970, Porto Alegre, RS, Brazil

\* Corresponding Author: Edilson V. Benvenutti  
Instituto de Química, UFRGS.  
CP 15003  
91501-970, Porto Alegre, RS, Brazil.  
Phone: 55 51 3316 7209  
Fax: 55 51 3316 7304  
e-mail: edilson@iq.ufrgs.br

## **Abstract**

The hybrid aniline/silica material was obtained by using the sol-gel synthesis. The hybrid material, characterized by FTIR and N<sub>2</sub> adsorption-desorption isotherms, shows a mesoporous structure. The metal ion adsorption capacity of the material was investigated by using the batch technique with CoCl<sub>2</sub>, ZnCl<sub>2</sub> and CdCl<sub>2</sub> in aqueous and ethanol solutions, at room temperature. It was observed that the metal ion adsorption capacity was strongly influenced by the solvent used. It was higher in ethanol than in aqueous solution. The metal adsorption capacity order was CdCl<sub>2</sub> > ZnCl<sub>2</sub> > CoCl<sub>2</sub> in ethanol solution and the inverse order in aqueous solution.

**Key words:** xerogel, hybrid material, porous material, metal sorption, organofunctionalized silicas.

## Introduction

The search for new sorbent materials with high metal adsorption capacity and selectivity have been growing in the recent years [1-3]. These sorbent materials can be used in analytical procedures with environmental chemistry interest. Among the large variety of the used adsorbents, organofunctionalized silicas are very common. Usually they were obtained by the immobilization of chelating organic groups on the surface by using grafting reactions [3-6]. However, in the last decade, a new class of organofunctionalized silicas arose, by using the sol-gel synthesis method. This method is based on hydrolysis and polycondensation of silicon alcoxides in basic or acidic medium. These new materials, commonly denominated as hybrid xerogels, can be obtained in mild reaction conditions, that allow the incorporation of organic functional chelating groups without damage, with controlled morphology [7-10]. The resulting hybrid xerogels, that present an homogeneous distribution of the organic groups on surface, are promising as metal sorbents. However, the sol-gel synthesis method was not extensively explored for this using. There are very few papers reporting hybrid xerogels used as metal sorbents [10-18] Among the cited papers some presented high adsorption capacity and selectivity for some pollutant metals like  $\text{Cu}^{+2}$ ,  $\text{Hg}^{+2}$  and  $\text{Sr}^{+2}$  [10-13]. Nowadays the extraction of metals cobalt, zinc and cadmium from wastewater have been also reported using different sorbents and process [19,20].

In the present work, we obtained a mesoporous aniline/silica sorbent material by using the sol-gel synthesis method. The hybrid material was characterized by  $\text{N}_2$  adsorption-desorption isotherms, CHN elemental analysis and infrared spectroscopy. The metal adsorption capacity of this material was investigated using aqueous and ethanol solutions of  $\text{CoCl}_2$ ,  $\text{ZnCl}_2$  and  $\text{CdCl}_2$  in the concentration range from  $10^{-4}$  to  $10^{-2}$  mol  $\text{dm}^{-3}$ .

## Experimental

### *Aniline/silica material synthesis*

The sol-gel synthesis used in this work has been already described elsewhere [21]. Aniline was activated, for 30 min, with sodium hydride using a mixture of aprotic solvents, toluene (5.0 cm<sup>3</sup>) and THF (5.0 cm<sup>3</sup>), and the 3-chloropropyltrimethoxysilane (CPTMS) was added. The amounts of aniline, NaH and CPTMS added were stoichiometric (8.0 mmol). The mixture was stirred for 5 h under argon at reflux temperature. The solution was centrifuged at 5000 rpm, for 20 min, to separate the byproduct NaCl, and the supernatant containing the anilinepropyltrimethoxysilane (APTMS) was used as organic precursor in the gelation process. In this solution it was added, under stirring, the tetraethylorthosilicate (TEOS) (5.0 cm<sup>3</sup>), ethyl alcohol (5.0 cm<sup>3</sup>), water (1.6 cm<sup>3</sup>), in stoichiometric ratio H<sub>2</sub>O/Si = 4/1 and HF (1.5 mmol). The gelation occurs on basic environment at pH 10. The mixture was stored for 5 days, just covered without sealing. The gel was then washed with toluene, THF, ethyl alcohol, water and ethyl ether, and finally dried for 30 min in an oven at 100 °C.

### *Elemental Analysis*

The organic phase content was obtained using a CHN Perkin Elmer M CHNS/O Analyzer, model 2400. The analysis was made in triplicate, after heating the material at 100 °C, under vacuum, for 1 h.

### *Infrared Analysis*

A self-supporting disk of the sample was prepared with 5 cm<sup>2</sup> of area, weighing ca. 100 mg. The disk was heated at 300 °C, under vacuum (10<sup>-2</sup> Torr) (1 Torr = 133.3 Pa), for 2 h, using a IR cell [22]. The self-supporting disk was analyzed in the infrared region using a Shimadzu FTIR, model 8300. The spectrum was obtained at room temperature with a resolution of 4 cm<sup>-1</sup>, with 100 scans.

### *Pore size distribution*

The pore size distribution was obtained by the N<sub>2</sub> adsorption-desorption isotherm, determined at liquid nitrogen boiling point, using a homemade volumetric apparatus, connected to turbo molecular Edwards vacuum line system, employing a Hg capillary

barometer and also an active Pirani gauge. The apparatus is frequently checked with alumina standard reference. The hybrid material was previously degassed at 150 °C, in vacuum, for 2 h. The data analysis was made using the BJH (Barret, Joyner, and Halenda) method [23].

#### *Surface Area*

The specific surface area of the previous degassed solid at 150 °C, under vacuum, was determined by the BET (Brunauer, Emmett and Teller) [24] multipoint technique in the volumetric apparatus, cited above, using nitrogen as probe.

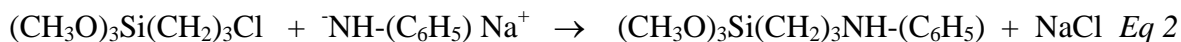
#### *Metal chloride adsorption isotherms*

The adsorption isotherms of metal chloride were obtained at 25 °C in aqueous and ethanol solutions using the batch technique. About 0.1 g of the aniline/silica material was immersed in 50 cm<sup>3</sup> of metal halide solution (Co(II), Zn(II) and Cd(II)), with variable concentration, at pH 5.5 for the aqueous solution. The mixture was shaken for 1 h. The metal adsorption capacity of the solid phase ( $N_f$ ), was calculated by applying the equation  $N_f = (N_a - N_s) / m$ , where  $N_a$  is the initial metal quantity added,  $N_s$  is the metal chloride quantity present in solution, at the equilibrium with the solid phase, and  $m$  is the mass of the solid phase. The metal quantities remaining in the solutions were determined by complexometric titration using 0.01 mol dm<sup>-3</sup> EDTA standard solution.

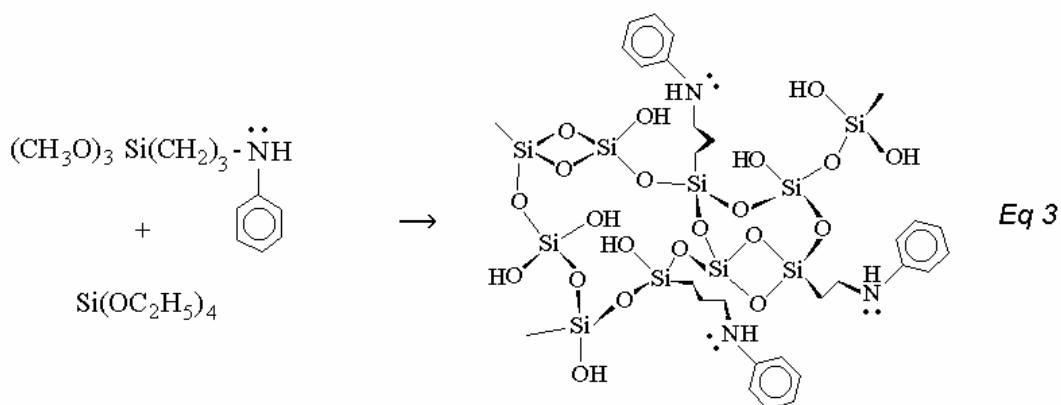
### **Results and discussion**

The synthesis procedure of the organic precursor anilinepropyltrimethoxysilane, was already described.[21] In the reaction of aniline with 3-chloropropyltrimethoxysilane, firstly the aniline was activated with sodium hydride in aprotic solvent mixture, as illustrated in Equations 1 and 2. The use of NaH as base activator results in drastic reduction in the reaction time [21]. Furthermore, the insoluble byproduct NaCl can be easily separated from the organic medium by centrifugation. In the absence of NaH there is a formation of HCl, that reacts with the aniline, resulting in the anilinium salt, which is more difficult to separate from the organic medium [22].





The organic precursor obtained in the Equation 2, anilinepropyltrimethoxysilane was then added to the inorganic precursor solution containing TEOS, water and HF, to gelation. The resulting hybrid material was assigned as aniline/silica. The gelation step is illustrated by the Equation 3.



The organic incorporation value obtained by using the CHN elemental analysis was 1.4 mmol of aniline groups per gram of material.

The immobilization of the aniline groups on the matrix surface was also confirmed by the infrared analysis showed in the Figure 1. It can be observed the typical spectra of hybrid material, with both components, organic and inorganic phases. The inorganic component can be identified from the Si-O-Si modes observed below  $1250 \text{ cm}^{-1}$ , the typical silica overtone bands at *ca.*  $1870 \text{ cm}^{-1}$  and the silanol stretching bands above  $3500 \text{ cm}^{-1}$ . The organic phase is clearly identified by the bands at  $1600$  and  $1500 \text{ cm}^{-1}$  corresponding to the aniline ring modes, bands at  $3060$  and  $2930 \text{ cm}^{-1}$ , attributed to aromatic and aliphatic C-H stretching modes, respectively, and also the N-H stretching at  $3410 \text{ cm}^{-1}$  [21]. The presence of the organics in the samples heat treated at  $300 \text{ }^\circ\text{C}$ , in vacuum, is an evidence of the high thermal stability of the organic phase, bonded in the covalent form as represented by the Eq 3.

The  $\text{N}_2$  adsorption-desorption isotherm of material is presented in the Figure 2. The curve was a typical type IV isotherm, characteristic of mesopore material [25,26]. The desorption curve presents hysteresis at high relative pressure ( $P/P_0 > 0.7$ ) and it was

interpreted considering the possibility of a small capillary condensation, possibly due to the organics presence. The pore size distribution curve, obtained by using BJH calculus [23], is presented in Figure 3. It was possible to observe that the material presents a mesoporous structure. The surface area and pore volume obtained were  $80 \text{ m}^2 \text{ g}^{-1}$  and  $0.10 \text{ cm}^3 \text{ g}^{-1}$ , respectively.

The shaking time condition for the metal chloride adsorption was previously evaluated using metal aqueous solution ( $10^{-2} \text{ mol dm}^{-3}$ ) according to the results showed in Table 1. The metal adsorption equilibrium was attained after 15 minutes. Therefore we have considered that the shaking time used in the bath experiments (1 h) was sufficient to reach the sorption equilibrium.

The metal adsorption isotherms of the hybrid aniline/silica material obtained in aqueous and ethanol solutions are shown in Figure 4. Using the Giles classification scheme [27], the isotherm curves were similar to subgroup 4 – L type. This kind of isotherms appears when the metal sorption occurs in different sites [28,29]. The first plateau was interpreted as due to the chelating groups while the second one was interpreted as a consequence of the other surface sites due to some matrix heterogeneity, basic centers or silica matrix itself adsorption.

Considering only the first plateau, it was observed a higher metal adsorption capacity of the aniline/silica material in ethanol than in water solution. This behavior was already reported for grafted silicas and it was interpreted taking into account a more effective interaction of the surface sites with water than with ethanol molecules [30], which sequence of metal adsorption capacity was the same for both solvents. However, in the present paper, the sequence of metal adsorption capacity was  $\text{CoCl}_2 > \text{ZnCl}_2 > \text{CdCl}_2$  in aqueous solution and the inverse order in ethanol solution. The low adsorption capacity of organofunctionalized silicas for cobalt in organic solvents was already reported and it was interpreted considering the metal solvation effects and the lower enthalpy of metal chelation. Thermochemical data showed a drastic decrease in the enthalpy for the interaction of divalent cobalt with similar surface sites in organic solvents [31].

The best metal adsorption capacity of the material was reached for cadmium chloride from ethanol solution ( $0.49 \text{ mmol g}^{-1}$ ). The metal adsorption capacities were similar to those reported by others using grafted surfaces [28,30,32,33]. Nevertheless, in the present work, the metal adsorption capacities were low when compared with the quantity of chelating groups present in the material ( $1.4 \text{ mmol g}^{-1}$ ). The lower values in

relation to the amine sites quantity was interpreted considering the blocking pores by the organics [34-37] due to a large quantity of organic groups presents in closed pores or in inaccessible small pores that were detected in large amount, as showed in Figure 3. Additionally the interactions such hydrogen bond between the amine groups could reduce the availability of the chelating groups.

## **Conclusions**

The hybrid aniline/silica sol-gel material was obtained with a mesoporous structure. The hybrid material showed positive results in metal chloride adsorption experiments, using Co(II), Zn(II) and Cd(II) from aqueous and ethanol solutions. The metal adsorption capacity sequence was  $\text{CoCl}_2 > \text{ZnCl}_2 > \text{CdCl}_2$  in aqueous solution and the inverse order in ethanol solution. The best adsorption capacity was reached for  $\text{CdCl}_2$  from ethanol solution.

## **Acknowledgement**

F. A. P is indebted to CNPq for his grant.

## References

1. A. M. Liu, K. Hidajat, S. Kawi and D. Y. Zhao, *Chem. Commun.*, (2000) 1145.
2. L. N. H. Arakaki, A. N. de Souza, J. G. P. Espinola, S. F. Oliveira and C. Airoidi, *J. Colloid Interface Sci.*, 249 (2002) 290.
3. M. E. Mahmoud and E. M. Soliman, *Talanta*, 44 (1997) 15.
4. M. G. Fonseca, J. G. P. Espinola, S. F. Oliveira, L. C. R. dos Santos, A. G. Souza and C. Airoidi, *Colloids Surf. A: Physicochem. Eng. Aspects*, 133 (1998) 205.
5. L. A. M. Gomes, P. M. Padilha, J. C. Moreira, N. L. D. Filho and Y. Gushikem, *J. Braz. Chem. Soc.*, 9 (1998) 494.
6. U. Deschler, P. Kleinschmit and P. Panster, *Angew. Chem. Int. Ed. Engl.*, 25 (1986) 236.
7. K. J. Shea and D. A. Loy, *Chem. Mater.*, 13 (2001) 3306.
8. F. A. Pavan, H. S. Hoffmann, Y. Gushikem, T. M. H. Costa and E. V. Benvenutti, *Mater. Lett.*, 55 (2002) 378.
9. U. Schubert, N. Hüsing and A. Lorenz, *Chem. Mater.*, 7 (1995) 2010.
10. H. J. Im, Y. Yang, L. R. Allain, C. E. Barnes, S. Dai and Z. Xue, *Environ. Sci. Technol.*, 34 (2000) 2209.
11. J. Brown, L. Mercier and T. J. Pinnavaia, *Chem. Commun.*, (1999) 69.
12. T. L. Yost, B. C. Fagan, L. R. Allain, C. E. Barnes, S. Dai, M. J. Sepaniak and Z. Xue, *Anal. Chem.*, 72 (2000) 5516.
13. B. Lee, Y. Kim, H. Lee, J. Yi, *Micropor. Mesopor. Mater.*, 50 (2001) 77.
14. J. Seneviratne and J. A. Cox, *Talanta*, 52 (2000) 801.
15. R. F. de Farias, A. G. de Souza, L. M. Nunes, and V. A. Cardoso, *Colloids Surf. A: Physicochem. Eng. Aspects*, 211 (2002) 295.
16. M. C. Burleigh, S. Dai, E. W. Hagaman and J. S. Lin, *Chem. Mater.*, 13 (2001) 2537.
17. J. C. P. Vaghetti, M. Z. K. R. S. Bentes, L. S. Ferreira, E. V. Benvenutti and E. C. Lima, *J. Anal. At. Spectrom.*, 18 (2003) 376.
18. I. M. El-Nahhal, B. A. El-Shetary, K. A. R. Salib, N. M. El-Ashgar and A. M. El-Hashash, *Anal. Letters*, 34 (2001) 2189.
19. J. S. Kim and J. Yi, *J. Chem. Technol. Biootechnol.*, 75 (2000) 359.
20. E. I. El-Shafey, M. Cox, A. A. Pichugin and Q. Appleton, *J. Chem. Technol. Biootechnol.*, 77 (2002) 429.

21. F. A. Pavan, S. Leal, Y. Gushikem, T. M. H. Costa and E. V. Benvenutti, *J. Sol-Gel Sci. Technol.*, 23 (2002) 129.
22. J. L. Foschiera, T. M. Pizzolato and E. V. Benvenutti, *J. Braz. Chem. Soc.*, 12 (2001) 159.
23. E. P. Barret, L. G. Joyner and P. P. Halenda, *J. Am. Chem. Soc.*, 73 (1951) 373.
24. S. Brunauer, P. H. Emmett and E. Teller, *J. Am. Chem. Soc.*, 60 (1938) 309.
25. S. J. Gregg and K. S. W. Sing, *Adsorption, Surface Area and Porosity*, Academic Press, London, 1982, Chapter 3 and 4.
26. K. S. W. Sing, *Adv. Coll. Interf. Sci.*, 76-77 (1998) 3.
27. C. H. Giles, T. H. MacEwan, S. N. Nakhwa and D. Smith, *J. Chem. Soc.*, (1960) 3973.
28. W. C. Moreira, Y. Gushikem and O. R. Nascimento, *J. Colloid Interface Sci.*, 150 (1992) 115.
29. T. Sismanoglu and S. Pura, *Colloids Surf. A: Physicochem. Eng. Aspects*, 180 (2001) 1.
30. A. G. S. Prado and C. Airoidi, *Anal. Chim. Acta*, 432 (2001) 201.
31. C. Airoidi and E. F. C. Alcântara, *J. Chem. Thermodynamics*, 27 (1995) 623.
32. A. M. Lazarin and Y. Gushikem, *J. Braz. Chem. Soc.*, 13 (2002) 88.
33. S. T. Fujiwara, Y. Gushikem and R. V. S. Alfaya, *Colloids Surf. A: Physicochem. Eng. Aspects*, 178 (2001) 135.
34. F. A. Pavan, W. F. de Magalhães, M. A. de Luca, C. C. Moro, T. M. H. Costa and E. V. Benvenutti, *J. Non-Cryst. Solids*, 311 (2002) 54.
35. B. Boury, R. J. P. Corriu and V. Le Strat, *Chem. Mater.*, 11 (1999) 2796.
36. L. Mercier and T. J. Pinnavaia, *Environ. Sci. Technol.*, 32 (1998) 2749.
37. J. C. D. da Costa, G. Q. Lu, and V. Rudolph, *Colloids Surf. A: Physicochem. Eng. Aspects*, 179 (2001) 243.

## **Caption of Figures**

Figure 1: Infrared absorbance spectra of aniline/silica material, obtained at room temperature, after been heated up to 300 °C, in vacuum.

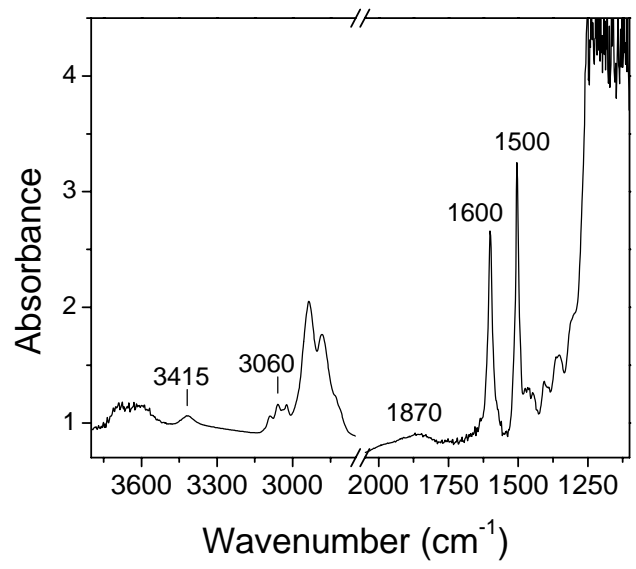
Figure 2: N<sub>2</sub> adsorption-desorption isotherms of aniline/silica material.

Figure 3: Pore size distribution of aniline/silica material, obtained by using BJH method.

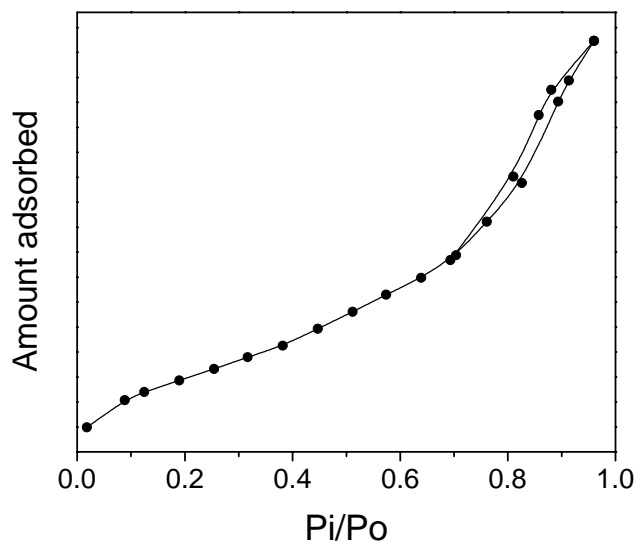
Figure 4: Metal chloride adsorption isotherms of the aniline/silica material, obtained at 25 °C in aqueous and ethanol solutions.

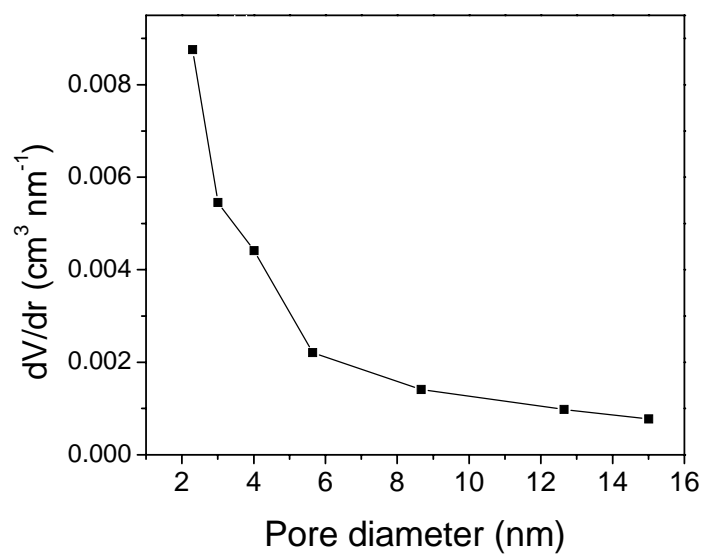
Table 1. Metal chloride adsorption capacity of the aniline/silica material in aqueous medium.

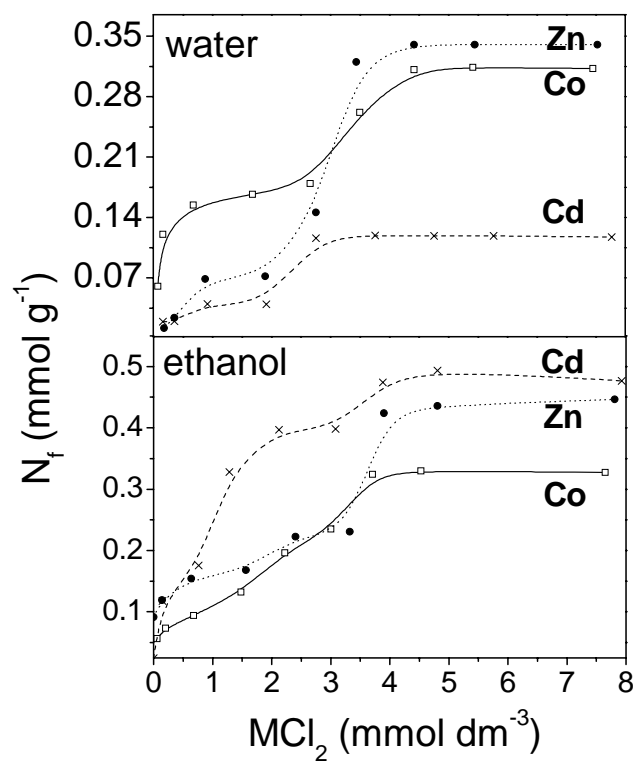
Metal chloride	Shaking time (min)	Adsorption capacity (mmol g <sup>-1</sup> )
CoCl <sub>2</sub>	5	0.24
	10	0.27
	15	0.30
	30	0.31
	120	0.31
CdCl <sub>2</sub>	5	0.05
	10	0.07
	15	0.11
	30	0.10
	120	0.11
ZnCl <sub>2</sub>	5	0.25
	10	0.31
	15	0.35
	30	0.34
	120	0.34











## 5. CONCLUSÕES

No presente trabalho foi obtido o precursor orgânico anilina-propiltrimetoxissilano de um modo satisfatório a partir da reação de anilina com 3-cloropropiltrimetoxissilano, usando-se hidreto de sódio como ativador básico. O uso de hidreto de sódio como ativador da base anilina, para a reação de substituição nucleofílica, diminuiu drasticamente o tempo da reação.

A partir da policondensação do precursor orgânico anilina-propiltrimetoxissilano em presença de tetraetilortossilicato obteve-se o xerogel híbrido anilina-propilsilica. Este xerogel foi obtido com diferentes frações de matéria orgânica (de 0,26 até 1,40 mmol g<sup>-1</sup>). A interface orgânica-inorgânica do xerogel anilina-propilsilica apresentou ligações covalentes. A fase orgânica mostrou-se termicamente estável, em alto vácuo, até a temperatura de 300 °C. Os xerogéis apresentam partículas nanométricas esféricas (*ca.* 100 nm) e estrutura de mesoporos. Uma fração de matéria orgânica encontrou-se ocluída em poros fechados.

O conteúdo orgânico incorporado influenciou significativamente as propriedades morfológicas do xerogel. O aumento da incorporação orgânica resultou em diminuição na área superficial, volume de poros e tamanho de poros. Entretanto, observou-se um ligeiro aumento no tamanho das partículas primárias. Quanto maior o grau de incorporação orgânica, menor foi a fração de orgânicos ocluídos em poros fechados.

Outros parâmetros de síntese também foram estudados como temperatura de policondensação, tipo e concentração de catalisador utilizado.

O aumento da temperatura de policondensação resultou em maior incorporação de matéria orgânica, menor tempo de policondensação e menor área superficial do xerogel, além de propiciar a formação de partículas mais esféricas e maiores.

Comparando-se o uso de HF e NaF como catalisador observou-se que os materiais obtidos usando-se HF apresentaram maior estabilidade térmica da fase orgânica. A presença do íon Na<sup>+</sup>, proveniente do NaF, diminuiu o grau de incorporação da matéria orgânica e inibe o crescimento das partículas primárias. Propõem-se que o íon Na<sup>+</sup> interage eletrostaticamente com os oxigênios do precursor orgânico hidrolisado inibindo sua policondensação. A preferência do íon Na<sup>+</sup> pelo precursor orgânico hidrolisado em relação ao ácido silícico, proveniente da hidrólise do tetraetilortossilicato, deve-se ao fato de que o primeiro apresenta-se mais nucleofílico devido ao efeito indutivo do grupo orgânico.

O aumento da quantidade de catalisador HF usado resultou em materiais com maior tamanho médio de poros e maior área superficial.

Através do conhecimento adquirido sobre a influência das variáveis de síntese nas propriedades finais do xerogel, foi possível estabelecer estratégias de sínteses que permitiram preparar um material híbrido seletivo para extração de íons Cu(II), em solução aquosa, na presença de Zn(II) e Cd(II), em concentrações equimolares. O xerogel também mostrou-se promissor como adsorvente de cádmio, zinco e cobalto em meio etanólico.

Com a realização deste trabalho acreditamos ter sido possível contribuir para o melhor entendimento das questões relacionadas a química do processo sol-gel de materiais híbridos, no que tange aos efeitos causados pelas variáveis aqui estudadas. Portanto, a partir dos resultados aqui apresentados, será possível traçar estratégias de síntese para arquitetar materiais com propriedades específicas, como por exemplo, grau de incorporação orgânica, tamanho e forma de partículas, tamanho de poros e área superficial.

## **6. SUGESTÕES PARA TRABALHOS FUTUROS**

- Otimizar a etapa de síntese do precursor orgânico, através da purificação do NaH, facilitando a separação do precursor orgânico de outros concomitantes indesejáveis;
- Estudar a influência de outras variáveis tais como: quantidade de água, surfactantes, solvente, pH etc, durante a polimerização dos precursores alcóxidos, nas propriedades finais dos híbridos;
- Conduzir estudos sobre as propriedades mecânicas e óticas dos híbridos anilina/sílica;
- Investigar a potencialidade de aplicação dos híbridos anilina/sílica na extração de outros metais e poluentes como também na adsorção de compostos orgânicos de interesse ambiental.

## 7. ANEXOS

### TRABALHOS APRESENTADOS EM CONGRESSOS NACIONAIS E INTERNACIONAIS

1. Estudo Comparativo de Retenção de Organoclorados em Sílica Quimicamente modificada,  
*Livro de Resumos do 10<sup>o</sup> Encontro Nacional de Química Analítica - ENQA*, Santa Maria,  
RS, 1999
2. Synthesis of Starionary Phase Based on Silica Orfanofunctionalized With Aromatic  
Groups.  
*Livro de Resumos do VIII Congresso Latino Americano de Cromatografia e Técnicas  
Afins*, Buenos Aires, Argentina 2000
3. Otimização da síntese de gel se sílica/anilina.  
*Livro de Resumos da 23<sup>a</sup> Reunião da Sociedade Brasileira de Química*, Poços de Caldas,  
MG, 2000
4. Estudo da estabilidade térmica da fase estacionária sílica/p-anisidina.  
*Livro de Resumos da VIII encontro de Química da Região Sul*, Santa Cruz do Sul, RS, 2000
5. Efeito do solvente usado nas propriedades do sólido organofuncionalizado.  
*Livro de Resumos do VIII Encontro de Química da Região Sul*, Santa Cruz –RS, 2000
6. Termo análise no infravermelho do xerogel anilina-propilsilica.  
*Livro de resumos do IX Encontro de Química da Região Sul*, Londrina, PR, 2001
7. Efeito da temperatura de geleificação na morfologia da anilina-propilsilica.

*Livro de resumos do IX Encontro de Química da Região Sul, Londrina, PR, 2001*

8. Evidência da presença de poros fechados em géis nanométricos de sílica/anilina.

*Livro de resumos da 24<sup>a</sup> Reunião anual da SBQ, 2001, Poços de Caldas, MG.*

9. Estudo Morfológico do Xerogel Anilinapropilsilica.

*Livro de Resumos da 25<sup>a</sup> Reunião da Sociedade Brasileira de Química, Poços de Caldas, MG, 2002*

10. Influência do catalisador fluoreto nas propriedades morfológicas do xerogel nanométrico amilinapropilsilica.

*Livro de Resumos do X Encontro de Química da Região Sul, Joinville – SC, 2002*